SOLID-LIQUID EQUILIBRIUM IN MULTI SOLUTE SYSTEMS

A Dissertation
Presented to
The Academic Faculty

By

Izumi Kurosawa

In Partial Fulfillment

of the Requirements for the Degree

Doctor of Philosophy in Chemical Engineering

Georgia Institute of Technology

April, 2004

SOLID-LIQUID EQUILIBRIUM IN MULTI SOLUTE SYSTEMS

Approved:

Dr. Ronald W. Rousseau, Chairman

Dr. Amyn S. Teja

Dr. Pete Ludovice

Dr. Athanassios Sambanis

Dr. Loren D. Williams

April 28, 2004

To my best friend and husband, Shutaro:

Without his love and encouragement, this thesis would not have been possible.

ACKNOWLEDGMENTS

from Tokyo Institute of Technology, and all the rest of my friends in Atlanta, Georgia and Japan.

Finally and most importantly, this thesis is dedicated to my parents, Kunio and Mariko Akiba, my parents-in-law, Dr. Hideo Kurosawa and Chikako Kurosawa, and my family whose continuous backing and encouragement made this possible.

TABLE OF CONTENTS

LIST OF TABLES

LIST OF FIGURES

LIST OF SYMBOLS

A	peak area in high performance liquid chlomatogram (HPLC)
A_{12}, A_{21}	fitting parameter in Margules equation
a_{mk}	group-interaction parameter between groups m and k.
A_W	van der Waals surface area
C	concentration of liquid solution
ΔC_p	difference between the heat capacities in the liquid and solid phases
d	d-spacing
$f^{bin,L}$	fugacity in a binary liquid solution
$f^{tern,L}$	fugacity in a ternary liquid solution
f^{oL}	fugacity of subcooled liquid
f^{oS}	fugacity of pure solid
g^E	excess molar Gibbs energy
$G^{E,s}$	molar excess Gibbs energy of a solid phase
g_c^E	combinatorial contribution to the excess Gibbs energy
g_r^E	residual contribution to the excess Gibbs energy
Δh^{fus}	enthalpy of fusion
hkl	cell parameters
I	mass of internal standard solution
k	response factor in HPLC analysis

M	mass of mixed solution
n_k	total number of groups of type k in a mixture
O	mass of OPA solution
R	volume parameter
S	mass of standard solution
T	temperature
T_t	triple point temperature
v	molar volume
V_W	van der Waals volume
W	mass of water
x	composition in liquid phase
$x*$	binary solubility of each amino acid in water
z	composition in solid solution
δ	solubility parameter
$\bar{\delta}$	average solubility parameter of mixture
ϕ	volume fraction
γ	symmetric activity coefficient
Γ	activity coefficient in a solid phase.
γ^l	activity coefficient in liquid phase
$\gamma_m{}^*$	unsymmetric activity coefficient
γ^S	activity coefficient in solid solution
γ^∞	infinite dilution activity coefficient
λ	wavelength of radiation source of X-ray diffractmetry

ν number of groups

θ peak angle

SUMMARY

Solid-liquid equilibrium in isomorphous amino acid systems has been investigated as a model for systems that form solid solutions. Solid- and liquid-phase compositions in L-valine + L-leucine, L-valine + L-isoleucine, and L-isoleucine + L-valine in water were measured over the entire range of solid composition, and it was shown (from mass balance and phase rule considerations) that these systems form solid solutions. The solid- phases resulting from isothermal and cooling crystallization experiments were also investigated using powder x-ray diffractometry which showed that homogeneous solid solutions could only be obtained in cooling crystallization experiments, whereas isothermal experiments generally produced inhomogeneous solids. This suggests that data reported in the literature from isothermal experiments may not represent true equilibrium values.

Solid-phase activity coefficients were estimated using binary and ternary equilibrium data and the UNIFAC-Kuramochi model for liquid-phase nonidealities. The solid phases in the three systems investigated exhibited significant nonidealities that were correlated using the Margules model. The model parameters exhibited a linear relationship with the ratio of binary solubilities of the two solutes. The analysis also showed that the model for crystal purity presented by Givand *et al*. represents a limiting case of the model presented in this work.

An empirical correlation was also proposed for crystal purity as a function of the liquid composition. The data exhibit sigmoid behavior and can be described with a two-parameter logarithmic function. Moreover, the parameters of this empirical model also exhibited a simple relationship with the binary solubility ratio. These results facilitate the prediction of crystal purity at an arbitrary liquid composition in other systems forming solid solutions since the parameters require only binary solubility data. Such simple relationship may be advantageous when solid-liquid equilibrium of thermally unstable solutes or components with unknown physical properties are crystallized.

CHAPTER 1

INTRODUCTION

Amino acids have been studied extensively as model compounds in biosciences such as medicine and protein chemistry. Solubilities of amino acids in various solvents, for instance, have been measured in association with protein denaturation (Nozaki et al, 1971; Dun and Ross, 1938; Cohn et al., 1934; McMeekin et al., 1936), and with protein stabilization in various solvents (Gekko and Idota, 1989, Lakshmi and Nandi, 1976; Back et al, 1979; Uedaira, 1980). This is because amino acids are essential substances for life, since they are the building blocks for proteins, and are also used in various metabolic processes in our body. For example, the essential amino acids tyrosine and tryptophan, are constituents for epinephrine, noreinephrine and serotonin, which take charge of neurological functions. Tryptophan is also converted by an enzyme to niacine, which is necessary for metabolizing sugars and fat. From an industrial perspective, the total consumption of amino acids in dietary additives and beverages is estimated to be over two million tons per year worldwide (Kusumoto, 2001). Since amino acids are rarely found in nature in a free form, they are produced by hydrolysis of proteins or fermentation processes, in which a product amino acid coexists with other by-products and inorganic salts in an aqueous solution. Not all the separation methods can be applied

to such bioproducts since they are sensitive to heat and decompose at temperatures below their melting points.

Recrystallization has been used as one of the most effective purification methods for biomolecules because it does not require excess heating for separation. Furthermore, crystals formed through recrystallization are thought to be in pure form, which is required in most cases for dietary or pharmaceutical applications. It has been pointed out in a survey of the types of the solid-liquid equilibrium for binary organic mixtures (Matsuoka, 1991) that more than 80 percent of the systems published in the literature fall into the category of simple eutectic systems or systems that include intermolecular compounds.

Even in such systems, however, it is often the case that some impurities are observed experimentally in crystal structures or on the surface of the crystals. This is because desired products in a fermentation broth are generally very similar to by-products in terms of structure and properties, and thus the difference in solubility is small in most cases. In order to improve recrystallization processes, additives and co-solvents have been designed based on their binary solubility data (Carta and Tola, 1996, Pradhan and Vera, 2000; Palecz, 1999, 2000; Ramasami, 2002).

So far, most efforts have been devoted to kinetic aspects of crystallization in order to eliminate the incorporation of impurity species. For example, Charmolue and Rousseau (1991) studied the effect of cooling rate on solvent incorporation in amino acid crystals, and reported that the slowest cooling rates yielded the most pure crystals in agreement with crystallization theories such as the theory of homogeneous nucleation. By contrast, there are a few studies of crystal purity in recrystallization processes from a thermodynamic point of view, especially in the case of ternary or higher multi-

component aqueous systems. Also, experimental compositions in both solid and liquid phases in the whole range of composition are rarely reported. Furthermore, in most studies on multi-component systems, pure seed crystals have been used in solubility measurements to saturate one of the components under the assumption that the solid phase is pure (Nyvlt, 1977; Jin and Chao, 1992; Kuramochi et al., 1996). This assumption is not valid in systems where the solutes have similar structure and/or functionality, since recrystallization could lead to the formation of solid solutions. For instance, Givand (1999a) and Givand et al. (2001) observed that the amount of impurity amino acid incorporated in the crystals of a product amino acid obtained from aqueous solutions was proportional to the relative solubility of the product and impurity amino acids in water. Furthermore, Koolman (1996) examined the powder x-ray diffraction patterns of amino acid crystals containing isomorphic impurities and found that the crystal patterns were different from those of the two pure amino acids, implying that the crystal phase was a solid solution. It should also be emphasized that the morphology of a solid crystal can affect its solubility even if the solid is composed of a single component; as in polymorphism (Giron, 1995, Beckmann, 2000; Wang et al., 2000, Lafferrere et al., 2003). Hence, simultaneous analysis of the solid and liquid phases should be implemented in order to eliminate any ambiguity in determination of solid-liquid equilibrium in such systems.

In this work, solid-liquid equilibrium of pairs of amino acids in aqueous solutions was investigated as a model for isomorphic systems. The following experiments and calculations were carried out; 1) simultaneous measurements of compositions in the solid and liquid phases in selected pairs of amino acids in water over a wide range of

composition to obtain their phase diagrams, 2) structural analysis of the solid phase using

powder x-ray diffractometry, and 3) estimation of activity coefficient of amino acids in

both liquid and solid phases.

CHAPTER 2

BACKGROUND

In this chapter, the literature on solid-liquid equilibrium in multi-component systems is reviewed. This includes general phase behavior and specific phase diagrams of multi-component systems. The literature on thermodynamic models applicable to solid-liquid equilibrium in multi-component systems is also reviewed.

2.1 Solid-Liquid Equilibrium in Multi-Component Systems

2.1.1 Binary Systems

Binary systems can have upto three degrees of freedom according to the Gibbs phase rule: $F=C-P+2$ where F is the degrees of freedom, C the number of components, and P the number of phases. Therefore, the state of binary components in equilibrium is defined by three variables such as temperature, pressure, and concentration. For example, at solid-liquid equilibrium (SLE) in a binary system, the composition in both solid and liquid phases changes with temperature at a given pressure.

Matsuoka (1991) investigated the frequencies of occurrence of particular kinds of SLE diagrams in binary organic mixtures and obtained the diagram shown in Figure 2-1. He found that more than half the systems in the literature exhibit simple eutectic behavior

(type (a)), and about a quarter form intermolecular compounds (type (b) and (c)) where

crystals formed are pure or compounds having a fixed composition. The rest of the

systems studied exhibit solid solutions (type (d), (e), and (f)).
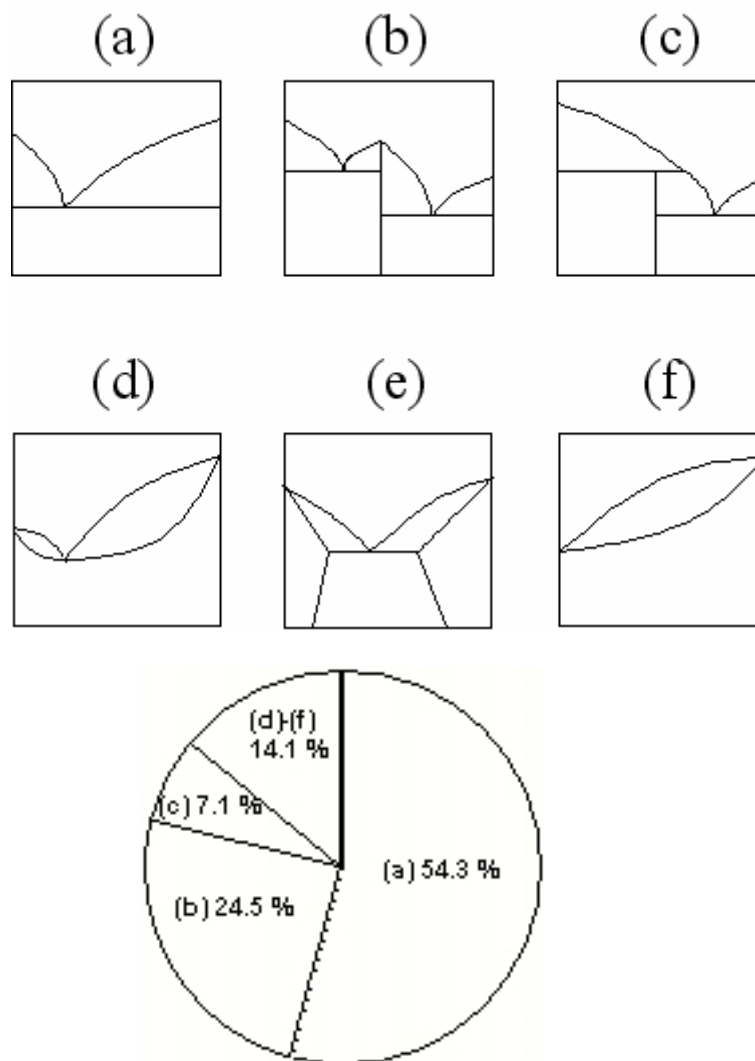
Figure 2-1 Types of organic binary SLE diagrams and the likelihood of their occurence

2.1.1.1 Systems that exhibit eutectic behavior

Figure 2-2 shows a phase diagram of a system in which the solid phases crystallize as pure crystals. The curve AEB and horizontal line CED represent liquidus and solidus curves, respectively. The area above AEB is the region of unsaturated and homogeneous liquids. The area enclosed by ACE and BED corresponds to the regions of pure crystal α (S_α) + liquid and pure crystal β (S_β) + liquid, respectively. Below the solidus curve CED, a mixture of S_α and S_β exists. For example, if a solution with a composition M_{T1} at a temperature T1 is cooled to a temperature T2, corresponding to M_{T2}, the system separates into a liquid phase F and solid S_β. The quantity of each phase can be determined by drawing a horizontal tie line FG and using the lever-arm rule. If the solution is cooled further, the composition of the liquid phase changes along the liquidus curve BE while the solid composition is kept at pure β. When the temperature reaches to T3, S_α appears.
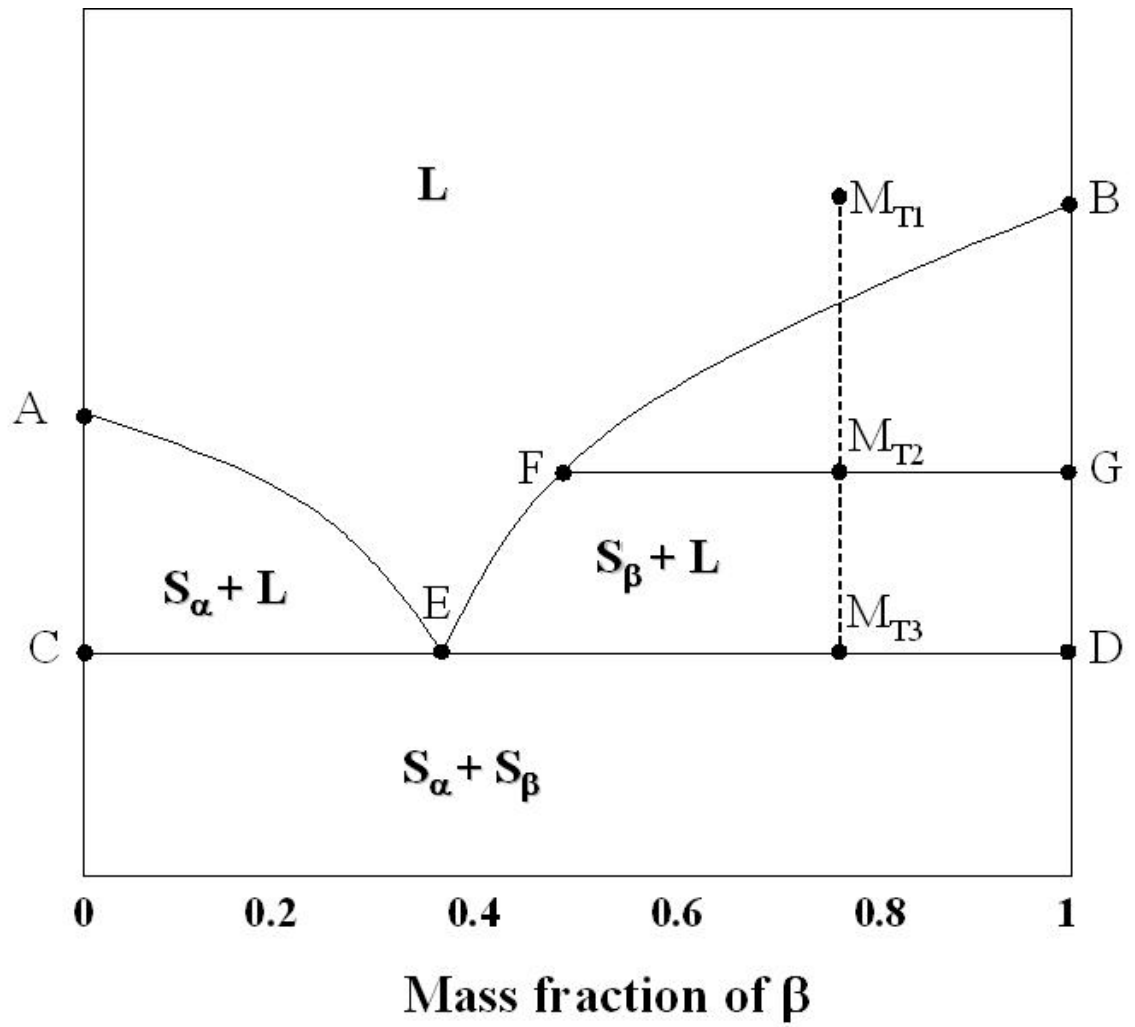
Figure 2-2 Temperature-composition phase diagram of a system that exhibits eutectic behavior

The thermodynamic relationship at equilibrium between a pure solid and a binary liquid solution is given by:

$$\mathbf{f}_i^{\circ S} = \boldsymbol{\gamma}_i^{L} \mathbf{x}_i \mathbf{f}_i^{\circ L} \qquad (i=\alpha,\beta) \qquad\qquad (2\text{-}1)$$

where $f_i^{\circ S}$ and $f_i^{\circ L}$ are fugacities of the pure solid and the subcooled liquid i, xi and γ_i^{L} are the composition and activity coefficient of component i in the liquid phase, respectively. The ratio of fugacities of the pure solid and the subcooled liquid at the temperature and pressure of the system, $f_i^{\circ S}/f_i^{\circ L}$, may be obtained using a thermodynamic path described by Prausnitz *et al.* (1986):

$$\ln\left(\frac{\mathbf{f}_i^{\circ S}}{\mathbf{f}_i^{\circ L}}\right) = \frac{\Delta \mathbf{h}_i^{\text{fus}}}{\mathbf{R}\mathbf{T}_{ti}}\left(1-\frac{\mathbf{T}_{ti}}{\mathbf{T}}\right) + \frac{\Delta \mathbf{C}_{pi}}{\mathbf{R}}\left(1-\frac{\mathbf{T}_{ti}}{\mathbf{T}}\right) - \frac{\Delta \mathbf{C}_{pi}}{\mathbf{R}}\ln\left(\frac{\mathbf{T}_{ti}}{\mathbf{T}}\right) \qquad (2\text{-}2)$$

where Δh_i^{fus} is the enthalpy of fusion of component i at its triple point temperature T_{ti}, and ΔC_{pi} is the difference between the heat capacities of the component i in the liquid and solid phases. The ΔC_{pi} terms are often omitted since their contribution is small compared to the Δh_i^{fus} term (Prausnitz *et al.*, 1999). The equation thus simplifies to:

$$\ln\left(\frac{\mathbf{f}_i^{\circ S}}{\mathbf{f}_i^{\circ L}}\right) = \frac{\Delta \mathbf{h}_i^{\text{fus}}}{\mathbf{R}\mathbf{T}_{ti}}\left(1-\frac{\mathbf{T}_{ti}}{\mathbf{T}}\right) \qquad\qquad (2\text{-}3)$$

If the pure-component properties (Δh_i^{fus}, ΔC_{pi}, and T_{ti}) are available, only the activity coefficient γ_i^{L} is required to obtain the phase diagram. If the solution is always very dilute, the activity coefficient in the liquid phase can be replaced by its value at infinite dilution. γ_i^{∞}. Furthermore, a simple equation can be used to represent the temperature-dependence of the infinite dilution activity coefficient as follows:

$$\ln \boldsymbol{\gamma}_i^{\infty} = \mathbf{a}_i^{'} + \mathbf{b}_i^{'}/\mathbf{T} \qquad\qquad (2\text{-}4)$$

If the liquid-phase is not dilute, thermodynamic models such as UNIFAC (Fredenslund *et al.*, 1977) may be used to estimate liquid-phase activity coefficient values.

2.1.1.2 Systems that form solid solutions

Figure 2-3 shows the phase behavior of a system that forms solid solutions. A solid solution may be thought of as a solid in which the atoms or molecules of one of the species occupy sites in the crystal lattice of the other species without modifying its crystal structure. Such a system is also called isomorphic because the components are completely miscible in both the liquid and solid phases. In the diagram, the curve ACB and ADB are the liquidus and solidus curves, respectively. The area above ACB represents the region of unsaturated and homogeneous liquid solutions. The area enclosed by ACBD corresponds to the region of liquid + solid solution. For example, a solution M_{T1} is cooled to temperature T2, the system M_{T2} becomes a mixture of liquid C and solid solution D. On further cooling, the solid composition changes continuously from D to G along the solidus curve, as does the liquid composition from C to F along the liquidus curve.

The thermodynamic relationship for equilibrium between a binary solid solution and a binary liquid solution are described by the following equation:

$$\gamma_i^S z_i f_i^{\circ S} = \gamma_i^L x_i f_i^{\circ L} \tag{2-5}$$

where γ_i^S and z_i are the activity coefficient and the composition of i in the solid solution, respectively.
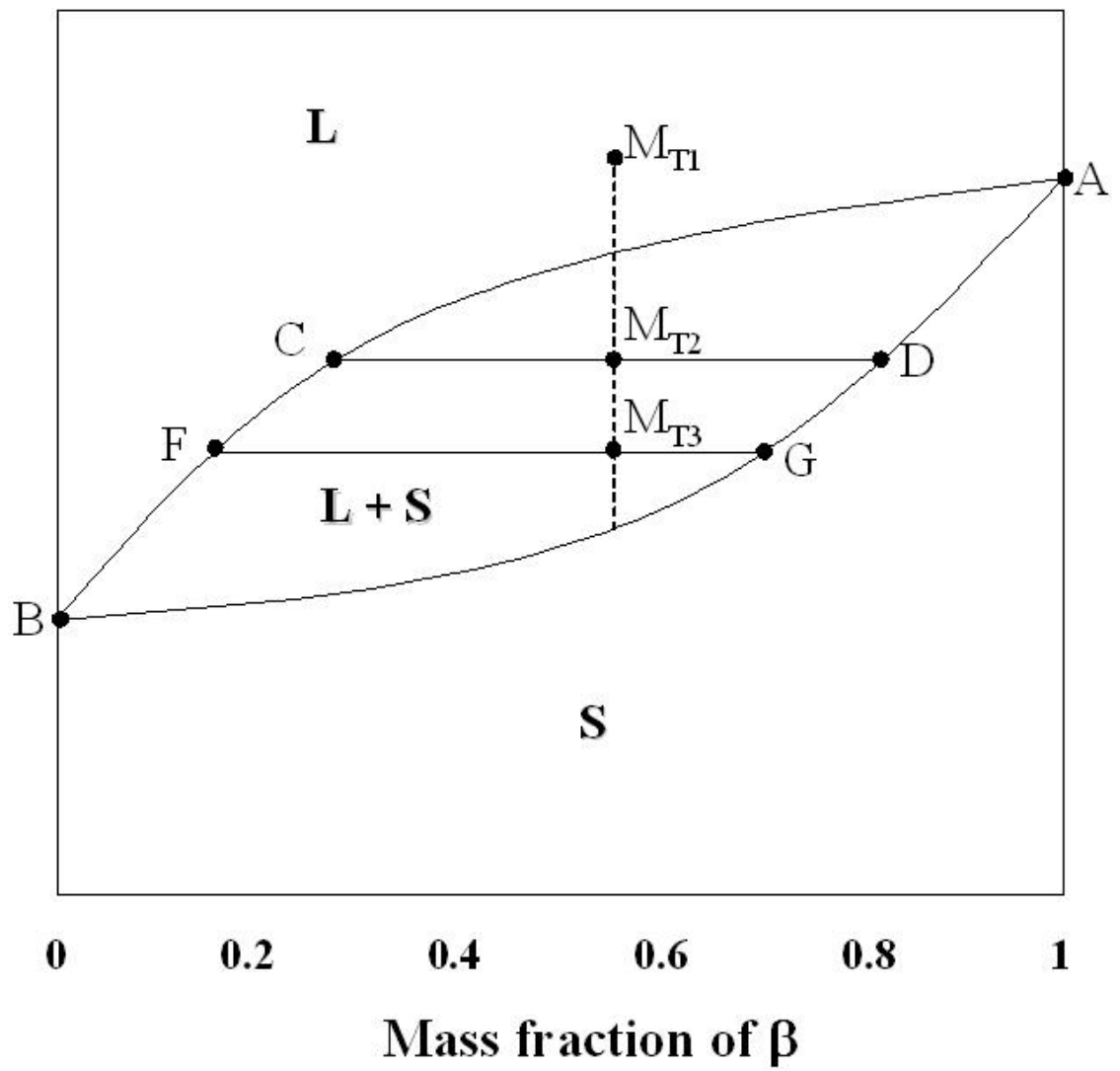
Figure 2-3 Temperature-composition phase diagram of a system forming solid solutions

2.1.2 **Ternary Systems**

Ternary systems such as those containing two solutes dissolved in a solvent exhibit different types of phase behavior depending on the state of the solids at a fixed temperature and pressure as shown in Figures 2-4(a) and (b). In the figures, a point S_α (or S_β) represents the solubility of pure solute α (or β) in a solvent, S, and the curve or curves $S_\alpha S_\beta$ corresponds to isothermal liquid compositions at equilibrium.

In Figure 2-4 (a), the point E is generally referred to as a *eutonic point* where a solution is saturated with mixed pure crystals of α and β. In the region $S_\alpha E\alpha$ (or $S_\beta E\beta$), a tie line always goes through the pure solid and the overall composition of the system since the precipitated solids are always pure α (or β). Therefore, a liquid composition at equilibrium, F, can be calculated from the overall composition, A, if the liquidus curve at the temperature is known. In the region $E\alpha\beta$, a tie line always goes through the point E and the overall composition of the system since the liquid composition is always fixed at a fixed temperature and pressure.

In Figure 2-4 (b), the area $S_\alpha S_\beta \beta\alpha$ represents the region of liquid + solid solutions (SS). In this type of system, the composition in the liquid and solid phases varies simultaneously. Therefore, a set of tie lines (FF', GG', and HH') is necessary in order to determine the composition in both phases from the overall composition.
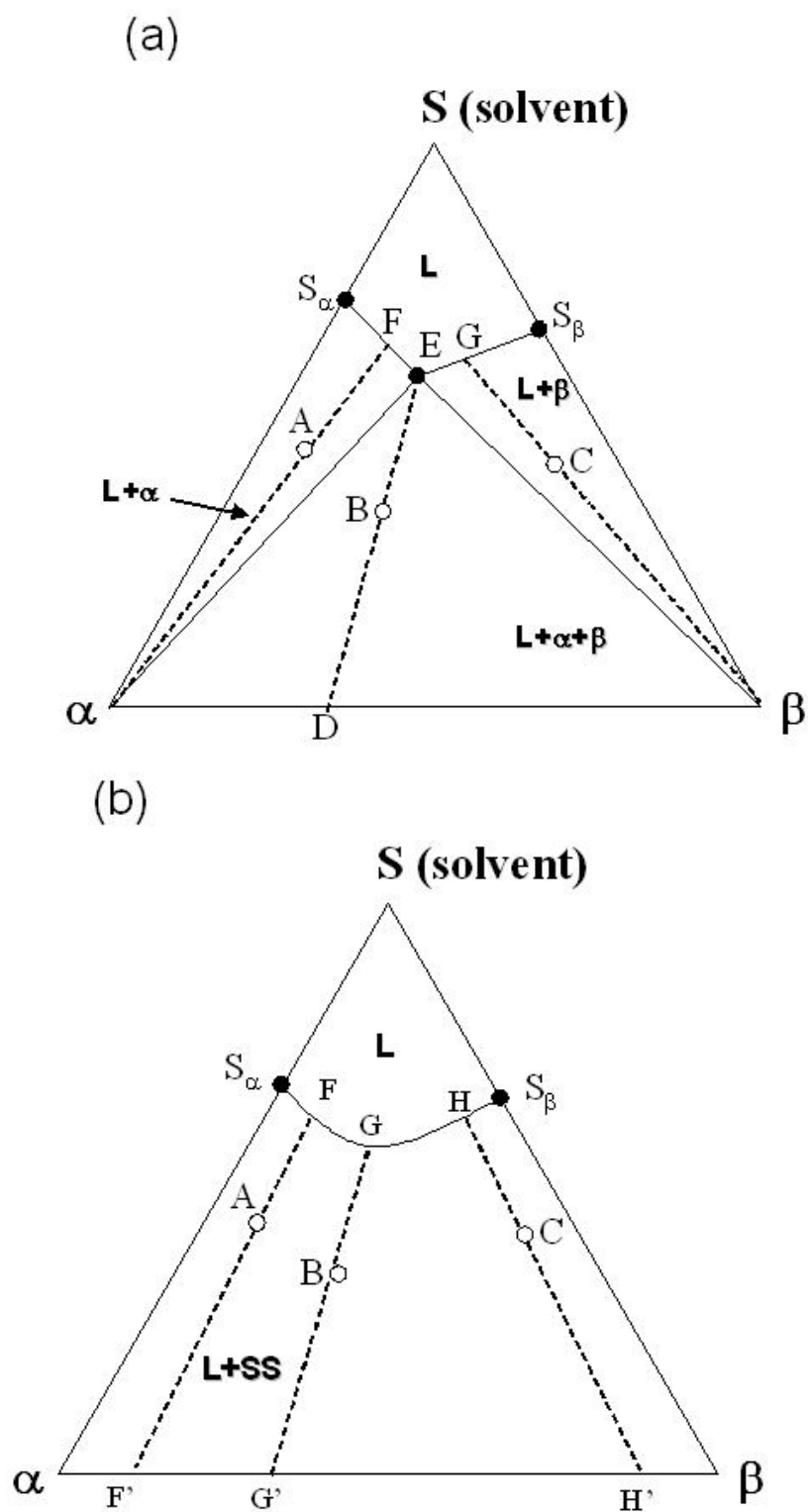
Figure 2-4 Ternary SLE phase diagrams for : (a) a system in which pure crystals are formed and (b) a ystem that forms solid solutions

2.2   Experimental Techniques to Observe Solid-Liquid Equilibrium

In order to design experimental procedures, one should take characteristics in phase behavior into account. As the number of components increases, the number of variables required to represent phase behavior also increases according to the Gibbs phase rule. Figure 2-5 is an example intended to highlight the differences between binary and ternary systems that exhibit similar eutectic behavior.

In a binary system, the system temperature is a typical variable in the isobaric phase diagram. For example, different feeds of A and B end up in the same mixture of S' and L' at a fixed temperature and pressure. Therefore, the phase diagram in binary systems is actually the temperature dependence of the composition in the solid and liquid phases.

In a ternary system, on the other hand, feeds A and B result in different mixtures of $L_A+\alpha$ and $L_B+\alpha$ at a fixed temperature and pressure. Therefore, a phase diagram in ternary systems is often composed of a set of isothermal and isobaric liquidus (and solidus) curves at different temperatures. Isothermal phase diagrams for multi-component systems are often obtained using analytical or synthetic techniques (Nyvlt, 1977). It should be noted that neither technique generally involves an analysis of the solid phase.
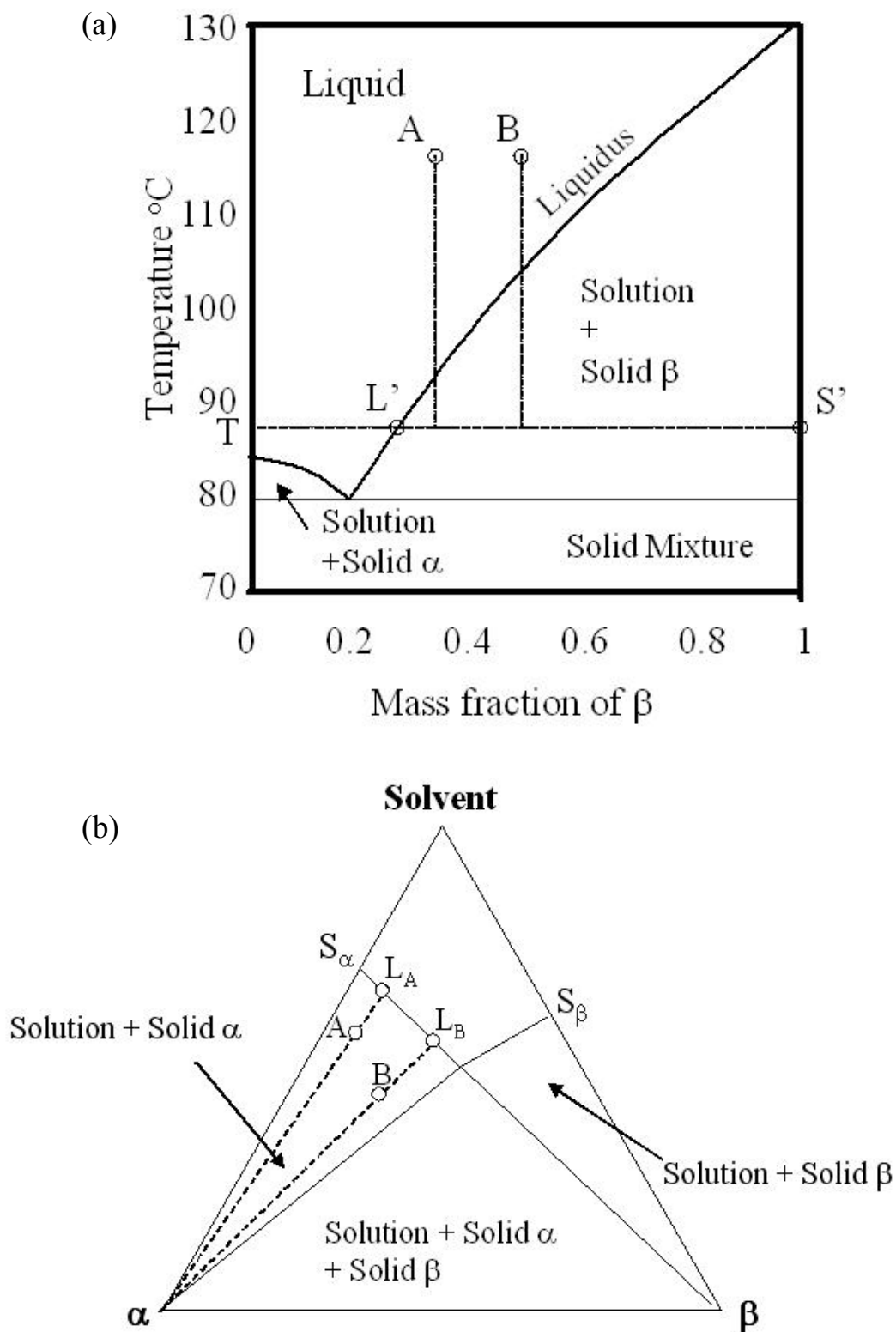
Figure 2-5 SLE phase diagrams of eutectic systems : (a) binary and (b) ternary

2.2.1   **Analytical Method**

Figure 2-6 shows a schematic diagram of the analytical method for a ternary system of solutes α and β in a solvent. In this method, an excess amount of α is added to an unsaturated solution of β so that some of the solid α remains undissolved in the solid phase throughout the experiment to ensure the saturation with α. After addition of α, the system is maintained at a constant temperature for a sufficient time to reach apparent equilibrium. The composition analysis in this method is based on an assumption that the solid crystals are exclusively of component α.

Figure 2-7 shows the change in the liquid composition along the isothermal solubility curve $S_\alpha S_\beta$. At first, the liquid composition is at S_i since the solution contains only the component β and the solvent. Then, the addition of α allows the liquid composition to move along a line $S_i A$, and to stop at S_f where the liquid phase is saturated with α.

The analytical method has been used for many multi-component systems due to its simplicity. However, this method should not be used for systems that form solid solutions because equilibrium cannot be attained in a realistic period of time due to low diffusivity in the solid phase. Besides, even if pseudo solid-liquid equilibrium is established between the contaminated surface of a pure crystal and the corresponding liquid solution, analysis of the solid composition will still be required. There are only a few studies that explicitly mentioned the purity of the crystals (Matsuoka, 1991; He *et al.*, 2003).

Excess amount of
pure α crystals

Unsaturated solution of β

Constant T

Pure α crystals
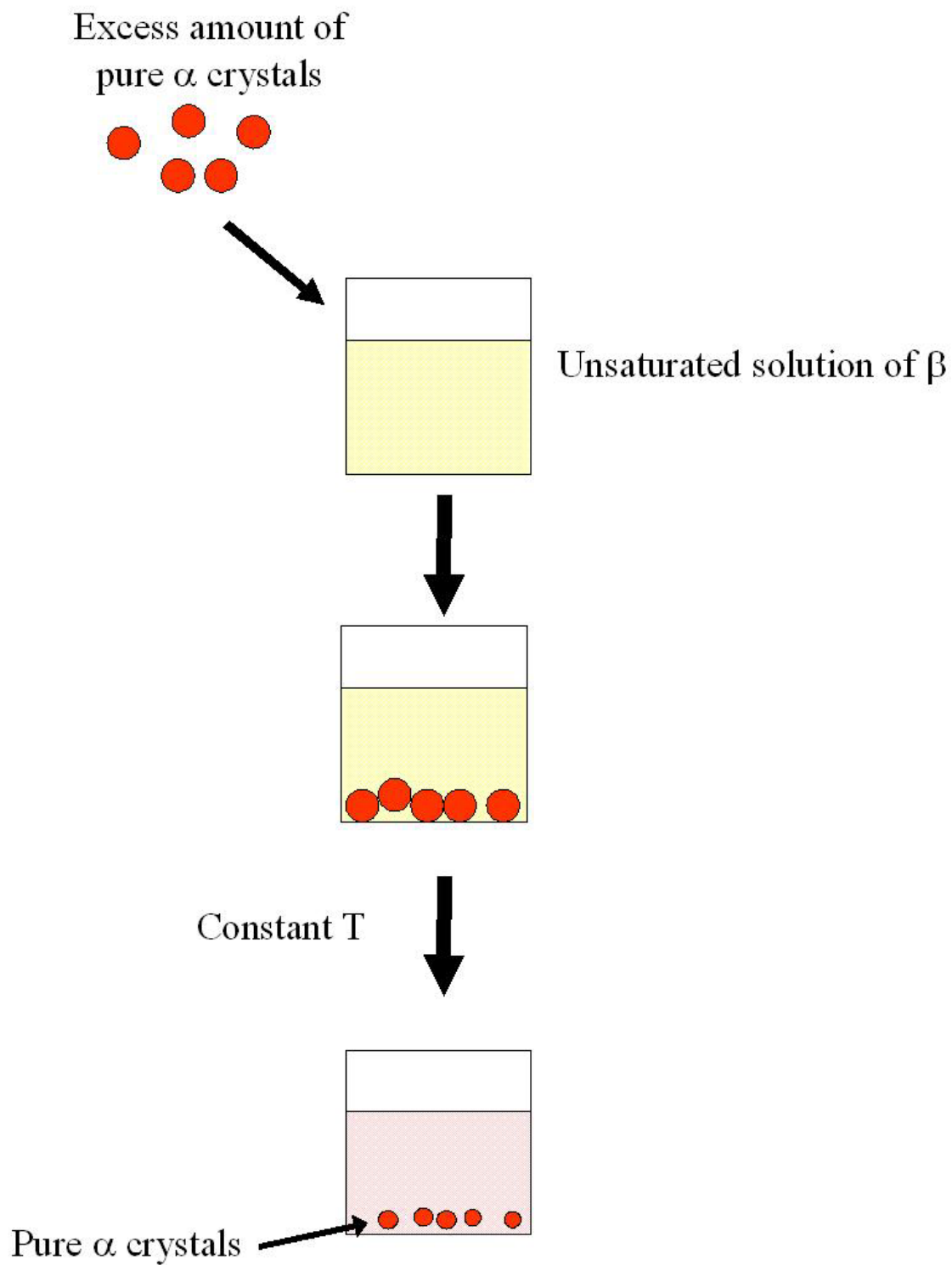
Figure 2-6 Schematic of the analytical method
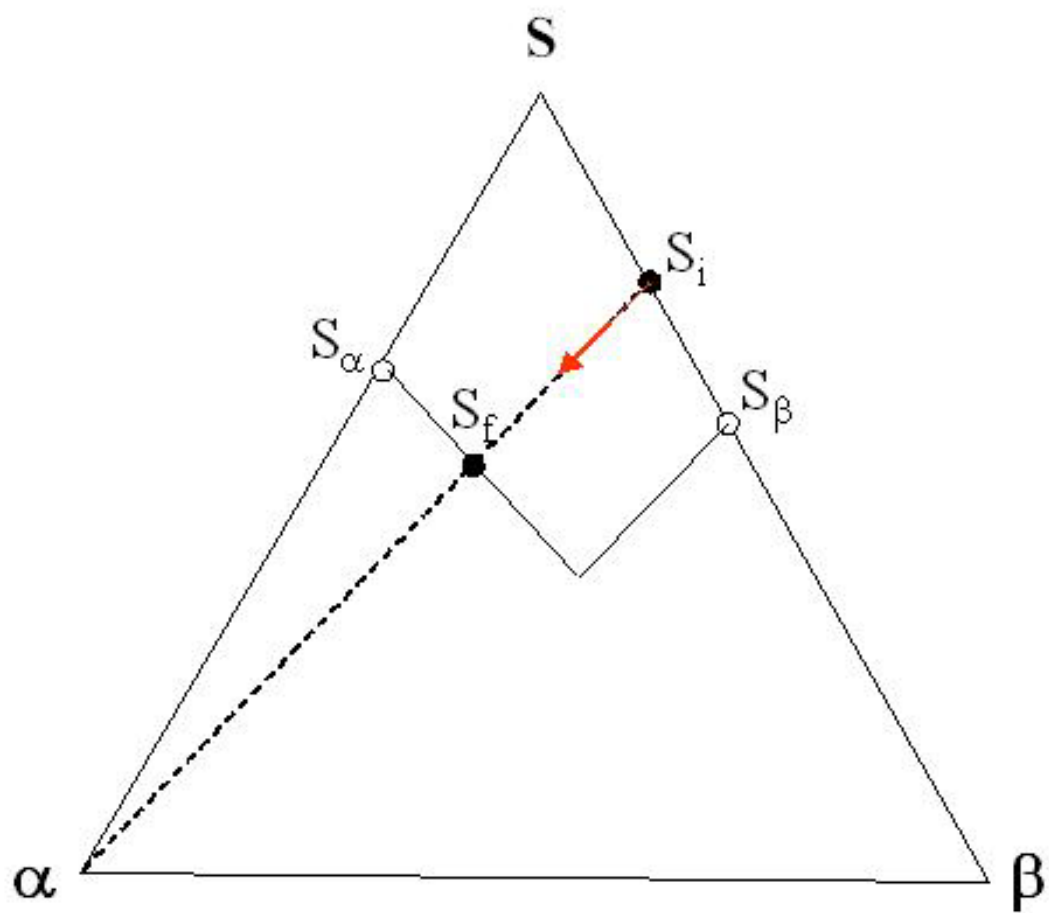
Figure 2-7 Phase diagram showing composition changes in the analytical method

2.2.2 Synthetic Method

The synthetic method determines the solubility by measuring the temperature at which solid crystals dissolve completely. The advantage of the method is ease of sampling. The disadvantage is that only "liquidus" compositions can be obtained.

Figure 2-8 shows a flow diagram of the changes in composition that occur in the synthetic method. Solutes are first added to a solvent in a certain ratio C until an excess amount of solid is present. Disappearance of the solid crystals is detected by a change in chemical and physical properties such as conductivity, refractive index, density and vapor pressure. The liquid composition at equilibrium with the last crystal at a particular temperature is considered to be the feed composition.

Figure 2-9 shows isothermal solubility curves $S_{\alpha,Ti}S_{\beta,Ti}$ and $S_{\alpha,Tf}S_{\beta,Tf}$ at T_i and T_f, respectively. At first, the feed composition C is within the saturation region at T_i. The system temperature is altered until all of the solids are dissolved. (C is on the solubility curve). It is assumed that the solid composition is the same as the feed composition. This assumption, however, may not be appropriate for systems with solid solutions in which solid composition changes with liquid composition.

Total composition
of the system: C

Changing T

Measure T
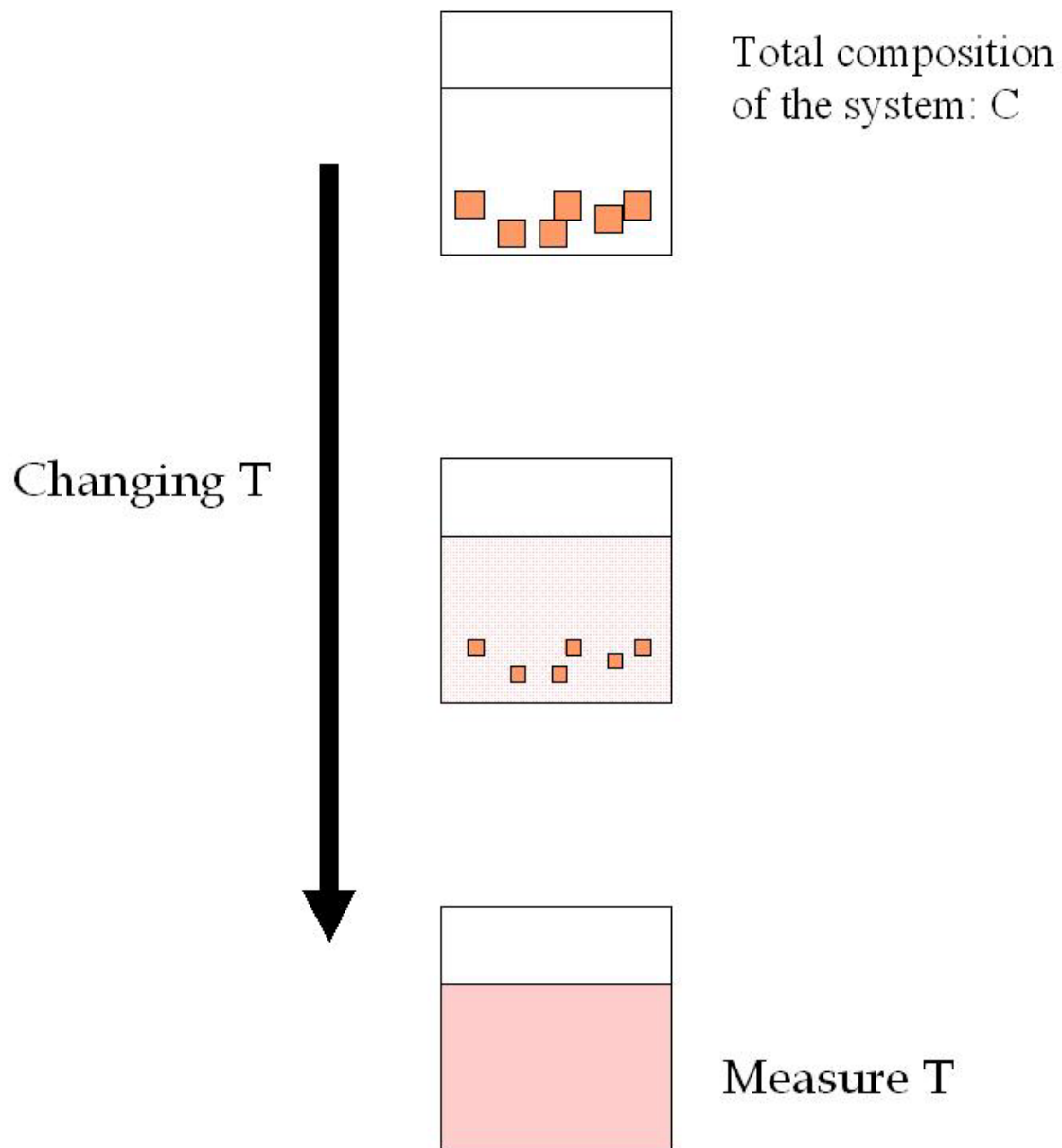
Figure 2-8 Schematic diagram of the synthetic method
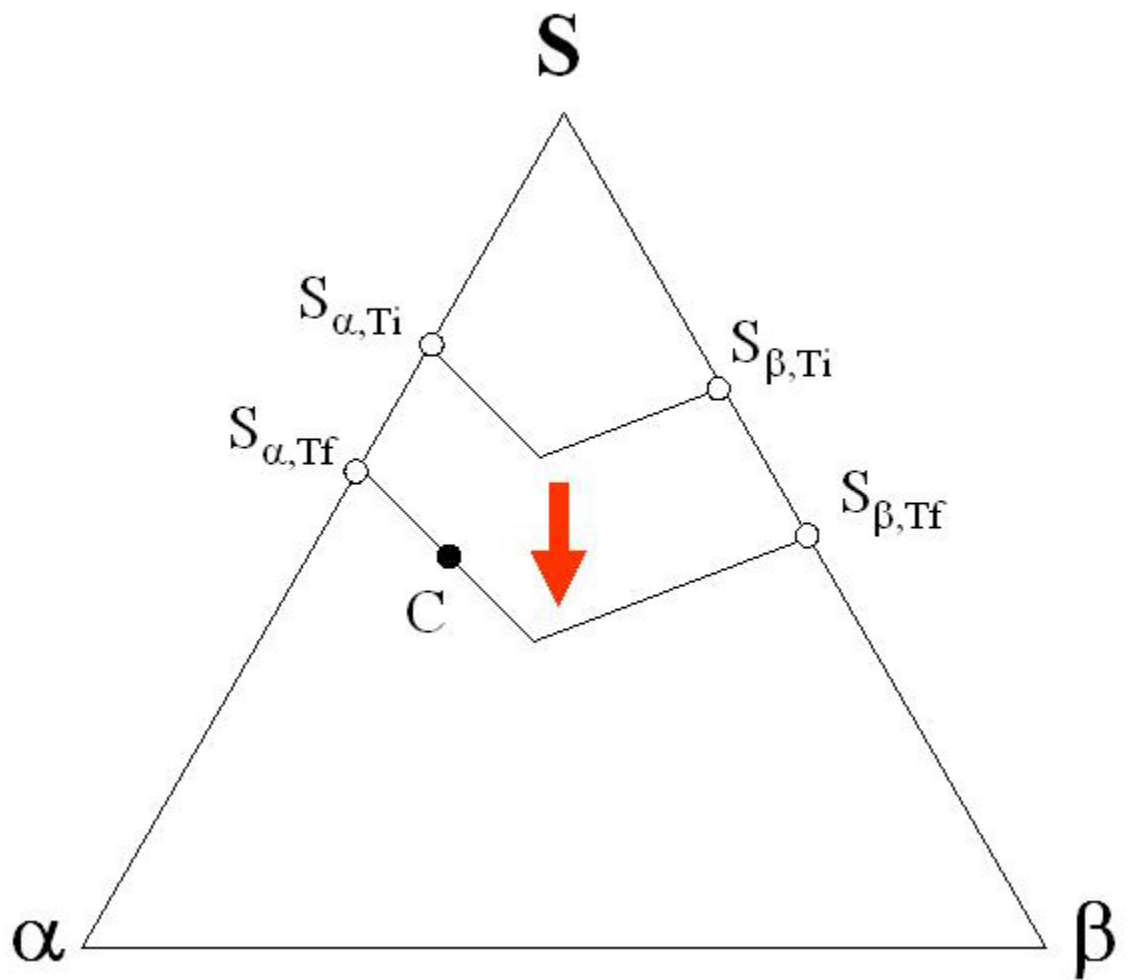
Figure 2-9 Phase diagram showing isothermal solubility curves at different temperature T_i and T_f.

2.3   Non-idealities in Solid-Liquid Equilibrium

Phase diagrams can be interpreted in terms of solid- and liquid-phase non-idealities. These non-idealities should also take account of the fact that crystal morphology can affect the phase diagram as in the case of polymorphs, racemates, and structural isomers.

2.3.1   Liquid-Phase Non-ideality

Keener *et al*. (1995) measured the freezing-point depression of aqueous amino acid solutions. They expressed non-ideality in the liquid phase with a single solute/solvent interaction parameter I_n, which corresponds to the number of perturbed water molecules per solute molecule. It was found that the parameter is directly proportional to the hydrophobic surface area of the solute and inversely proportional to the dielectric strength. This indicates that the non-ideality in the liquid phase is due to water structuring and destructuring induced by solute molecules. These results are consistent with the molecular dynamics study for solvent perturbations at molecular surfaces (Rossky and Karplus, 1979; Sonnenschein and Heinzinger, 1983; Geiger, 1981; Marlow *et al*., 1993) and with the NMR study of solvent motions and structure changes (Fullerton *et al*., 1986; Grosch and Noack, 1976; Zimmerman *et al*., 1985).

Pradhan and Vera (2000) measured the solubility of amino acids (glycine, DL-alanine, DL-valine, and DL-serine) in aqueous electrolyte solutions (NaNO$_3$, KNO$_3$, NaCl, and KCl) at 298.2 K. They found that the solubility of the amino acids in solutions containing the nitrate anion is always higher than that of solutions containing the chloride

anion. In terms of cations, the solubility with potassium in solution was always higher than that with sodium at the same concentration, except in the case of DL-alanine. The solubility of DL-alanine in solution with sodium is larger than with potassium in the presence of nitrate anion.

Kalra *et al.* (2001) investigated hydration on hydrophobic solutes in three tetramethylammonium salt solutions at various concentrations using molecular dynamics simulations. They evaluated salting-in and salting-out effects on the solubility of hydrophobic solutes. This simulation showed that kosmotropes, small and strongly hydrated ions, are excluded from the vicinity of hydrophobic solutes, leading to an increase in local water densities near hydrophobic solutes. This increases the excess chemical potential of hydrophobic solutes in solution, resulting in salting-out. The opposite behavior was observed for chaotropes, large and less favorably hydrated ions.

2.3.2 **Solid-Phase Non-ideality**

2.3.2.1 *Polymorphism*

Materials that exhibit more than two crystal structures are called polymorphs. Polymorphs often have different physical properties such as melting and sublimation temperatures, dissolution rate, solubility, hygroscopicity, and solid-state reactivity (Beckmann, 2000; Wang *et al.*, 2000, Giron, 1995; Lafferrere *et al.*, 2003).

There are two types of polymorphs: monotropic and enantiotropic. Monotropic polymorphs are not interconvertible, which means that the crystal structures seldom change into another one just by heating or dissolution. Graphite and diamond are examples of monotropic polymorphs. Enantiotropic polymorphs have interchangeable

crystal structures induced by melting or dissolution. For example, 5-methyl-2-[(4-methyl-2-nitrophenyl)amino]-3-thiophenecarbonitrile crystallizes in four modifications. These polymorphs have different solubilities in ethanol and different crystal shapes at ambient temperature. However, three of them transform to a stable form at 373 K ~ 388 K (He *et al.*, 2001). Such a transformation can cause a significant change in volume (e.g. ammonium nitrate) (Mullin, 2001).

The presence of polymorphism is not always beneficial especially in the pharmaceutical industry. For example, the production of ritonavir (Norvir)- an HIV protease inhibitor- was halted in 1998 because an unexpected polymorph was observed. This new polymorph had a different dissolution rate in water (Rowe, 2001). Another example involves Glaxo Wellcome, who sued Novopharm in 1997 for alleged patent infringement, maintaining that Novopharm patented a different polymorphic form of Glaxo's drug, Zantac. Glaxo lost its case and now Novopharm and other companies sell generic Zantac drugs with the new polymorph.

2.3.2.2 Racemate

A racemate is a mixture of equal amounts of enantiomers. In the gas or liquid state, a racemate behaves as an ideal mixture, and its physical and chemical properties are indistinguishable from those of individual enantiomers (Mitchell, 1998). In the solid state, however, the properties depend on whether the racemate is a racemic mixture or a racemic compound. In a racemic mixture, each enantiomer exists in the solid phase as a pure compound. Therefore, solid-state properties such as density or structure are identical to those of pure enantiomers. For example, a racemic mixture always has solubility

higher than the pure enantiomers, and the solubility will be twice that of a pure

enantiomer if both phases are ideal (Lorenz *et al*., 2002). A racemic compound, on the

other hand, is a homogeneous mixture of enantiomers, and its solid-state properties are

different from those of pure enantiomers. Therefore, solubility of a racemic compound is

not always greater than that of the pure enantiomers. For example, the solubility of

racemic compound of dexclamol hydrochloride in water is about five times less than that

of the pure enantiomers (Liu and Hurwitz, 1978).

2.3.2.3 *Multi Amino Acids in Water*

The synthetic method has been used to obtain the solubility of pairs of L-amino

acids in water as a function of temperature between 20 ˚C and 140 ˚C (Messer *et al*.,

1981). The amino acid pairs studied include phenylalanine-leucine, methionine-leucine,

methionine-norleucine, methionine-isoleucine, leucine-isoleucine, and aspartic acid-

leucine. The total molal concentration of amino acids was constant in the experiments so

that the system could be assumed to be a pseudo-binary mixture. In the case of the

isoleucine-leucine system, composition-independent solubility-temperature behavior was

reported in the range 20 to 50 mol % leucine. The authors also pointed out that solid

solutions were formed in the L-isoleucine-L-leucine system. However, they did not

analyze the solid phase.

The analytical method has been used to obtain the solubility of pairs of amino

acids in water by Jin and Chao (1992). They examined the effect of one amino acid A on

the solubility of another amino acid B for four pairs: L-glutamic acid (L-Glu) + glycine,

L-Glu + L-aspartic acid, L-Glu + L-serine, and L-aspartic acid + L-serine. For all of the

pairs, the solubility of one amino acid was always increased by the presence of the other. However, Jin and Chao based their analysis of liquid composition on the assumption that the crystals were pure. This assumption may not be applied to systems where the solid includes both amino acids. Furthermore, the effect of pH in the solutions via addition of acid was not investigated. Kuramochi *et al*. (1996) measured the solubility of two amino acids in water at 298 K including DL-alanine/DL-serine and DL-alanine/DL-valine in order to understand the effect of a hydrophobic molecule (DL-valine with a hydrophobic side chain) or hydrophilic amino acid molecule (DL-serine with a hydrophilic side chain) on the solubility of another amino acid in water. The solubility of DL-alanine decreased proportionally with the molality of DL-valine. The solubility of DL-alanine, on the other hand, increased with DL-serine molality. They also assumed that the crystal was pure without further analysis of the solid phase.

Koolman (1996) has provided experimental evidence that L-isoleucine (L-ILE) and L-leucine (L-LEU) can form solid solutions upon recrystallization. Powder x-ray diffraction patterns of crystals grown from L-ILE and L-LEU solutions revealed that diffraction peaks of the crystals appear at different reflection angles from those of each pure amino acid. This indicates that the crystals obtained from the solutions are not a mixture of pure L-ILE and L-LEU crystals, but their solid solution. The structural similarity may allow the substitution of one amino acid with another in the crystal lattice during recrystallization.

Kitamura and Nakamura (1999) studied the effect of the additives, L-valine (L-VAL), L-LEU, L-ILE and L-norleucine (L-NLE), on the crystallization of L-Glu. The concentration change of L-Glu was measured with time as a supersaturated solution of L-

Glu was cooled in the presence of each additive. It was found that L-VAL had a larger effect on the formation of crystals than does L-LEU, although L-VAL has a smaller substituted group than others. The additive most included in the L-Glu crystals was L-VAL. They suggested that the results might be due to the strong adsorption of L-VAL on L-Glu crystal surfaces.

Note that in the analytical method, an excess amount of pure crystals of a main amino acid is placed on the bottom of a vessel to ensure saturation throughout the equilibration process. The mechanism of nucleation and growth of crystals would be different from spontaneous recrystallization because pure crystals can play the role of "seeds" to crystallize the same species preferentially. Therefore, the solubility behavior can be different depending on the state of solids as suggested by Liu and Nagahama (1997), who measured the solubility of anthracene and phenanthrene in supercritical carbon dioxide at 35˚C and between 10.6 MPa and 24.6 MPa. The feed solids were prepared as either a mixture of pure solids or solid solutions. In the case of a pure solids mixture, the solubility of each component in the fluid was independent of the feed composition. In the case of solid solution, on the other hand, a moderate effect of the feed composition on the solubility was observed. This may be attributed to the difference in the degrees of freedom. This result suggests that experimental data obtained by both methods should be compared to understand the impact of the experimental procedures

2.4   Thermodynamic Models for Solid-Liquid Equilibrium

2.4.1   Thermodynamic Models for Non-Polar Solutes

Won (1986) developed a thermodynamic model to predict vapor-liquid-solid equilibrium in paraffinic hydrocarbon mixtures. In the model, the Soave Redlich-Kwong equation of state was used for vapor-liquid equilibrium, and a modified regular solution theory was used for liquid-solid phase equilibrium. In the modified regular solution theory, a solid solubility parameter that is a function of heats of vaporization and fusion was used instead of the conventional solubility parameter. For the systems studied, Won's model was not able to predict the experimental data better than an alternative model assuming mixed pure crystals in the solid phase. However, the assumption in the alternative model did not follow the Gibbs phase rule.

Coutinho *et al*. (1996a) predicted the solid appearance temperature in long-chain n-alkane mixtures by a predictive local composition model. In the model, the activity coefficient in the liquid phase was described as the sum of two terms: the Flory free-volume term (Continho *et al*., 1995) and UNIFAC residual term (Fredenslund *et al*., 1977; Hansen *et al*., 1991). The non-ideality in the solid phase was calculated with a version of the Wilson equation (Coutinho *et al*., 1996b) where local volumetric fractions were substituted with local mole fractions. The model predicted the phase behavior accurately for selected ternary systems, n-$C_{22}H_{46}$/n-$C_{24}H_{50}$/ethylbenzene (EB) , n-$C_{23}H_{48}$/n-$C_{24}H_{50}$/EB (Ghogomu *et al*., 1989), n-$C_{20}H_{42}$/ n-$C_{22}H_{46}$/n-C_7H_{16}, and n-$C_{22}H_{46}$/n-$C_{24}H_{50}$/n-C_7H_{16} (Brownawell and Hollyday, 1962).

Liu and Nagahama (1997) correlated solid solution- supercritical fluid equilibrium of a ternary system of anthracene, phenanathracene, and carbon dioxide. They assumed that the solid phase is a hypothetical liquid solution to which a simple thermodynamic representation can be applied. The activity coefficient in the solid solution was calculated by the Wilson model, and the Peng-Robinson equation of state was used for the fugacity coefficient in the fluid phase. The correlation was in good agreement with the experimental data, which implies the assumption of a hypothetical liquid solution was valid in this system.

Cottin *et al.* (1997) predicted the phase diagrams of hard-sphere mixtures using classical thermodynamics where both the fluid and solid phases behave as ideal solutions or an ideal fluid mixture in equilibrium with pure solids. Comparison with accurate calculations from computer simulation (Cottin *et al*., 1995; Mansoori *et al*., 1971) showed that the prediction deviated from simulation data. This failure may be ascribed to lack of consideration of non-ideality in the solid phase in the predictive model.

Khan *et al*. (2000) developed a thermodynamic model based on liquid-solid equilibrium principle to express liquid adsorption isotherms. They treated the adsorbent and sorbate as a solid phase in equilibrium with the liquid phase. In the model, the activity coefficient of the solid phase was a function of the weight fraction of sorbate in the solid phase using a Redlich-Kister expansion. The activity coefficient in the liquid phase was assumed to be constant and independent of the solute concentration. This model was able to correlate solubility data for 14 different systems with an average error of about 6 %, better than other available methods such as a vacancy solution theory, exponential model, and modified forms of the Freudlich isotherm.

2.4.2 **Thermodynamic Models for Polar Solutes: Alkali Halide and Amino Acid**

Rosenberger and Riveros (1974) developed an equilibrium segregation theory for solid solutions derived from the data of alkali halide solutions and melts. In this model, major and minor components in the solid phase are called host and impurity, respectively. The segregation coefficient was defined as the product of (1) the ratio of activity coefficients of impurity at a trace level and at saturation in the liquid phase, (2) the solubility ratio of host to impurity, and (3) an exponential term consisting of the heat of dissolution of the impurity in the solid host and the vibrational part of the entropy change of dissolution of the impurity in the solid host. In the model, (1) was set to unity, and (2) was obtained from experimental data. The heat of dissolution of alkali and halogen impurities in (3) was computed based upon a consistent set of empirical parameters derived from pure salts (Douglas, 1966). The vibrational entropy change in (3) was estimated from the Debye model of a solid (Morse, 1969). Rosenberger and Riveros reported that the calculation underestimated the segregation coefficient in most cases due to kinetic effects and a coarse estimation of the heat of dissolution.

Gupta and Heidemann (1990) attempted to build a predictive model for the effects of temperature and pH on the solubility of amino acids in water. The amino acids studied were alanine, aminobutyric acid, glycine, hydroxy-proline, proline, serine, threonine, and valine. Activity coefficients of the amino acids were correlated with the modified UNIFAC group contribution model (Larsen *et al*. 1987) where glycine and proline groups were considered. For example, alanine, aminobutyric acid, and valine were thought of as glycine with methyl (CH, CH_2, or CH_3) groups, and hydroxy-proline as proline and a

hydroxy group. However, this model failed to predict even the limited activity coefficient of glycine, alanine, amino butyric acid and valine.

Chen and Zhu (1989) analyzed activity coefficients of amino acids in water using an electrolyte nonrandom two liquid (NRTL) model. In this model, a long-range interaction is a Pitzer-Debye-Huckel form (Pitzer 1980), and short-range interaction is a modified form of the NRTL equation (Renon and Prausnitz 1968). The impact of other dipolar or ionic species on aqueous amino acid solubility was considered as well as temperature and pH effects using only one parameter for each pair of amino acids. Experimental data of solubility of amino acids in the presence of another amino acid showed nonlinear increase on a logarithmic scale with the amount of another amino acid. However, the model predicted that the solubility linearly increases with the concentration of another amino acid.

Kuramochi *et al*. (1996) introduced additional groups, α-CH, and sc-CH$_2$ (side chain-CH$_2$), into Larsen's modified UNIFAC model. Interaction parameters were determined from available osmotic coefficient data and the model was able to correlate liquid-phase activity coefficients of amino acids in water. The model was also able to predict the solubility of amino acids in the presence of another amino acid using a solid-liquid equilibrium concept developed by Prausnitz (1986). The predicted values were in good agreement with experimental data.

Givand (1999b) observed that the purity of amino acid crystals obtained from aqueous solutions is proportional to the relative solubility of the product and impurity amino acids in water. A simple thermodynamic relationship was applied to the experimental data, and the data could be correlated within experimental error.

Furthermore, the purity of crystals of the same amino acids in other solvents using the parameters obtained from the available data in water was reasonably successful. This success suggests that thermodynamic models could potentially have the ability to describe impurity incorporation during recrystallization.

CHAPTER 3

EXPERIMENTAL

In order to obtain solid-liquid phase equilibrium data for pairs of amino acids in water, simultaneous measurements of composition in the equilibrated solid and liquid phases and structural analysis of the solid phase using powder x-ray diffractmetry (XRD) were conducted. In this chapter, the experimental procedures and results of pure amino acid crystals are presented.

3.1 **Solubility and Crystal Purity Measurements**

3.1.1 **Materials**

Amino acids – L-leucine (L-LEU), L-isoleucine (L-ILE), and L-valine (L-VAL) – were obtained from Ajinomoto Company (Tokyo, Japan) and used as received. HPLC-grade water was purchased from Fisher Chemicals (catalog# W5SK-4, Fair Lawn, NJ) to prepare solutions of the amino acids and mobile phases for High Performance Liquid Chromatography (HPLC) analysis.

3.1.2 **Experimental Procedures**

3.1.2.1 *Solubility Measurements*

a) Binary Systems

The solubility of the pure amino acids (L-ILE, L-LEU, and L-VAL) in water was measured at temperatures between 293 K and 333 K. A predetermined amount of each amino acid, corresponding to the literature values of solubility at 343 K was loaded in 300-ml of water in a 350 mL jacketed glass vessel. The vessel was sealed with rubber sleeve stoppers (Catalog # 14-126DD, Fisher Scientific, Pittsburgh, PA) with small holes made by a needle for ventilation. The system was heated until all crystals were dissolved. The amount of water vaporized during heating is negligible because the time of heating was 10~20 minutes and the ventilation holes were small. The homogeneous solution was cooled to a set temperature, and left for more than 2 days with a constant stirring by a magnetic bar. The solution temperature was controlled to ± 0.01 K via water circulation in a jacket around the vessel using a programmable water bath (VWR Scientific Model 1157, VWR international, West Chester, PA). Typical cooling rates were in the range 0.5-0.8 K/min.

After the set temperature was attained, a small amount of liquid (2.0 mL) was withdrawn through a stainless steel needle (3½" length 22 gauge needles with a fitting stylet, catalog # 7307, Popper & Sons, New Hyde Park, NY) connected to a 5-mL plastic syringe (sterilized, VWR international, West Chester, PA). The syringe was subsequently detached from the needle and connected to a filter (Fisher brand filters 25mm 0.2μm pore size sterilized, Catalog # 09-719A, Fisher Scientific, Pittsburgh, PA). About 6 drops (~ 0.3 ml) of the solution were introduced into each of three 2-mL screw top vials (catalog #

34

2-SVG, Chromacol, Wilmington, NC) through the filter, followed by an injection of 0.4 mL of an internal standard solution (see Section 3.1.3.2 (d)-(g)) for HPLC analysis. The vials were capped with 8-mm screw caps (catalog # 8-SCJY-ST15, Chromacol, Wilmington, NC), and agitated with a vortexer (vortexer 2, model G-560, VWR international, West Chester, PA). The samples in the vials were diluted with pure water and analyzed by HPLC. The composition of the three samples was determined to $\pm$ 0.03 g/kg H_2O. The sampling and HPLC analysis were repeated until the liquid composition did not change with time.

b) Ternary system

Two methods were used in this work for solubility measurement in ternary systems of pairs of amino acids in water. These methods will be referred to as the cooling and isothermal methods. In the cooling method, recrystallization from a homogeneous solution produces solids that exist in equilibrium with a liquid. In the isothermal method, an excess amount of pure amino acid is introduced into an unsaturated solution of another amino acid. This is identical to the analytical method discussed in Chapter 2 (Kuramochi *et al.* 1996, Zin and Chao 1992, Soto *et al.*, 1999).

b-1) Cooling method

Predetermined quantities of two amino acids were mixed with 100 mL of water in a 150ml jacketed glass vessel. The mixture was heated until all solids were dissolved. After complete dissolution of the solids, the initial composition was measured by the same method as in binary systems. The solution was then cooled to 298 K with a cooling

rate of about 50 K/h. The temperature was maintained at 298 K for 2 days before HPLC

analysis, although equilibrium was attained within 24 h for all systems (Appendix A). It

should be noted that the initial concentration was optimized by trial and error in order to

produce as small an amount of crystals as possible at 298 K so that uniform crystals were

obtained.

b-2) Isothermal Method

At first, one of the amino acids (A1) was added to 100 ml of water in a jacketed

glass vessel where the concentration of A1 was less than its saturation value at 298 K.

After all crystals were dissolved, the initial concentration of A1 was measured by HPLC

analysis. An excess amount of the other amino acid (A2) was then mixed in the solution.

The amount of A2 was 1.5 times as much as required to prepare a saturated solution with

A2 at 298 K in the case of L-VAL, and twice in the case of L-ILE or L-LEU. Analysis of

the liquid composition was conducted periodically until the liquid composition was

constant with time.

3.1.2.2 Crystal Purity Measurements

After the achievement of solid-liquid equilibrium, the contents of the vessel were

filtered to collect the solids. The solids were not washed with water in this work since

washing could result in preferential removal of one component. Instead, a correction was

made in order to determine a true solid composition as follows: a wet solid sample after

filtering was weighed in a Petri dish. The sample was then dried overnight in an oven at

373 K, and weighed again. The difference in weight before and after drying was the

weight of water included in the sample. The weight of each solute precipitated upon drying was calculated to be a product of the mass of the evaporated water and the concentration in the liquid phase. Subsequently, a small amount (< 0.1 g) of the dry solid sample was dissolved in fresh water, and the mole fraction of the solutes in the solid phase was determined by HPLC. The rest of the solid samples were utilized for structural analysis via powder XRD measurements.

It should be pointed out that in all the experiments not more than 5 g of mother liquor was attached to the crystals and filter paper. This indicates that the contribution of the correction is not significant compared to the total mass of the solids. For example, if the L-LEU concentration in a mother liquor is 20 g/kg water, the amount of L-LEU in 5 g of the mother liquor is 0.1 g. A total amount of the solid sample was generally more than 3 g; therefore, the amount of L-LEU from the mother liquor is less than 5 wt % of the total mass. Moreover, the solvent-free composition of the mother liquor was very close to the composition in the crystals. Therefore, the crystal deposition via evaporation would not affect the crystal compositions significantly.

3.1.3   HPLC Analysis

Reverse-phase HPLC apparatus was used to determine the concentration of the amino acids in the samples. The apparatus, materials, experimental, and analytical procedures for these experiments are described in the following sections.

3.1.3.1 Apparatus

The apparatus consists of a reverse-phase packed HPLC column (Microsorb-MV 100-3 C18, 100 × 4.6 mm VALCO, catalog # R0086200E3, Varian, Palo Alto, CA), a UV-VIS spectrophotometric detector (SPD-10AV, Shimadzu, Kyoto, Japan), two solvent delivery units (LC-10A, Shimadzu), an automatic sample injector (SIL-10A, Shimadzu), and a system controller module (SCL-10A, Shimadzu). Data collection and processing were conducted by a Shimadzu CLASS-VP Chromatography Data System version 4.2 software.

3.1.3.2 Procedures

(a) Preparation of Mobile Phases

A linear gradient elution method was adopted in order to obtain distinctive peaks (Synder et al., 1983). This method allows the composition of the mobile phase to change with time using two solutions with different polarity. One mobile phase (solution A) was an aqueous methanol solution and the other (solution B) was pure methanol in this work.

The procedure to make a 1-L solution of A is the following: 5 g of sodium phosphate dibasic heptahydrate (catalog# MK-7914-500, Fisher Scientific, Pittsburgh, PA) was dissolved in 680 ml of water in a glass bottle. The pH of the solution was adjusted to 7.2 chosen to minimize the damage to the HPLC column by dropwise addition of a concentrated hydrochloric acid solution (catalog # 9535-00, J. T. Baker, Phillipsburg, New Jersey). Then, 300 mL of pure methanol (Methanol OPTIMA[*], catalog # A454-4, Fisher Scientific) and 20 mL of tetrahydrofuran (HPLC grade, 99.9%, catalog#

AC610100040, Fisher Scientific) were added and mixed thoroughly. The solution was stored in a refrigerator before use.

(b) Pre-Column Derivatization

The pre-column derivatization of amino acids with an o-phthaldialdehyde (OPA) solution yields highly fluorescent derivatives, thio-substituted isoindoles, detectable by the UV-VIS detector at low concentrations (Jones et al., 1981). Therefore, the pre-column derivatization has been widely used to detect amino acids with good selectivity and sensitivity (Brückner et al., 1995).

In this research, Fluoraldehyde™ Reagent Solution (catalog# 26025, Pierce, Rockford, IL) was used as a derivatization agent. The reagent solution was supplied as a ready-to-use solution containing OPA, boric acid, 2-mercaptoethanol, potassium hydroxide, Brij® 35, water and methanol. The solution is so sensitive to air, light, and heat that a small amount of the solution (100 mL) was stored into a 125-mL amber bottle (Boston round bottles, catalog # EP115-125A, VWR International, West Chester, PA) wrapped with aluminum foil in a refrigerator.

The derivatization procedure was as follows: 50 µL of a diluted sample solution was pipetted into 950 µl of the reagent solution in a 2-mL vial and mixed well by the vortexer. A 5-minutes interval was taken before the initialization of an auto injection sequence in HPLC analysis since the maximum of fluorescence intensity is observed 5 minutes after the mixing (Roth, 1971). The molality of OPA was about 5 times as much as that of the amino acids in the samples (Givand, 1999a).

(c) Linear Gradient Elution Method

As mentioned in (a), the composition of the mobile phases changes with time so that chemicals of interest elute out separately with distinct retention times. The total flow rate was fixed at 1 mL/min, and the concentration profile is shown in Table 3-1. After 17 minutes of analysis, approximately 5 minutes were taken before the next measurement so that the column was refilled with the initial mobile phase (40 volume % of solution B). A representative chromatogram is shown in Figure 3-1. Within 1-2 minutes after injection of the sample, peaks from components in the OPA solution are observed. The peaks corresponding to L-VAL, L-ILE and L-LEU appear at 3.5, 5.2, and 5.7 minutes, respectively.

Table 3-1 Flow rate of solution B with time

Time [min]	Solution B [volume %]
0	40
0.01 → 10	40 → 65
10 → 11	65 → 90
11 → 12	90 → 90
12 → 17	90 → 35
17.01	STOP
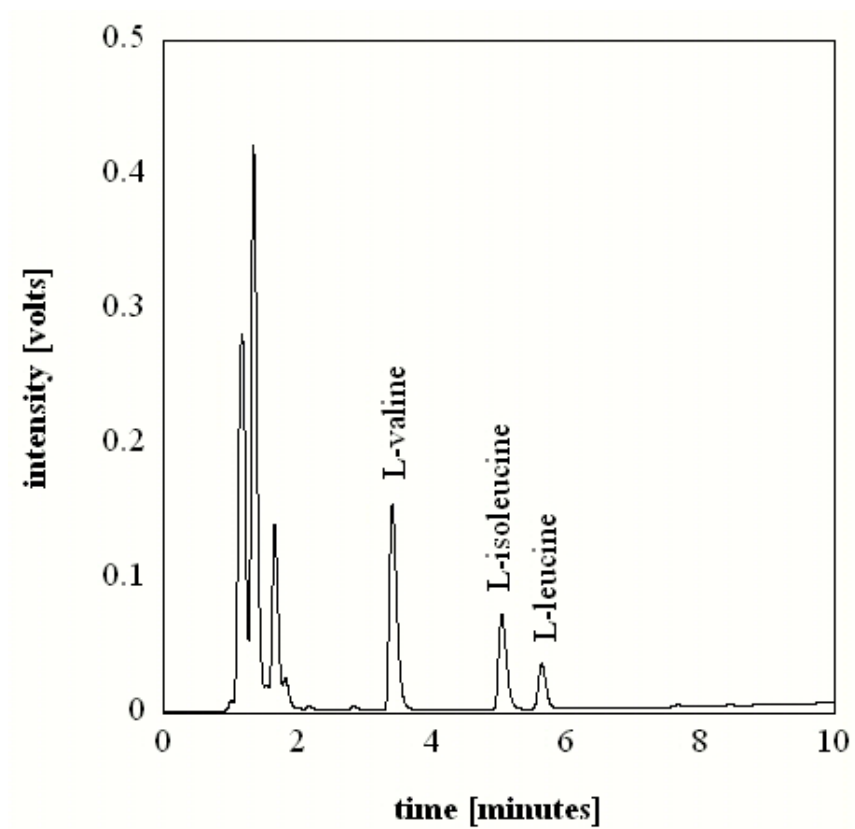
Figure 3-1 Typical HPLC separation of L-isoleucine, L-leucine, and L-valine

(d) Internal Standard Method

The peak area calculated by integration of the peak intensity with time is generally proportional to the concentration of a component in the sample. However, this is not always the case because HPLC conditions such as pressure inside the column, the amount of the sample injected, and the sensitivity of the UV/VIS detector may not be exactly the same in all runs. Every-time calibration of HPLC is one way to obtain experimental consistency, but is time consuming. Instead, an internal standard method was used in this study since the ratio of peak areas of sample and standard solutions is not affected by fluctuation in the HPLC conditions. This can be represented in the following equation:

$$\frac{C_s}{C_i} = k_{s,i} \frac{A_s}{A_i} \qquad\qquad (3\text{-}1)$$

where C, A, and k are the concentration, the peak area, and the response factor, respectively. The subscripts s and i denote the sample and internal standard, respectively. If the concentration of i and the response factor $k_{s,i}$ are known, the unknown concentration C_s can be calculated with equation (3-1). In order to obtain the response factor, the calibration described in (e) was carried out every time the column was exchanged.

(e) Calibration

A flow chart of the calibration is shown in Figure 3-2. Two amino acid solutions with known concentrations, C_{s0} [g amino acid/ g solution] and C_{i0} [g amino acid/ g solution], were prepared as a standard and internal standard amino acid solutions,

respectively. The concentration of both solutions was set at about 1 g-amino acid / g-solution. The internal standard solution was also used in the solubility measurements.

Six samples with different concentrations were analyzed to obtain a calibration curve for each pair of the amino acids. Among the six samples, three were prepared by diluting S_0 g of the standard solution with W_0 g of water. The concentration of the diluted samples, C_{s1}, is then:

$$C_{s1} = \frac{C_{s0} \cdot S_0}{S_0 + W_0} \qquad (3\text{-}2)$$

Then, S_1 g (~ 0.05 g) of the diluted sample solution was mixed with I g (~ 0.05 g) of the internal standard and W_1 g (~ 0.95 g) of water. The rest samples were made with S_1 g of the standard solution ($C_{s1} = C_{s0}$), water, and the internal standard. The concentrations of the amino acids in the standard and internal standard solutions were expressed in the following equations, respectively:

$$C_{s2} = \frac{C_{s1} \cdot S_1}{S_1 + I + W_1} \qquad (3\text{-}3)$$

$$C_{i2} = \frac{C_{i0} \cdot I}{S_1 + I + W_1} \qquad (3\text{-}4)$$

Finally, M g (~ 0.05 g) of the mixed solution was added to O g (~ 0.95 g) of the OPA solution before analysis. The final concentrations of the standard and internal standard solutions are:

$$C_{s3} = \frac{C_{s2} \cdot M}{M + O} \qquad (3\text{-}5)$$

$$C_{i3} = \frac{C_{i2} \cdot M}{M + O} \qquad (3\text{-}6)$$

Since the ratio of peak area of the standard, A_s, to that of internal standard, A_i, is proportional to the ratio of C_{s3} to C_{i3}:

$$\frac{C_{s3}}{C_{i3}} = k_{s,i} \frac{A_s}{A_i}$$

(3-7)

From equations (3-1)-(3-7), the following relationship can be obtained:

$$\frac{C_{s3}}{C_{i3}} = \frac{C_{s2}}{C_{i2}} = \frac{C_{s1} \cdot S_1}{C_{i1} \cdot I} = k_{s,i} \frac{A_s}{A_i}$$

(3-8)
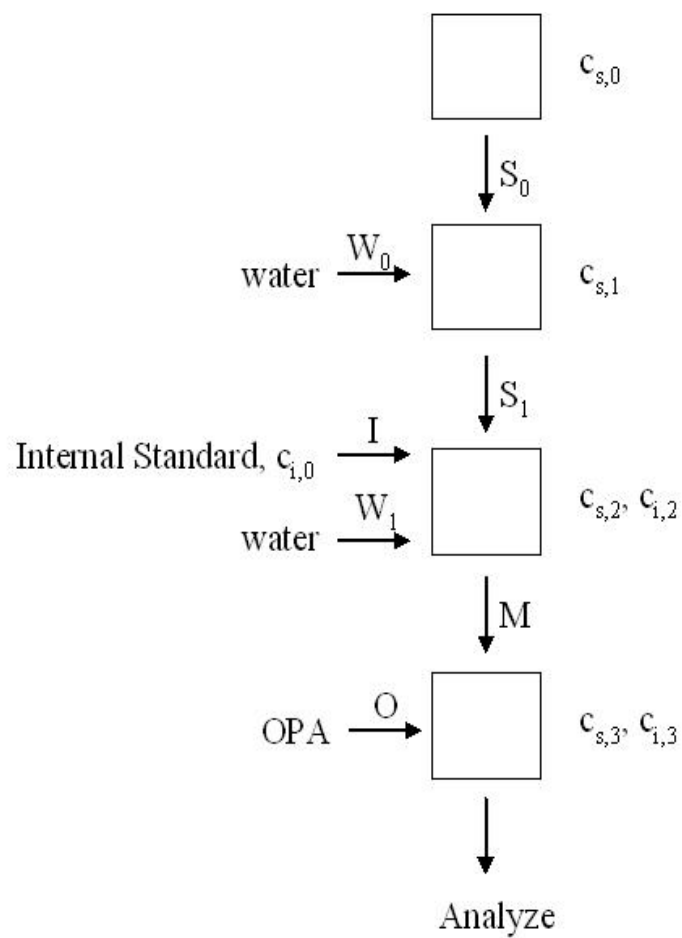
Figure 3-2 Calibration procedure for HPLC

(f) Contamination of L-VAL crystals with L-LEU

When the calibration for L-VAL (standard) and L-ILE (internal standard) solutions was conducted, a peak corresponding to L-LEU appeared in the chromatogram as shown in Figure 3-3. This suggests that L-VAL crystals were contaminated with L-LEU since the peak area of L-LEU is proportional to that of L-VAL when L-VAL solutions with different concentrations were analyzed. Using the calibration data of L-LEU with L-ILE (internal standard), the concentration of L-LEU in the L-VAL crystals was determined to be 3 weight %. Taking into account this contamination, the response factors, $k_{s,i}$, for every pair of the amino acids were corrected by the following equations:

For L-VAL (standard) and L-ILE (internal standard):

$$\frac{C_{s1} \cdot S_1 \cdot (1 - 0.03)}{C_{i1} \cdot I} = k_{s,i} \frac{A_s}{A_i} \qquad (3\text{-}9)$$

For L-VAL (standard) and L-LEU (internal standard):

$$\frac{C_{s1} \cdot S_1 \cdot (1 - 0.03)}{C_{i1} \cdot I + C_{s1} \cdot S_1 \cdot 0.03} = k_{s,i} \frac{A_s}{A_i} \qquad (3\text{-}10)$$

For L-ILE (standard) and L-VAL (internal standard):

$$\frac{C_{s1} \cdot S_1}{C_{i1} \cdot I \cdot (1 - 0.03)} = k_{s,i} \frac{A_s}{A_i} \qquad (3\text{-}11)$$

For L-LEU (standard) and L-VAL (internal standard):

$$\frac{C_{s1} \cdot S_1 + C_{i1} \cdot I \cdot 0.03}{C_{i1} \cdot I \cdot (1 - 0.03)} = k_{s,i} \frac{A_s}{A_i} \qquad (3\text{-}12)$$
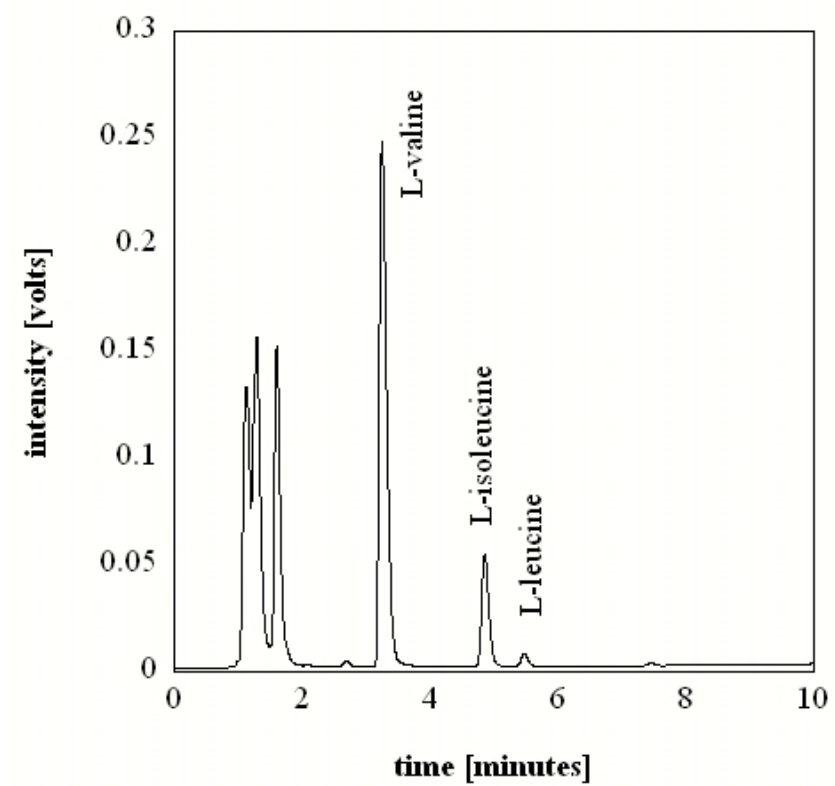
Figure 3-3 Chromatogram for the calibration of L-VAL with L-ILE as an internal standard

(g) Composition Measurements

The solubility of the amino acids was obtained using the following procedure as shown in Figure 3-4: Firstly, an empty vial with a cap was weighed (M_e [g]). Then, about 400 µL of the internal standard was added in the vial and weighed (M_i [g]). A sample solution was added to the vial and weighed (M_s [g]) and stirred with the vortexer. Then 50 µL of the solution was taken and mixed with 950 µL of water. Finally, 50 µL of the diluted solution was mixed with 950 µL of the OPA solution, and the composition of the solution was analyzed with HPLC. The final ratio of the concentrations of the sample to the internal standard solution can be described as:

$$\frac{C_{s3}}{C_{i3}} = \frac{C_{s2}}{C_{i2}} = \frac{C_{s1}}{C_{i1}} = \frac{C_{s0} \cdot (M_s - M_i)}{C_{i0} \cdot (M_i - M_e)} = k_{s,i} \frac{A_s}{A_i} \tag{3-13}$$

Therefore, the concentration of the sample, C_{s0}, is:

$$C_{s0} = k_{s,i} \frac{A_s}{A_i} \frac{(M_i - M_e)}{(M_s - M_i)} C_{i0} = R_{s,i} \frac{m_i}{m_s}$$

$$\text{where } R_{s,i} = k_{s,i} \frac{A_s}{A_i}, \quad m_i = M_i - M_e, \quad m_s = M_s - M_i \tag{3-14}$$

To take into account the contamination of the L-VAL crystals with the L-LEU, equation (3-14) was corrected. In this correction, it was assumed that all the L-LEU molecules contained in the L-VAL crystals always dissolve in water:

For L-VAL and L-ILE with L-LEU (internal standard):

$$C_{VAL,0} = \frac{R_{VAL,LEU} \cdot C_{i,0} \cdot m_i}{(1 - \frac{0.03}{1 - 0.03} \cdot R) \cdot m_s} \tag{3-15}$$

$$C_{ILE,0} = R_{ILE,LEU} \cdot (C_{i,0} \cdot m_i + C_{VAL,0} \cdot \frac{0.03}{1 - 0.03} m_s) \cdot \frac{1}{m_s} \tag{3-16}$$

For L-ILE and L-LEU with L-VAL (internal standard):

$$C_{ILE,0} = R_{ILE,VAL} \cdot C_{i0} \cdot \frac{m_i}{m_s} \cdot (1 - 0.03) \qquad\qquad (3\text{-}17)$$

$$C_{ILE,0} = C_{i0} \cdot \frac{m_i}{m_s} \cdot \left[R_{LEU,VAL} - (1 + R_{LEU,VAL}) \cdot 0.03 \right] \qquad (3\text{-}18)$$
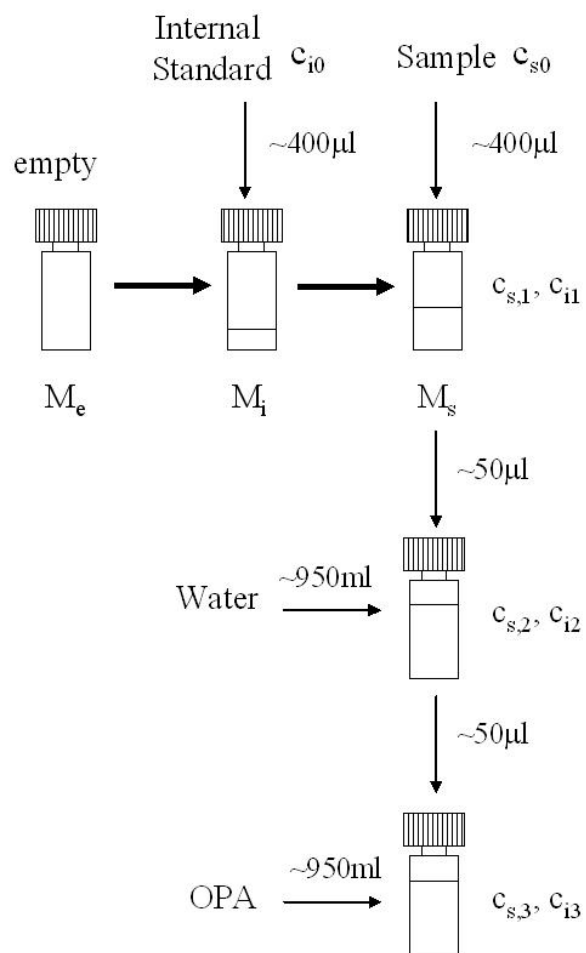
Figure 3-4 Analysis of the samples

3.2   Structural Analysis of Crystals

There are two techniques to analyze crystal structure using X-ray diffractometry: single-crystal XRD and powder XRD. Single-crystal XRD is a powerful tool to determine the position of atoms in crystals; however, it generally requres large sample dimensions of single crystals (> 50 μm) to yield distinctive intensity of reflected signals. In this study, single-crystal XRD was not conducted since small and homogeneous crystals of amino acids were intentionally produced from low-concentration solutions to assure equilibrium between crystals and mother liquor. Furthermore, the amino acid crystals tend to exhibit flake- or needle-like morphology (Torii and Iitaka, 1970, 1971), and they are easy to break by mechanical agitation during recrystallization. Therefore, solid samples were analyzed using a powder XRD module to yield the information on change in crystal structure with its composition. The apparatus used in the experiment is described, and the diffraction patterns of the pure amino acid crystals are presented in the following sections.

3.2.1   Apparatus and Procedures

A Scintag XDS-2000 (Scintag, Sunnyvale, CA) X-ray diffraction module equipped with a Cu Kα radiation source (wavelength = 1.54184 Å) was used in this work. Scintag software (DMSNT Version 1.37) was used to convert signals to diffraction patterns. At the beginning of the experiment, sample crystals were packed on a stainless-steal sample holder taking care to remove any preferred orientations of the crystals for accurate crystal structure determination in XRD analysis (Campbell-Roberts *et al.*, 2002).

Since the amino acid crystals have either flake- or needle-like morphology, a side-packing method was adopted in this research. In this method, the sample crystals were first ground to reduce crystal size, and the ground particles were poured in a gap of two flat-plate sample holders (side-loading). Figure 3-5 shows an example of the powder XRD patterns of pure L-VAL crystals obtained in this method. This result shows that the peak intensity exceeded the limit of the detector, resulting in an artificial peak split. In order to avoid this splitting, the current of the radiation source was reduced from typical 30.0 mA to 15.0 mA in all the measurements. The settings are summarized in Appendix B.
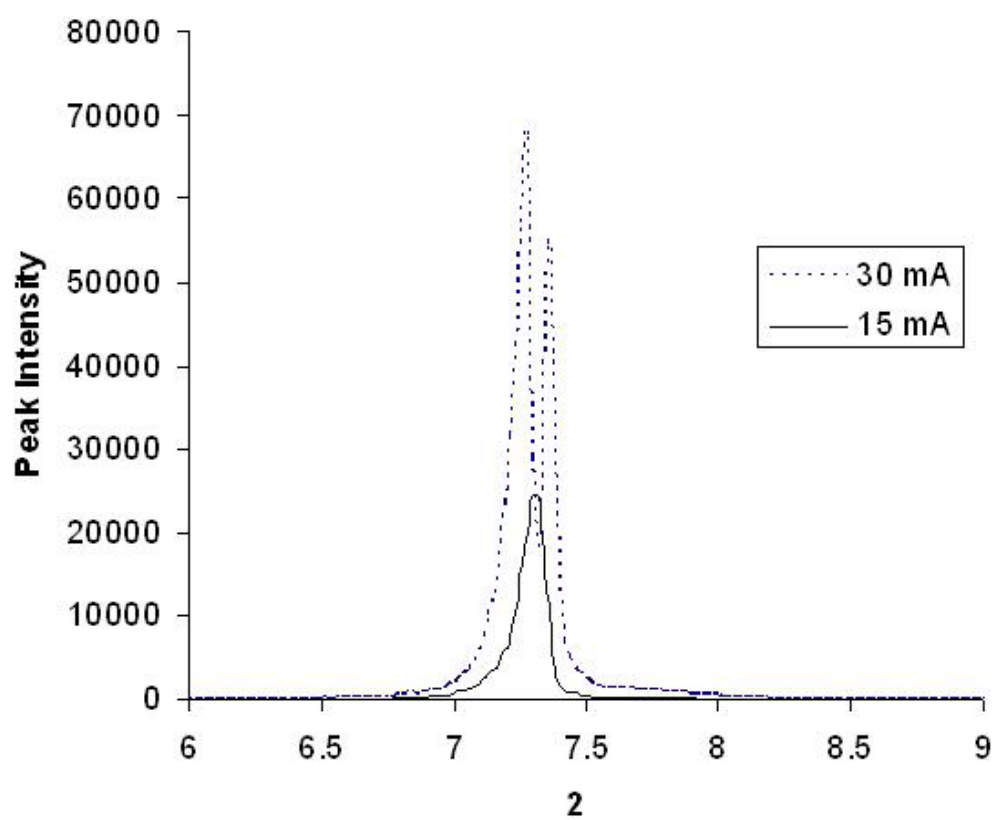
Figure 3-5 Peak splitting in the diffraction pattern of L-VAL pure crystals due to preferred orientation.

3.2.2 Analysis of XRD Diffraction Patterns

The peak intensity in XRD patterns has been used to calculate a structure factor
that is related to the position of each atom in the crystal lattices. However, its absolute
value is affected strongly by preferential ordering mentioned in the previous section. This
ordering effect was actually observed in this study as shown in Figures 3-6, 3-7, and 3-8
that are the diffraction patterns of pure L-LEU, L-ILE, and L-VAL crystals, respectively.
The crystal structure was therefore speculated by an alternative way using the position of
the first peaks in diffraction patterns described below.

According to single-crystal XRD measurements, pure crystals of the amino acids
studied in this work are monoclinic (Torii and Iitaka, 1970 and 1971), and belong to the
same space group, $P2_1$ (Torii and Iitaka, 1971). A schematic diagram of the monoclinic
unit cell is shown in Figure 3-9. The relationship between the measured peak angle, θ,
and d-spacing of the corresponding face can be written as:

$$ d = \frac{n\lambda}{2\sin\theta} \tag{3-19} $$

where λ is the wavelength of the radiation source, and n is an integer. If a crystal belongs
to the monoclinic space group, the d-spacing of a face (hkl) is expressed as a function of
cell parameters as follows:

$$ \frac{1}{d^2} = \frac{1}{\sin^2\beta}\left(\frac{h^2}{a^2} + \frac{k^2}{b^2} + \frac{l^2}{c^2} - \frac{2hl\cos\beta}{ac}\right) \tag{3-20} $$

According to the single-crystal XRD measurements (Torii and Iitaka, 1970, 1971),
the first peak in the powder XRD patterns corresponds to the crystal face (001). This

indicates that the first peak corresponds to the c-axis length in a unit cell. Thus, the d-spacing of the first peak can be represented by:

$$\frac{1}{d^2} = \frac{1}{\sin^2 \beta} \frac{l^2}{c^2} \propto \frac{l^2}{c^2} \qquad (3\text{-}21)$$

In order to investigate differences in the crystal structure, the first peak corresponding to the crystal face (001) or c-axis length is used for simplicity. Figure 3-10 shows a schematic diagram of the crystal structure of pure L-ILE crystals along the b axis. It can be seen that the smallest constituent in a layer is made of four molecules connected by hydrogen bonds, and aliphatic groups between layers lie along to the c-axis. The structures of L-LEU, L-ILE, and L-VAL molecules differ only by the length of the aliphatic side-groups. Therefore, as the size of the alkyl group increases, the unit cell constant along the c-axis also increases, which is reflected in a decrease in the first peak angle. In other words, the first peak position shifts toward a higher angle as the size of the aliphatic group decreases. This is shown in Figure 3-11 where the intensity counts are normalized by the maximum intensity in each diffraction pattern.

If crystals of solid solutions belong to the same space group as the pure amino acids, the length of c-axis in the unit cell would also change with the composition of the solids. This assumption has also been proposed by several investigators (Blasdale, 1927; Yoshimura *et al.*, 1997; Abel *et al.*, 1999; Chae *et al.*, 2003, Suda, *et al.*, 2002) in the XRD study of solid solutions of metal oxides. This assumption allows one to calculate unit cell constants simply from powder diffraction patterns.

The unit cell constants of pure crystals of the amino acids studied in this work were reported in the literature and tabulated in Table 3-2. The position of the first peak and the corresponding d-spacing were determined using PowderX

(http://www.ccp14.ac.uk/tutorial/powderx/index.html) which is a graphical powder

diffraction analysis program and freely available for academic and non-commercial use.

For comparison, the first peak position was also estimated by a CMPR program

developed by Toby (2000). This program can simulate a powder XRD pattern from a set

of unit cell constants, for example, from those determined by single-crystal XRD

measurements (Koolman, 1992; Torii and Iitaka, 1970, 1971). The d-spacing values of

the pure amino acid crystals are tabulated in Table 3-3, in which the d-spacing values

estimated in this work are consistent with those reported in the literature.

Additionally, as a measure of crystal uniformity, full-width-at-half-maximum

(FWHM) of the first peaks was also calculated by PowderX. The broadening of FWHM

is caused mainly by the crystall size distribution and atomic level distortion in the solids

(Chae *et al*., 2003).
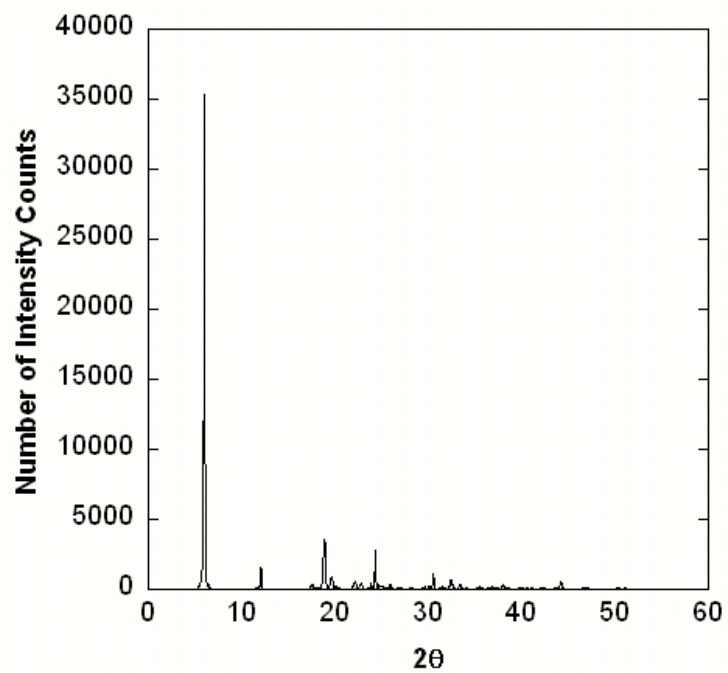
Figure 3-6 X-ray diffraction patterns of pure L-LEU crystals.
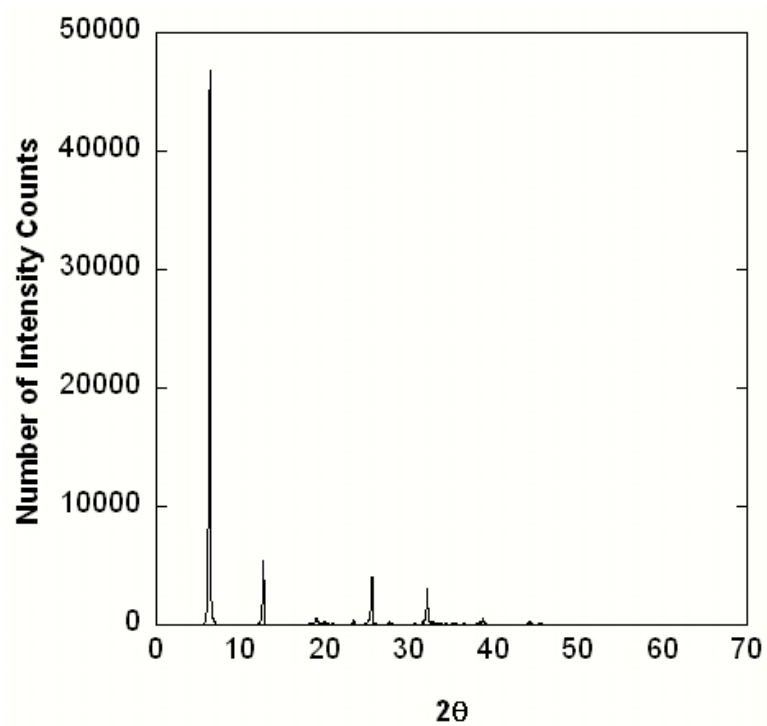
Figure 3-7 X-ray diffraction patterns of pure L-ILE crystals.
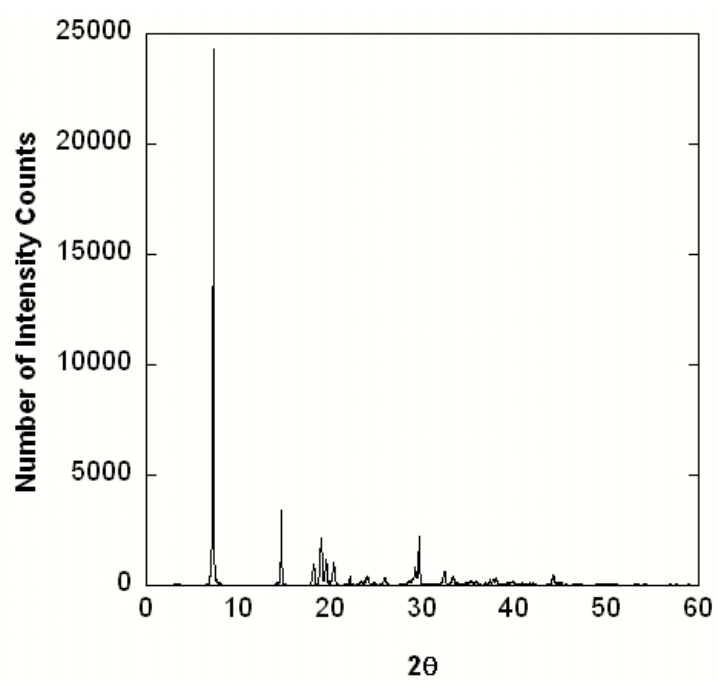
Figure 3-8 X-ray diffraction patterns of pure L-VAL crystals.
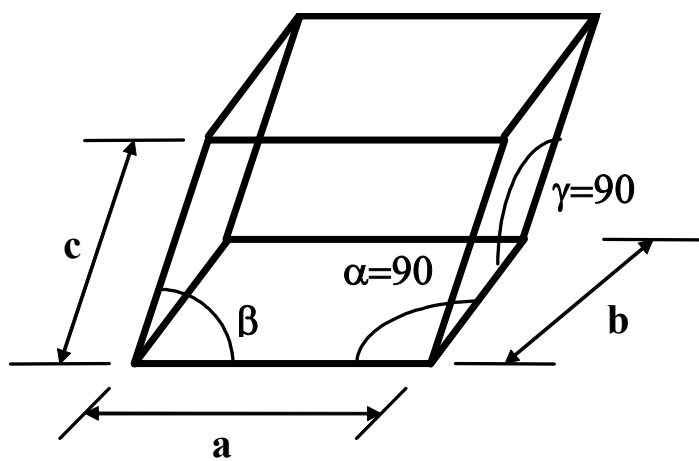
Figure 3-9 Dimensions of monoclinic unit cell.
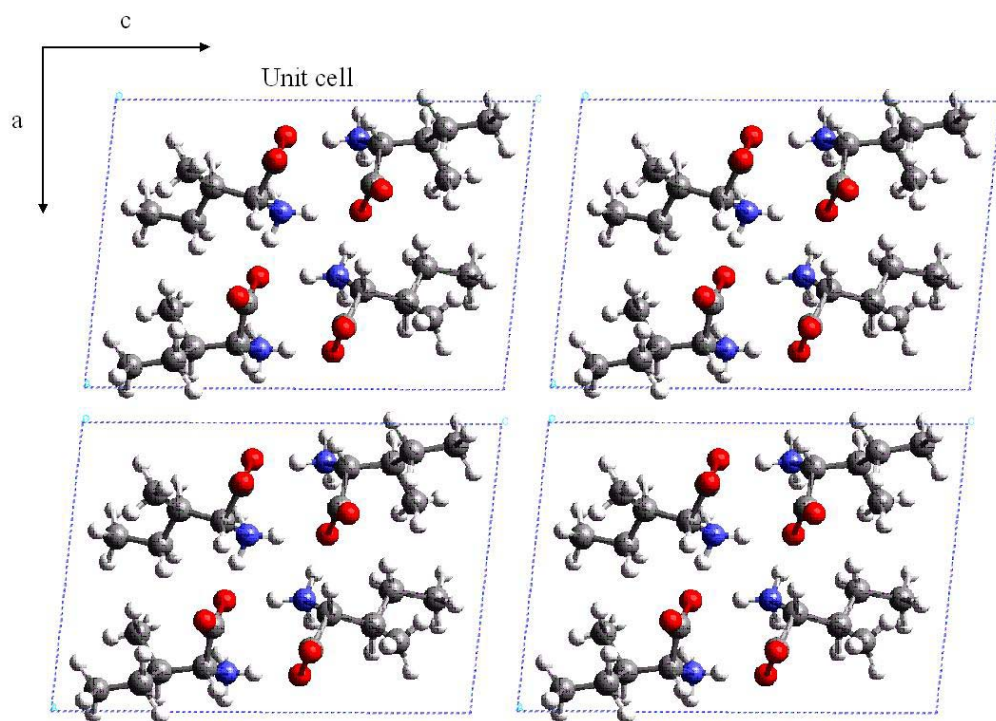
Figure 3-10 Crystal structure of L-ILE. Black, white, red, and blue dots represent carbon, hydrogen, oxygen, and nitrogen atoms, respectively.
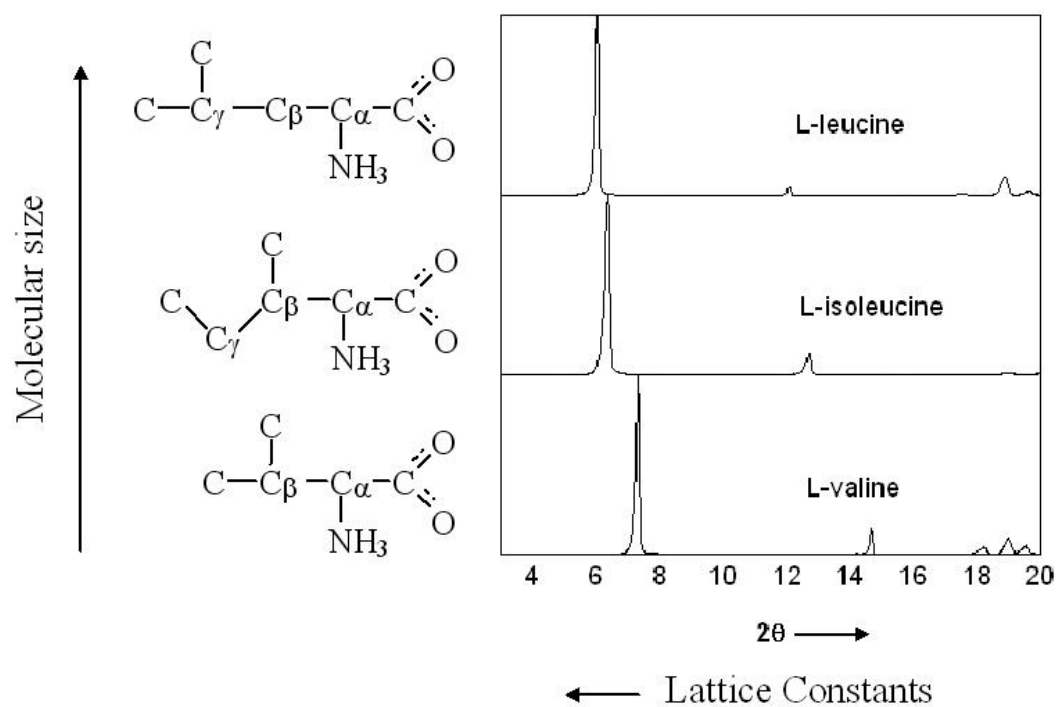
Figure 3-11 Diffraction patterns of pure L-LEU, L-ILE and L-VAL crystals. The position of the first peak corresponds to the length of c-axis in a unit cell.

Table 3-2 Unit cell constants from single X-ray diffraction measurements (Torii and Iitaka, 1970, 1971; [*]Koolman, 1992).

Unit Cell Dimension	L-LEU	L-ILE		L-VAL
a [Å]	9.63	9.75	9.71[*]	9.71
b [Å]	5.33	5.32	5.29[*]	5.27
c [Å]	14.62	14.12	14.02[*]	12.06
β [º]	93.9	95.8	95.8[*]	90.8

Table 3-3 The d-spacing values calculated from unit cell constants and estimated from powder diffraction patterns of L-ILE, L-LEU, and L-VAL crystals.

	L-LEU [Å]	L-ILE [Å]	L-VAL [Å]
Estimated (This study)	14.59	13.92	12.06
Calculated (Torii et al., 1971)	14.67	14.04	12.10
Calculated (Koolman, 1992)	–	13.94	–
Estimated (Khawas, 1970)	–	14.13	–

CHAPTER 4

RESULTS AND DISCUSSION

Solid-liquid equilibria of amino acids in water are presented in this chapter. The measurements were conducted as described in Chapter 3; firstly, the solubilities of single amino acids in water were obtained in order to confirm the validity of experimental procedures. Secondly, the solubilities of pairs of amino acids in water were measured using the isothermal and cooling methods. Finally, structural analysis of crystals obtained through recrystallization was carried out using powder X-ray diffractometry in order to correlate the change in crystal structure with equilibrium compositions.

4.1 Solubility of One Amino Acid in Water

The solubility of each chiraly pure amino acid (L-ILE, L-LEU and L-VAL) in water was measured to validate the experimental procedure by comparison with literature data. The experimental data are listed in Table 4-1, and plotted in Figures 4-1, 4-2 and 4-3 for L-ILE, L-LEU, and L-VAL, respectively. Each figure also includes the corresponding literature data. The solubility data are in good agreement with the literature values, except for the data on L-VAL reported by Dalton and Schmidt (1935). The deviation in this data set could be due to experimental errors or insufficient optical

and chemical purity in their samples. For example, contamination of D-valine in L-VAL would increase the solubility because the solubility of DL-valine in water is much larger than L-VAL (Pradhan and Vera, 1998).

Table 4-1 Solubility of L-ILE, L-LEU, and L-VAL in pure water.

Temperature[K]	L-ILE [g/kg water]	L-LEU [g/kg water]	L-VAL [g/kg water]
292			58.05
293	32.04	21.19	
298	33.24	21.61	
301			61.09
303	34.21	21.96	
311			64.94
313	37.09	23.72	
321			69.64
323	40.89	26.00	
331			77.12
333	44.26	29.31	
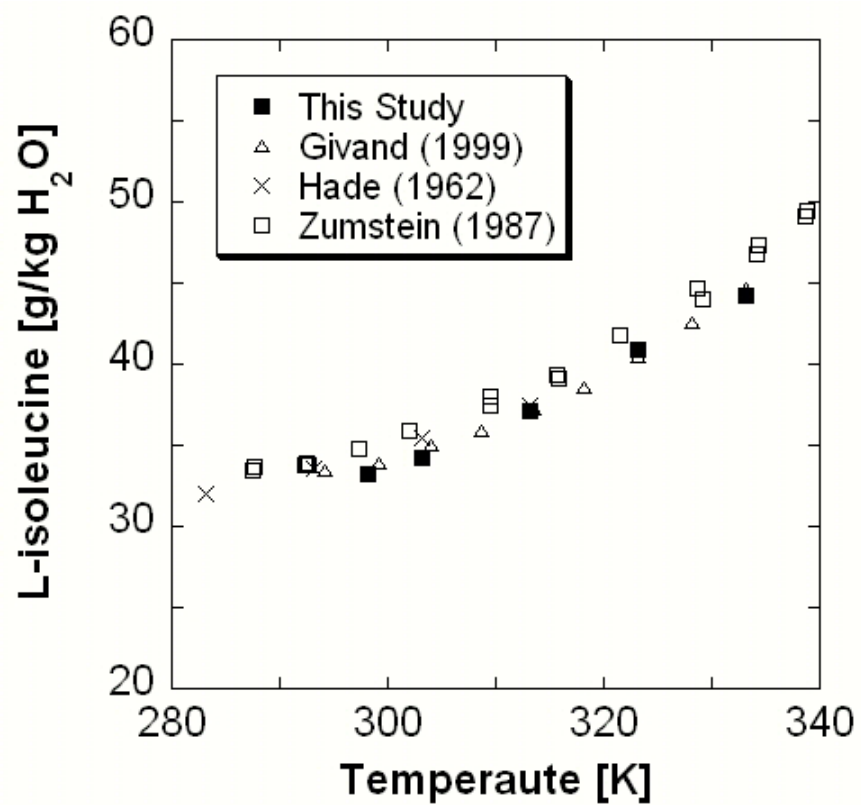
Figure 4-1 Solubility of L-ILE in water. Data of ■ this work; ∆Givand (1999a); × Hade (1962); and □ Zumstein (1987).
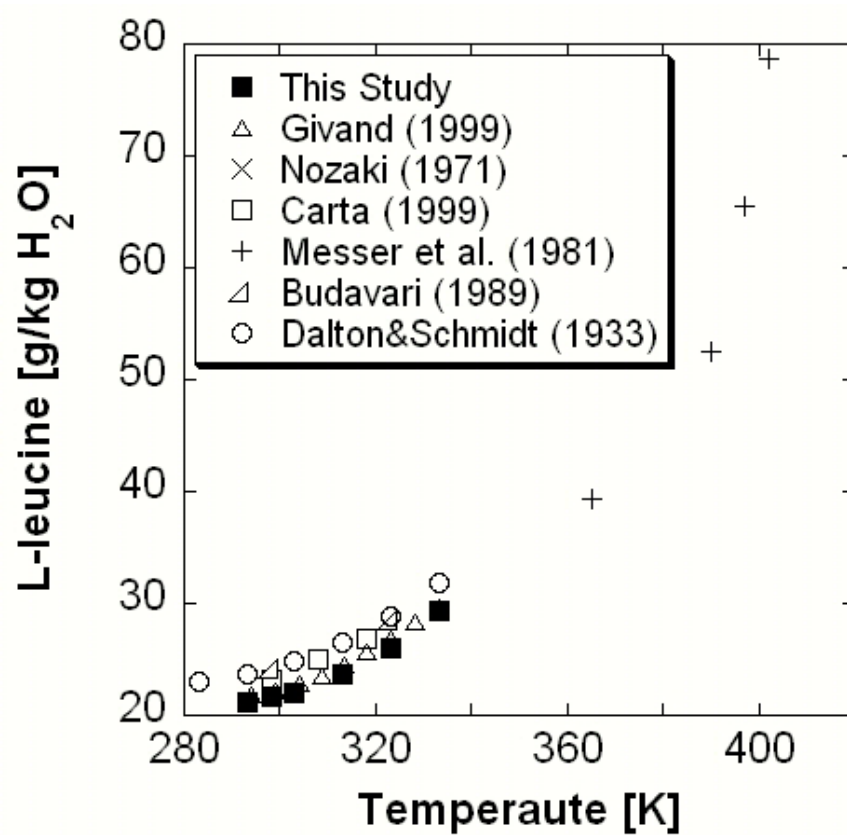
Figure 4-2 Solubility of L-LEU in water. Data of ■ this work; △ Givand (1999a); × Nozaki and Tanford (1971); □ Carta (1999); + Messer et al. (1981); ⊿Budavari (1989); and ○ Dalton and Schmidt (1933).
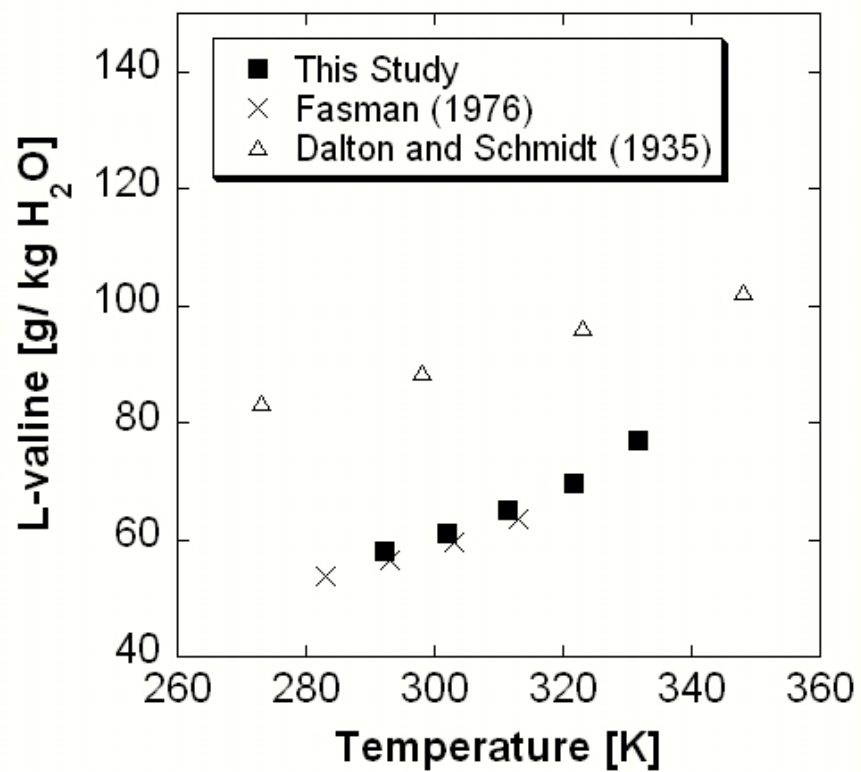
Figure 4-3 Solubility of L-VAL in water. Data of ■ this work; × Fasman (1976); and △ Dalton and Schmidt (1935).

4.2   Solubility of Two Amino Acids in Water

Solubility data in ternary systems (two amino acids in water) were measured using the isothermal and cooling methods as described in Chapter 3. The experimental data of the L-ILE + L-LEU + water system are listed in Tables 4-2 and 4-3. Figures 4-4 and 4-5 show the phase behavior obtained by the isothermal and cooling methods, respectively.

In Figure 4-4, only the liquid composition is plotted since the solid composition was not measured in the isothermal method. This method relies on the assumption that solids are pure, and therefore assumes equilibrium to have been established when no more pure seed crystals will dissolve. The initial composition plotted on the axes is connected to the equilibrium composition in order to visualize the transition of the liquid composition. It can be seen that the lines between the initial and equilibrium compositions are neither parallel nor normal to the axes, indicating that a minor component is recrystallized during the experiments.

The upper figure in Figure 4-5 shows the whole phase diagram including both solid and liquid compositions at equilibrium. The lower figure is an enlargement of the liquid region in the upper figure. The open and closed symbols denote mole fractions at initial and equilibrium conditions, respectively, and the solid lines correspond to tie lines connecting the equilibrated solid and liquid compositions. It can be seen in the figure that all of the tie lines pass through or near the corresponding initial compositions, indicating that mass balances are satisfied within experimental error. Moreover, the formation of solid solutions is suggested by the absence of a distinct eutonic point and the continuous change in the liquid composition with the solid composition.

Table 4-2 Initial and equilibrium compositions of amino acids in L-ILE + L-LEU + water systems obtained by the isothermal method

(Unsaturated L-ILE solution + L-LEU pure crystals)

Vessel #	Initial [mol/mol] $\times 10^3$		Equilibrium [mol/mol] $\times 10^3$	
	L-ILE	L-LEU	L-ILE	L-LEU
IL_I1	0.47	0.02	0.45	3.03
IL_I2	0.93	0.01	0.92	2.97
IL_I3	1.34	0.01	1.34	2.94
IL_I4	1.86	0.02	1.82	2.82
IL_I5	2.75	0.02	2.53	2.49
IL_I6	3.64	0.02	2.78	2.32
IL_I7	4.53	0.02	2.75	2.24

(Unsaturated L-LEU solution + L-ILE pure crystals)

Vessel #	Initial [mol/mol] $\times 10^3$		Equilibrium [mol/mol] $\times 10^3$	
	L-ILE	L-LEU	L-ILE	L-LEU
LI_I1	0.00	0.30	4.57	0.31
LI_I2	0.00	0.56	4.57	0.57
LI_I3	0.00	0.89	4.35	0.73
LI_I4	0.01	1.26	4.13	1.03
LI_I5	0.01	1.85	3.98	1.16
LI_I6	0.00	2.40	3.41	1.77
LI_I7	0.00	3.12	3.38	1.70
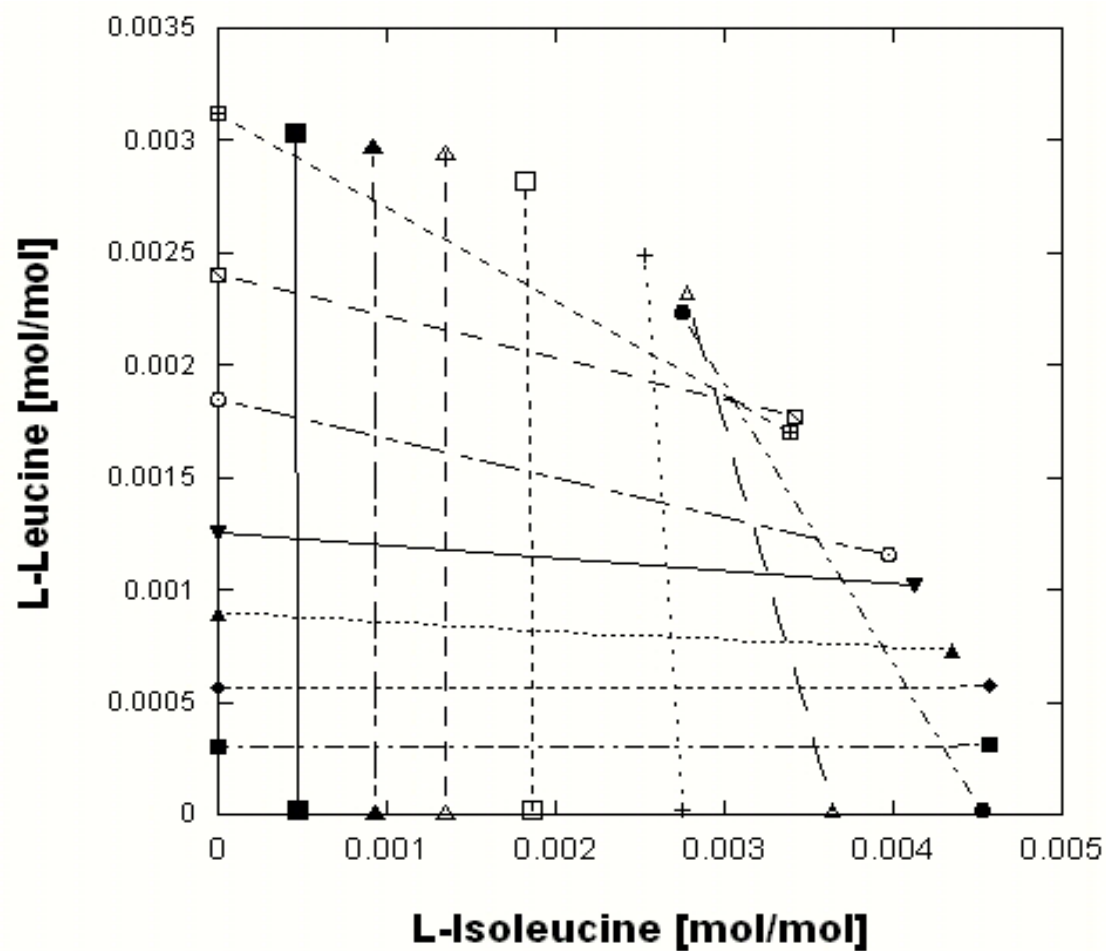
Figure 4-4 Initial and final liquid compositions in the L-ILE + L-LEU + water system in isothermal experiments. The data points on the axis are compositions at initial conditions, and each of the points is connected to the corresponding equilibrium composition with a line.

Table 4-3 Initial and equilibrium compositions of amino acids in L-ILE + L-LEU + water systems obtained by the cooling method

Vessel#	Initial [mol/mol] × 10³			Equilibrium at 298 K			
				Liquid [mol/mol] × 10³		Solid [mol/mol]	
	Temp to dissolve all crystals [K]	L-ILE	L-LEU	L-ILE	L-LEU	L-ILE	L-LEU
IL_C1	353	0.55	3.62	0.48	3.10	0.02	0.98
IL_C2	353	0.99	3.71	0.95	3.02	0.09	0.91
IL_C3	353	1.71	3.61	1.49	2.84	0.15	0.85
IL_C4	348	2.07	3.23	1.97	2.67	0.23	0.77
IL_C5	353	3.52	3.52	2.68	2.27	0.40	0.60
IL_C6	348	4.10	2.78	3.01	1.89	0.54	0.46
IL_C7	353	4.91	2.04	3.55	1.44	0.66	0.34
IL_C8	353	5.35	1.31	4.02	0.96	0.77	0.23
IL_C9	353	5.71	0.62	4.52	0.48	0.86	0.14
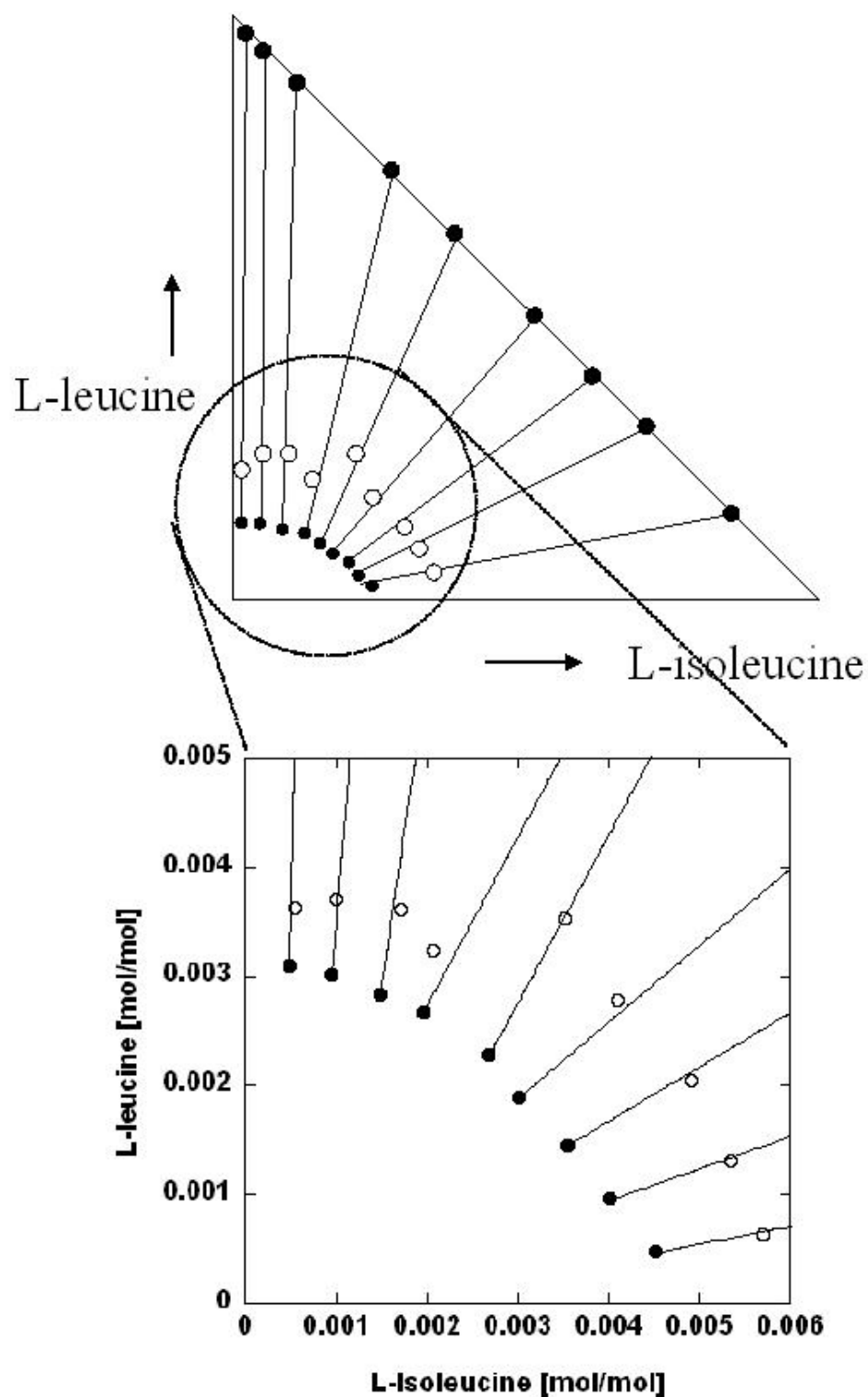
Figure 4-5 Initial and equilibrium composition of L-ILE + L-LEU + water systems obtained by the cooling method. The closed symbols denote mole fractions of liquid- and solid-phases at equilibrium. The open symbols denote mole fractions at initial conditions. Solid lines are tie lines connecting the solid- and liquid- compositions at equilibrium.

Figures 4-6, 4-7, and 4-8 show comparisons of the final (equilibrium) liquid compositions obtained by the isothermal and cooling methods in L-ILE + L-LEU + water, L-ILE + L-VAL + water, and L-LEU + L-VAL + water, respectively. The experimental data for L-ILE + L-VAL + water obtained by the cooling method and isothermal method are listed in Tables 4-4 and 4-5, and for L-LEU + L-VAL + water in Tables 4-6 and 4-7, respectively.

In the L-ILE + L-LEU + water system, all the data lie on a single continuous curve, regardless of the experimental method. In the other systems, on the other hand, the behavior of liquidus curves depends clearly on the experimental methods used to obtain the data. This can be seen in the phase diagrams shown in Figures 4-9 and 4-10 for L-ILE + L-VAL + water and L-LEU + L-VAL + water systems, respectively. The figures indicate that solid solutions are formed only by the cooling method, and that a minor component is not recrystallized by the isothermal method except a few points where the concentration of the minor component is about at saturation. The information on crystal structure would impart evidence on what happens during recrystallization when coupled with the composition analysis. Therefore, the structural analysis of the crystals was also carried out in order to complement the liquidus data.
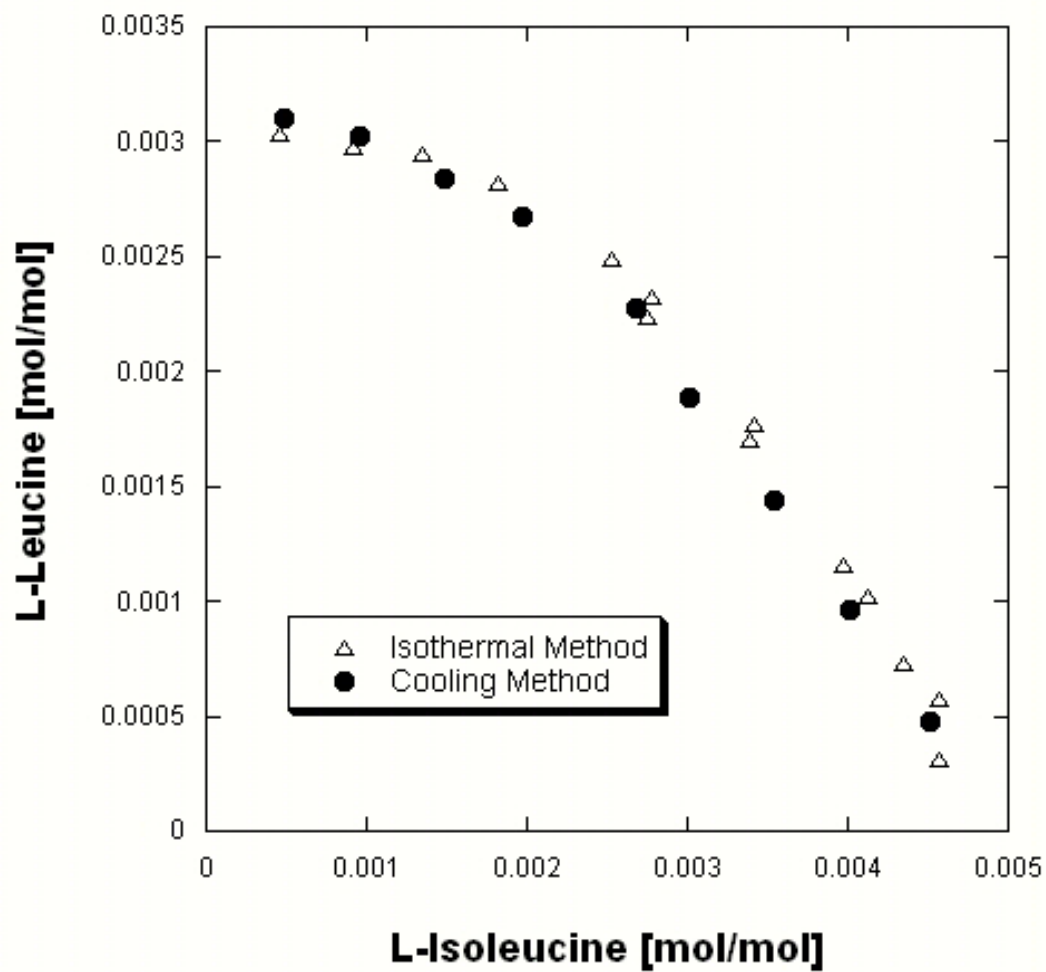
Figure 4-6 Comparison of the equilibrium liquid compositions of amino acids in L-ILE + L-LEU + water systems obtained by two experimental methods
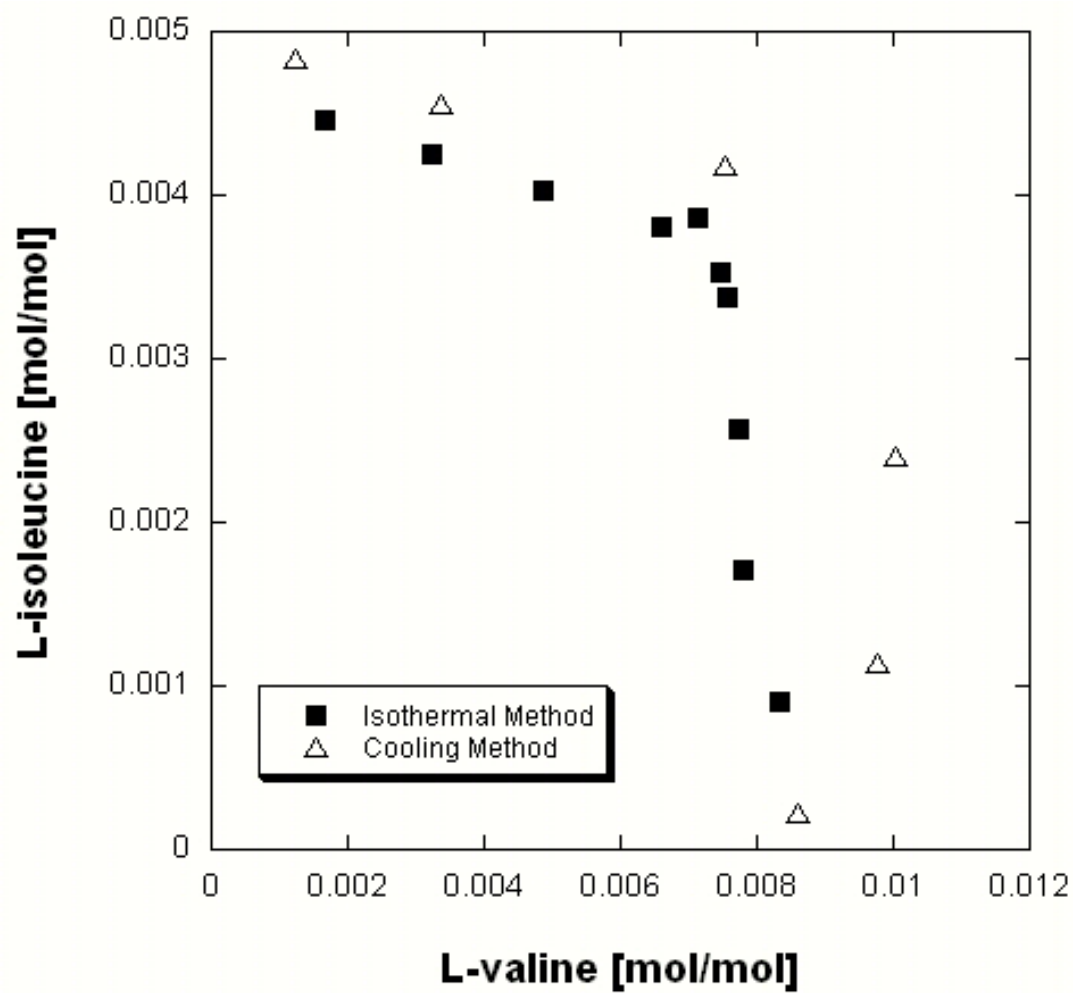
Figure 4-7 Comparison of the equilibrium liquid compositions of amino acids in L-ILE + L-VAL + water systems obtained by two experimental methods
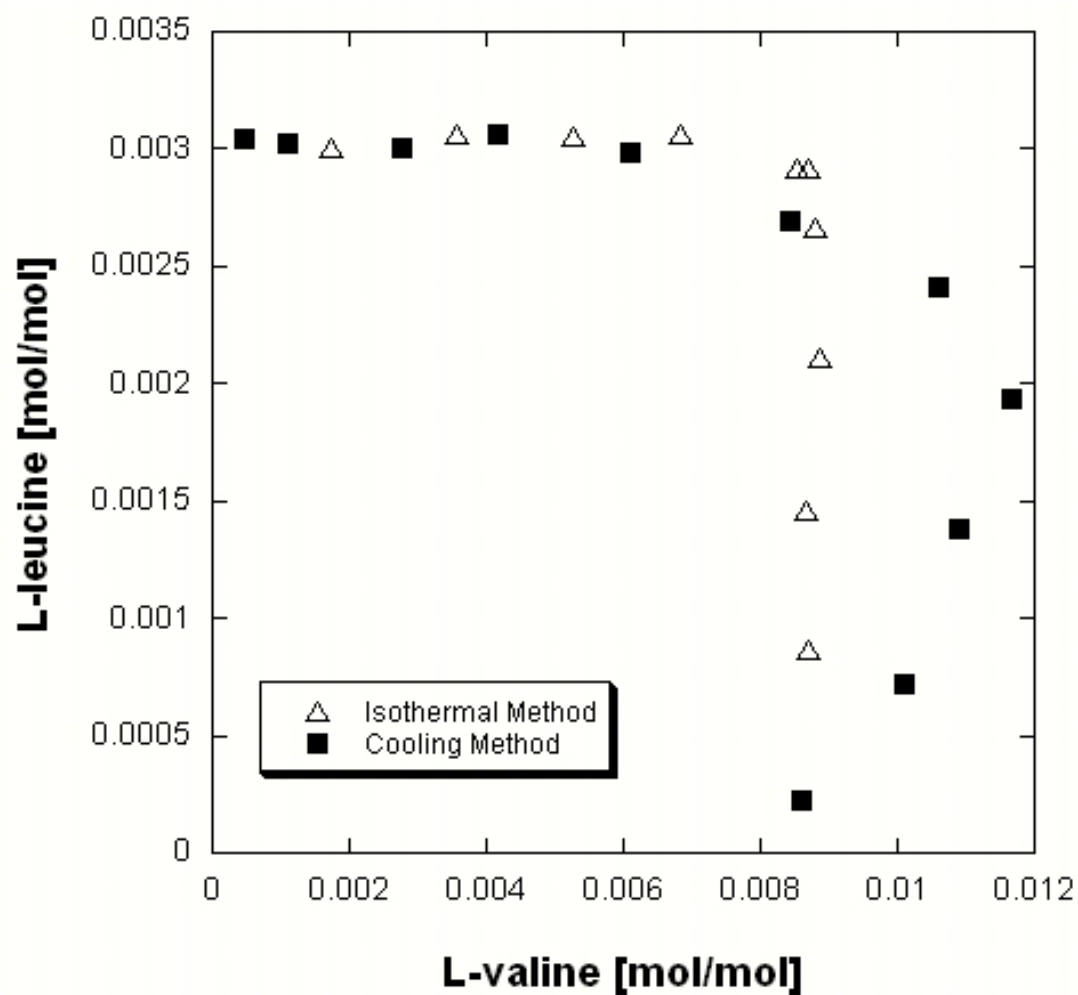
Figure 4-8 Comparison of the equilibrium liquid compositions of amino acids in L-LEU + L-VAL + water systems obtained by two experimental methods

Table 4-4 Initial and equilibrium compositions in L-VAL + L-ILE + water systems obtained by the isothermal method.

(Unsaturated L-ILE solution + L-VAL pure crystals)

Vessel #	Initial		Equilibrium	
	L-VAL	L-ILE	L-VAL	L-ILE
	[mol/mol] x 10^3	[mol/mol] x 10^3	[mol/mol] x 10^3	[mol/mol] x 10^3
IV_I1	0.00	0.94	8.33	0.91
IV_I2	0.00	1.90	7.80	1.70
IV_I3	0.00	2.74	7.73	2.57
IV_I4	0.00	3.60	7.56	3.37
IV_I5	0.00	4.47	7.13	3.86

(Unsaturated L-VAL + L-ILE pure crystals)

Vessel #	Initial		Equilibrium	
	L-VAL	L-ILE	L-VAL	L-ILE
	[mol/mol] x 10^3	[mol/mol] x 10^3	[mol/mol] x 10^3	[mol/mol] x 10^3
VI_I1	1.77	0.00	1.68	4.46
VI_I2	3.42	0.00	3.23	4.26
VI_I3	5.03	0.00	4.86	4.03
VI_I4	6.73	0.00	6.59	3.81
VI_I5	8.27	0.00	7.46	3.53

Table 4-5 Initial and equilibrium compositions of amino acids in L-VAL + L-ILE + water systems obtained by the cooling method.

Vessel#	Initial [mol/mol] $\times 10^2$			Equilibrium at 298 K			
				Liquid Phase [mol/mol] $\times 10^2$		Solid Phase [mol/mol]	
	Temp [K]	L-VAL	L-ILE	L-VAL	L-ILE	L-VAL	L-ILE
VI_C1	353	1.21	0.14	0.98	0.11	0.89	0.11
VI_C2	360	1.20	0.32	1.00	0.24	0.72	0.28
VI_C3	359	0.87	0.64	0.75	0.42	0.42	0.58
VI_C4	353	0.35	0.60	0.34	0.46	0.11	0.89
VI_C5	359	0.12	0.57	0.12	0.48	0.05	0.95

Table 4-6 Initial and equilibrium compositions of amino acids in L-VAL + L-LEU + water systems obtained by the isothermal method.

(Unsaturated L-VAL solution + L-LEU pure seed crystals)

Vessel #	Initial [mol/mol] x 10³		Equilibrium [mol/mol] x 10³	
	L-VAL	L-LEU	L-VAL	L-LEU
VL_I1	1.72	0.05	1.73	3.00
VL_I2	3.50	0.10	3.57	3.06
VL_I3	5.26	0.16	5.27	3.05
VL_I4	6.78	0.21	6.85	3.06
VL_I5	8.69	0.26	8.69	2.92

(Unsaturated L-LEU solution + L-VAL pure seed crystals)

Vessel #	Initial [mol/mol] x 10³		Equilibrium [mol/mol] x 10³	
	L-VAL	L-LEU	L-VAL	L-LEU
LV_I1	0.00	0.61	8.71	0.87
LV_I2	0.00	1.21	8.68	1.46
LV_I3	0.00	1.84	8.86	2.11
LV_I4	0.00	2.41	8.81	2.66
LV_I5	0.00	2.99	8.54	2.92

Table 4-7 Initial and equilibrium compositions of amino acids in L-VAL + L-LEU + water system obtained by the cooling method.

				Equilibrium			
	Initial [mol/mol] ×10²			Liquid Phase [mol/mol] ×10²		Solid Phase [mol/mol]	
Vessel#	Temp [K]	L-VAL	L-LEU	L-VAL	L-LEU	L-VAL	L-LEU
VL_C1	353	1.32	0.03	0.86	0.02	-	-
VL_C1	360	1.37	0.10	1.01	0.07	-	-
VL_C1	366	1.34	0.17	1.09	0.14	0.87	0.13
VL_C1	366	1.32	0.26	1.17	0.19	0.72	0.28
VL_C1	358	1.10	0.30	1.06	0.24	0.45	0.55
VL_C1	353	0.87	0.39	0.84	0.27	0.23	0.77
VL_C1	353	0.63	0.44	0.61	0.30	0.15	0.85
VL_C1	353	0.43	0.44	0.42	0.31	0.08	0.92
VL_C1	353	0.28	0.45	0.28	0.30	0.05	0.95
VL_C1	358	0.11	0.49	0.11	0.30	0.02	0.98
VL_C1	353	0.04	0.44	0.05	0.30	0.01	0.99
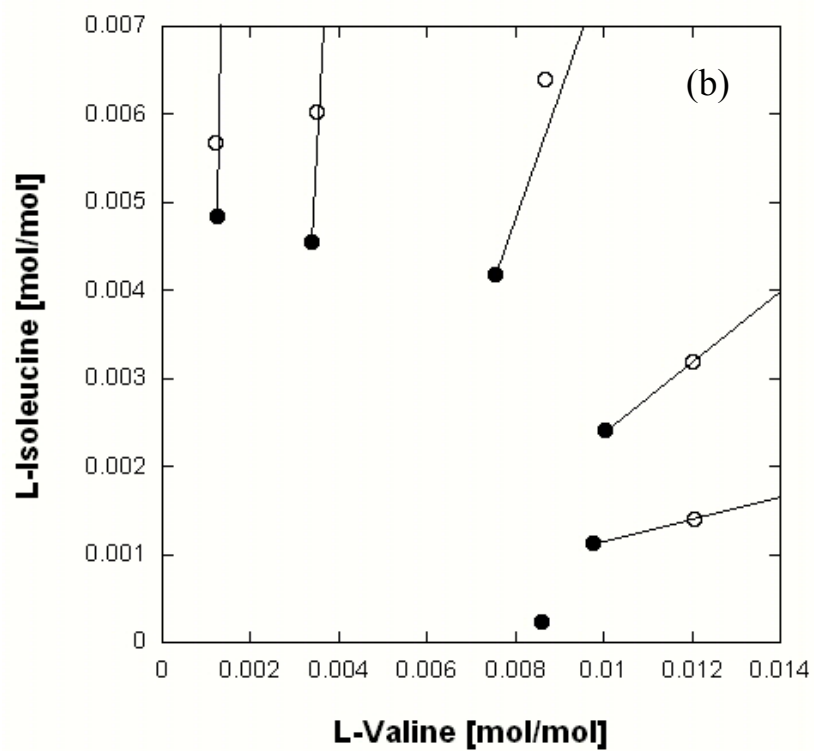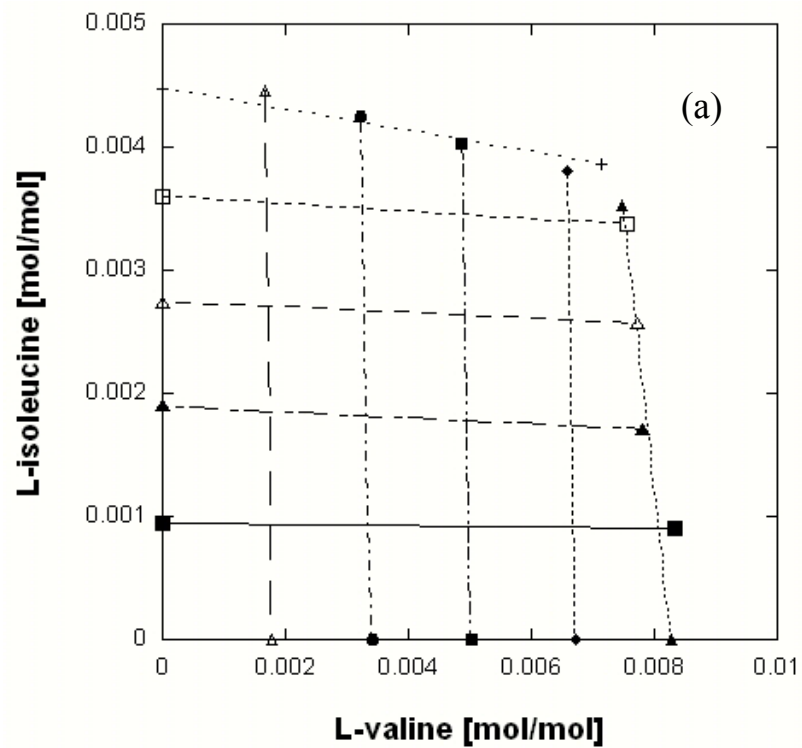
Figure 4-9 Initial and equilibrium composition of L-ILE + L-VAL + water systems obtained by (a) the isothermal method and (b) the cooling method.
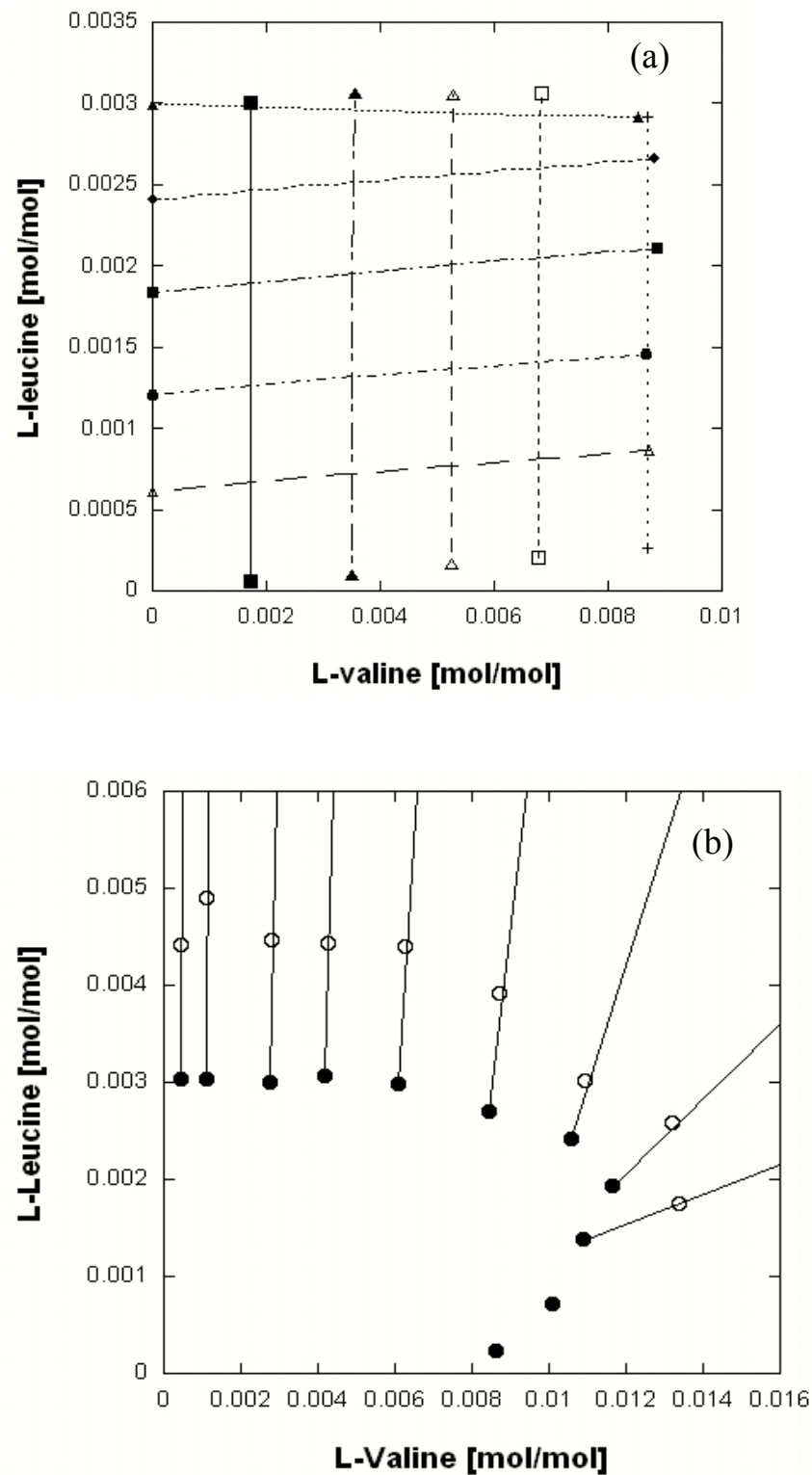
Figure 4-10 Initial and equilibrium composition of L-LEU + L-VAL + water systems obtained by (a) the isothermal method (b) the cooling method.

4.3   **Analysis of Crystal Structure**

a) Cooling Experiments

Figures 4-11, 4-12, and 4-13 show powder XRD diffraction patterns of crystals around the first peak position for the three pairs. The sample name, peak position, FWHM, and calculated d-spacing of the peak are listed in Tables 4-8, 4-9, and 4-10. It can be seen in the figures that the position of the first peak shifts with composition, and that the patterns are not superposition of patterns of pure crystals. A diffraction pattern of mixed crystals of two amino acids (pure L-LEU and pure L-VAL) was shown in Figure 4-13 as a reference. It is evident that the solids do not contain pure crystals. The d-spacing with the solid composition will be discussed further in Chapter 5.
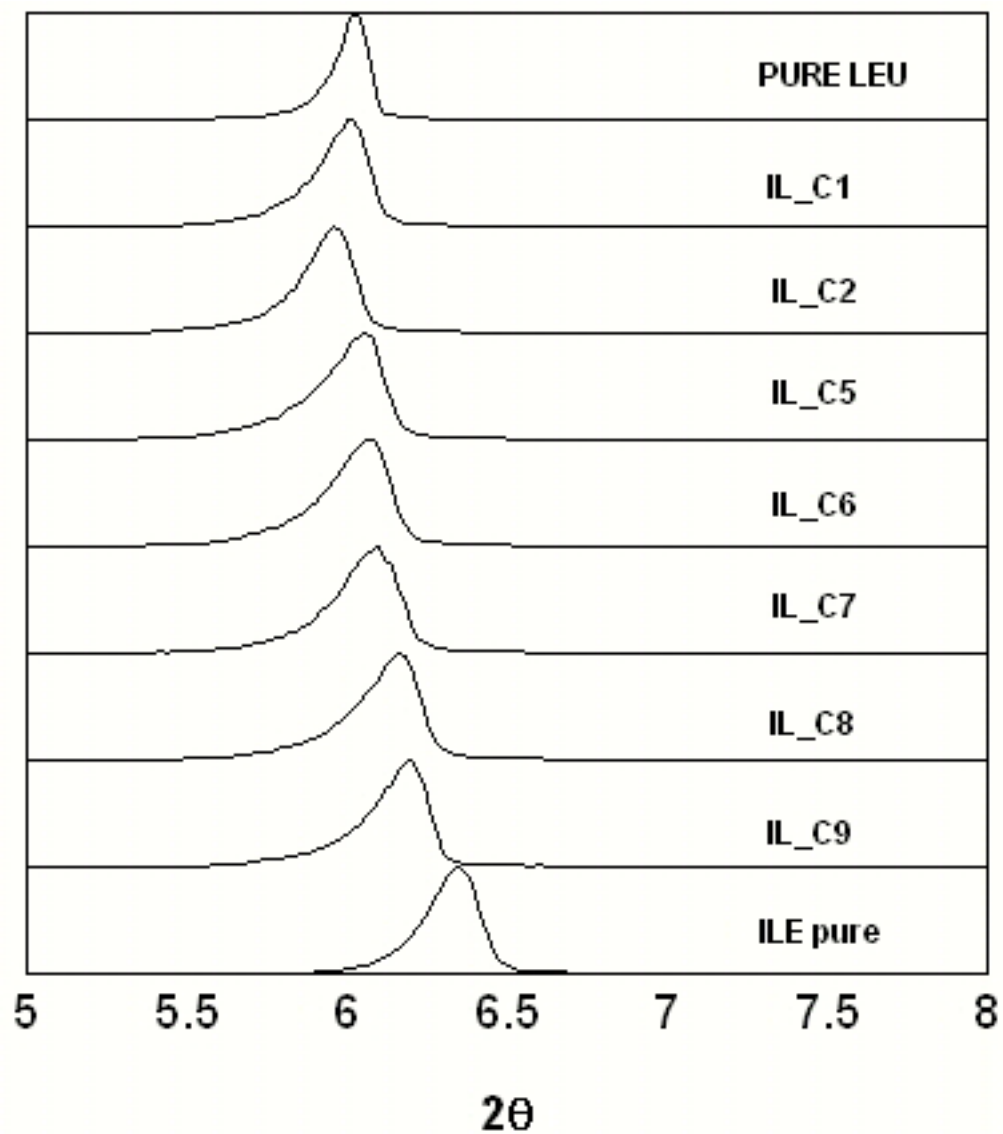
Figure 4-11 Powder XRD patterns of the crystals of L-ILE + L-LEU + water systems obtained by the cooling method (IL_C# is the sample name). The liquid- and solid-phase compositions of the corresponding samples are tabulated in Table 4-3.
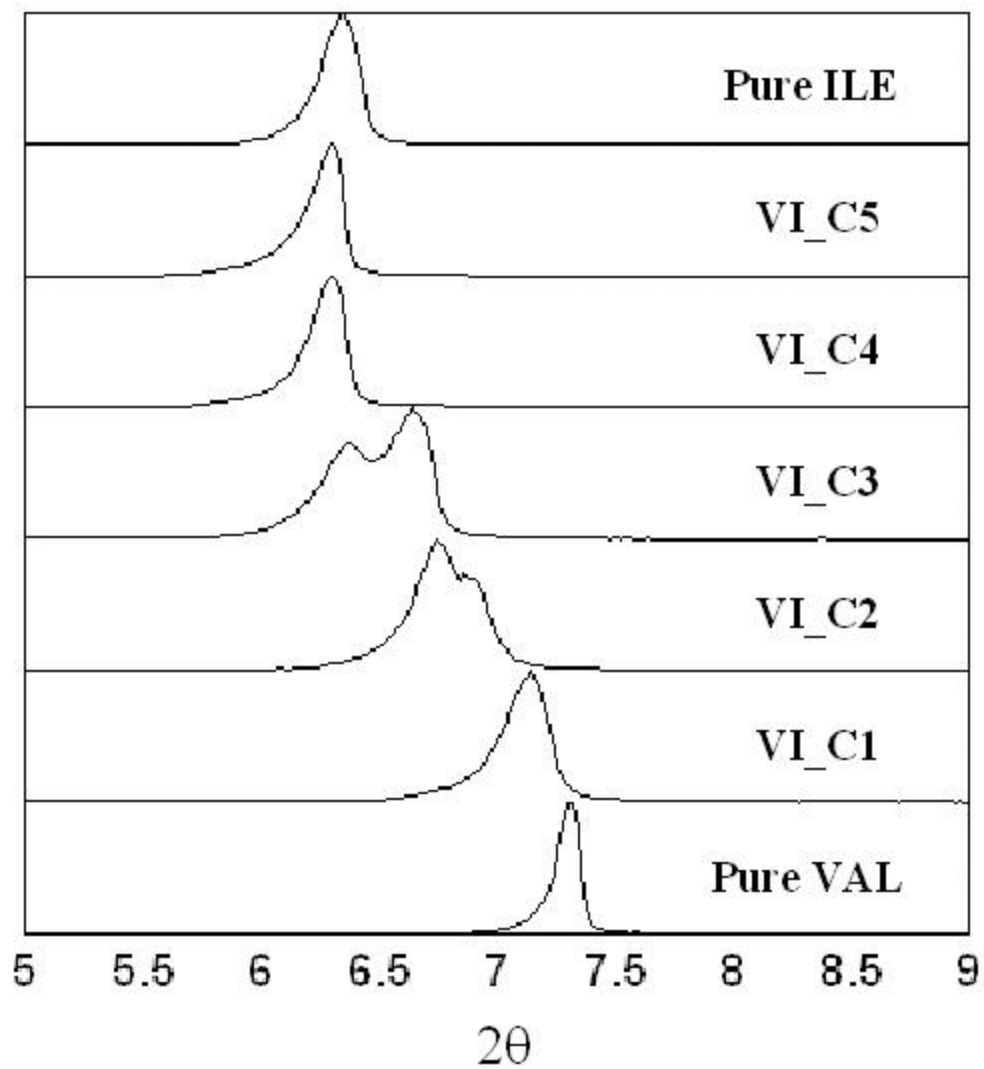
Figure 4-12 Powder XRD patterns of the crystals of L-ILE + L-VAL + water systems obtained by the cooling method (VI_C# is the sample name). The liquid- and solid-phase compositions of the corresponding samples are tabulated in Table 4-5.

.
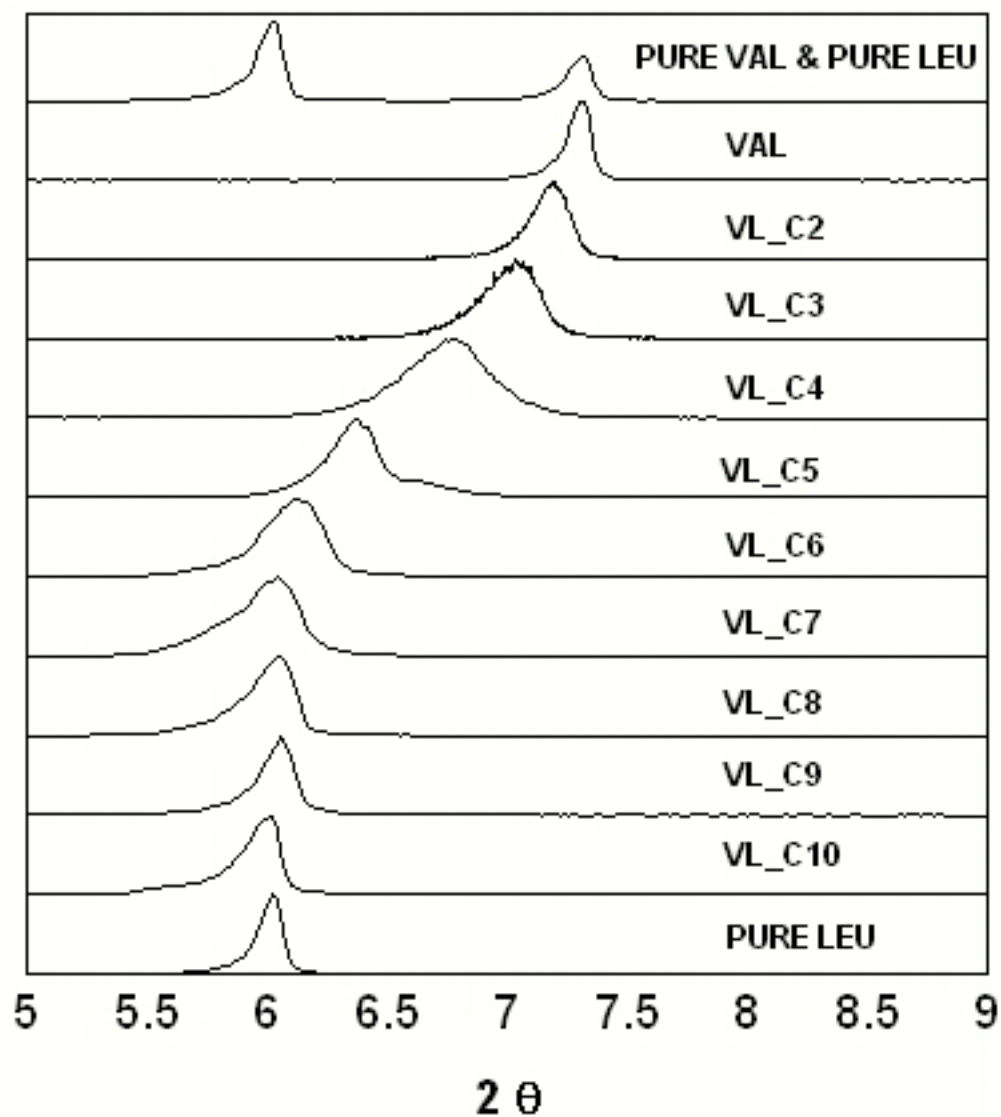
Figure 4-13 Powder XRD patterns of the crystals of L-LEU + L-VAL systems obtained by the cooling method (VL_C# is the sample name). The liquid- and solid-phase compositions of the corresponding samples are tabulated in Table 4-7.

.

Table 4-8 The peak position, FWHM, and calculated d-spacing of the crystals of L-ILE + L-LEU + water systems obtained by the cooling method with the composition in solid phase.

	2 Theta	d	FWHM	Area	L-LEU in Solid
	[θ]	[Å]	[θ]		[mol/mol]
Pure L-LEU	6.02	14.66	0.12	146894	1.00
IL_C1	6.02	14.68	0.16	205781	0.98
IL_C2	5.97	14.80	0.16	195961	0.91
IL_C5	6.07	14.56	0.16	141916	0.6
IL_C6	6.08	14.52	0.18	141197	0.46
IL_C7	6.10	14.48	0.20	158088	0.34
IL_C8	6.17	14.31	0.14	110784	0.23
IL_C9	6.20	14.24	0.16	143334	0.14
Pure L-ILE	6.35	13.91	0.16	256793	0.00

Table 4-9 The peak position, FWHM, and calculated d-spacing of the crystals of L-ILE + L-VAL + water systems obtained by the cooling method with the composition in solid phase.

	2 Theta [2θ]	d [Å]	FWHM [2θ]	Area	L-ILE in Solid [mol/mol]
Pure L-VAL	7.31	12.09	0.12	104121	0.03
VI_C1	7.14	12.36	0.20	129430	0.11
	6.72	13.14	0.08	4861	
VI_C2	6.74	13.11	0.14	90016	0.28
	6.90	12.80	0.12	54506	
VI_C3	6.38	13.85	0.14	62650	0.58
	6.68	13.23	0.18	99594	
VI_C4	6.31	13.99	0.16	178447	0.89
	6.62	13.34	0.18	7105	
VI_C5	6.31	14.01	0.14	147079	0.95
	6.66	13.26	0.10	2268	
Pure L-ILE	6.35	13.92	0.16	256793	1.00

Table 4-10 The peak position, FWHM, and calculated d-spacing of the crystals of L-LEU + L-VAL + water systems obtained by the cooling method with the composition in solid phase.

	2 Theta [θ]	d [Å]	FWHM [θ]	Area	L-LEU in Solid [mol/mol]
Pure L-VAL	7.31	12.09	0.12	104121	0.03
VL_C2	7.19	12.29	0.17	746464	–
VL_C3	7.06	12.50	0.24	402633	0.13
VL_C4	6.77	13.04	0.32	121566	0.28
VL_C5	6.38	13.84	0.20	172880	0.55
	6.60	13.37	0.08	15566	
VL_C6	6.17	14.32	0.28	204903	0.77
VL_C7	6.08	14.54	0.20	120814	0.85
VL_C8	6.07	14.56	0.16	141916	0.92
VL_C9	6.06	14.57	0.14	216552	0.95
VL_C10	6.02	14.68	0.14	137510	0.98
Pure L-LEU	6.02	14.66	0.12	146894	1.00

b) Isothermal Experiments

b-1) L-ILE + L-LEU + water system

Figure 4-14 shows the powder XRD patterns of crystals around the first peak in

L-ILE + L-LEU + water system. The sample name, peak position, FWHM, and

calculated d-spacing of the peak are listed in Table 4-11. In Figure 4-14, the first peak

shifts with the liquid composition, which is similar to the results in the cooling

experiments. However, two peaks are observed when the concentration of a minor

component is close to saturation, which means that two structures exist in the solid phase.

Since the first peak position is close to that of pure crystals, it was assumed that solid

solutions are formed on the surface of pure seed crystals.

It should be pointed out again that the cooling and isothermal methods exhibit

identical behavior of the liquid composition in this system (see Figure 4-6). This suggests

that identical solid solutions at each composition are in contact with liquids. In order to

evaluate the hypothesis, d-spacing of the peak is plotted with the liquid composition in

Figure 4-15. It can be seen in the figure that the two sets of d-spacing are almost

superimposed over a whole range of concentration tested, which indicates that the solid

solutions are identical, and that their structure depends solely on the liquid composition

with which it is in contact.
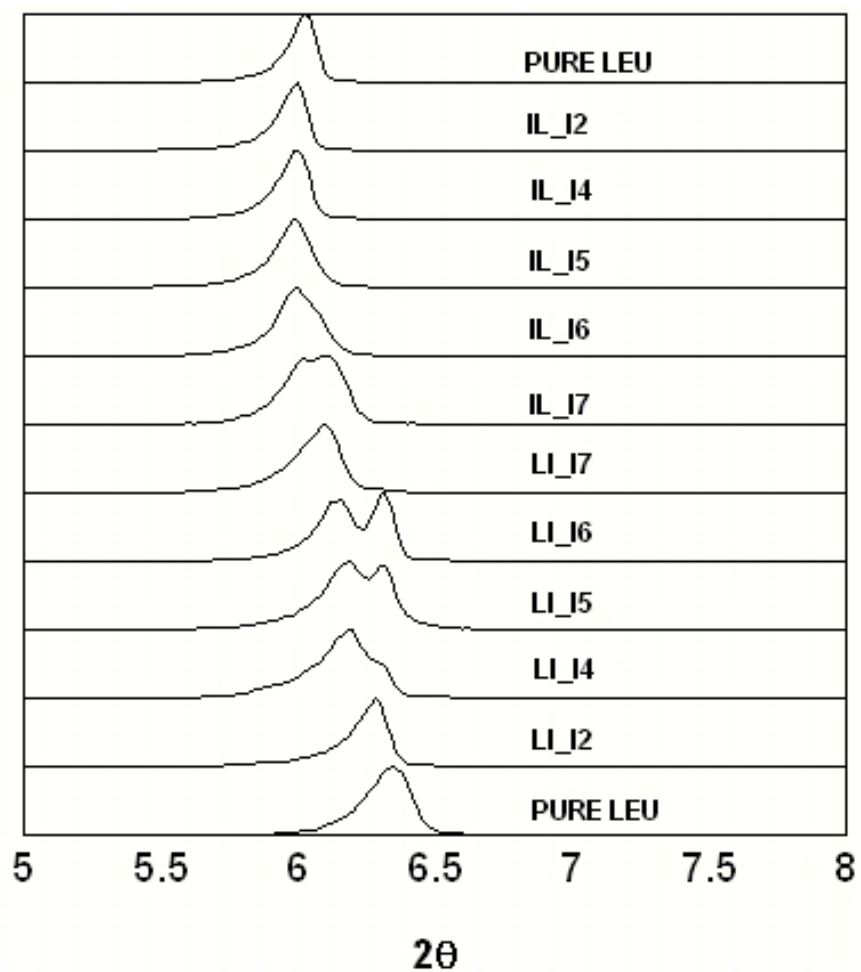
Figure 4-14 Powder XRD patterns of the crystals of L-ILE + L-LEU + water systems obtained by the isothermal method (IL_I# and LI_I# are the sample name). The liquid- and solid-phase compositions of the corresponding samples are tabulated in Table 4-2.

Table 4-11 The peak position, FWHM, and calculated d-spacing of the crystals of L-ILE + L-LEU + water systems obtained by the isothermal method with the equilibrium concentration of amino acids in liquid phase.

	2 Theta [θ]	d [Å]	Area	FWHM [θ]	L-ILE in Liquid [mol/mol] × 10³	L-LEU in Liquid [mol/mol] × 10³
Pure L-LEU	6.02	14.66	146894	0.12	0.00	2.96
IL_I2	5.99	14.73	125458	0.12	0.92	2.97
IL_I4	6.00	14.72	113179	0.12	1.82	2.82
IL_I5	5.98	14.76	199669	0.14	2.53	2.49
IL_I6	5.99	14.74	141825	0.18	2.78	2.32
IL_I7	6.00	14.72	75099	0.12	2.75	2.24
	6.12	14.43	80884	0.12		
LI_I7	6.10	14.47	70930	0.14	3.38	1.70
LI_I6	6.13	14.41	73918	0.14	3.41	1.77
	6.31	14.00	56844	0.1		
LI_I5	6.17	14.31	50703	0.12	3.98	1.16
	6.32	13.99	39486	0.1		
LI_I4	6.18	14.28	35288	0.12	4.13	1.03
	6.31	13.99	9662	0.08		
LI_I2	6.29	14.05	64801	0.12	4.57	0.57
Pure L-ILE	6.35	13.91	256793	0.16	4.54	0.00
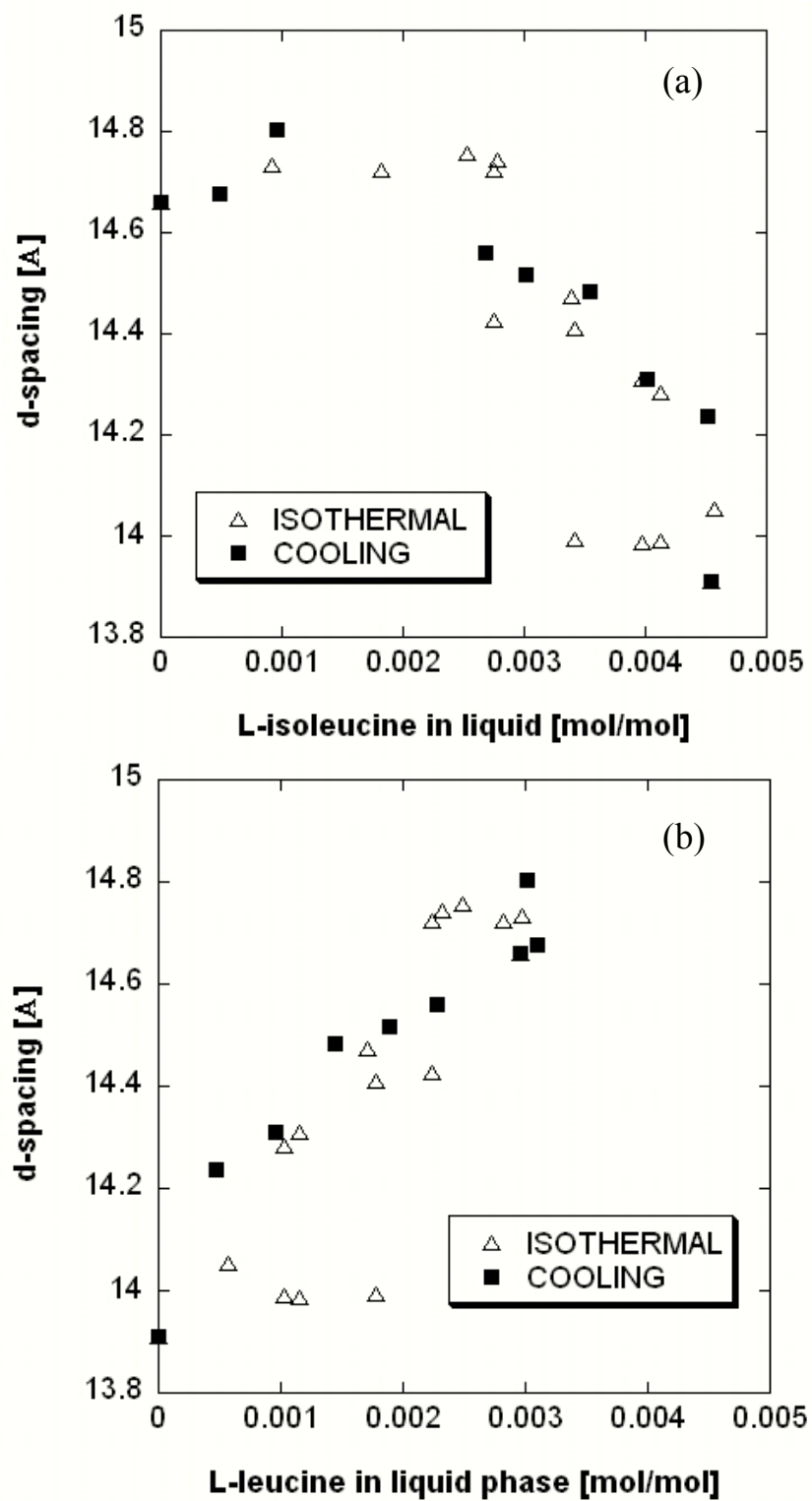
Figure 4-15 d-spacing of the crystals in isothermal and cooling method with (a) equilibrium L-ILE concentration and (b) equilibrium L-LEU concentration in liquid phase.

b-2) L-ILE + L-VAL + water and L-LEU + L-VAL + water systems

Figures 4-16 and 4-17 show the diffraction patterns of crystals around the first peak in L-ILE + L-VAL + water and L-LEU + L-VAL + water systems, respectively. The d-spacing of the crystals are tabulated in Table 4-12 and 4-13 and plotted with the liquid composition in Figures 4-18 and 4-19.

In both systems, it is shown that a distinct peak corresponding to the pure seed crystals is observed, and that a small second peak appears when a minor component concentration is at about saturation. The solids corresponding to the second peak in L-ILE + L-VAL + water system might be identical to the compounds identified in the cooling method since the d-spacing of the solids is 13.1-13.3 Å in the both experiments. The additional d-spacing in L-LEU + L-VAL + water systems is around 13.10 Å, close to the average value, 13.38 Å, of those of pure L-LEU and pure L-VAL crystals. This suggests the presence of equimolar compounds in L-LEU + L-VAL + water systems, which was not identified in the cooling method.

Note that the composition of phases at equilibrium should be specified in order to discuss experimental results from a thermodynamic point of view. The isothermal experiments in this work assumed that the solids are in a pure form; however, this may mislead the construction of true phase diagrams where non-pure and/or inhomogeneous solids are formed.
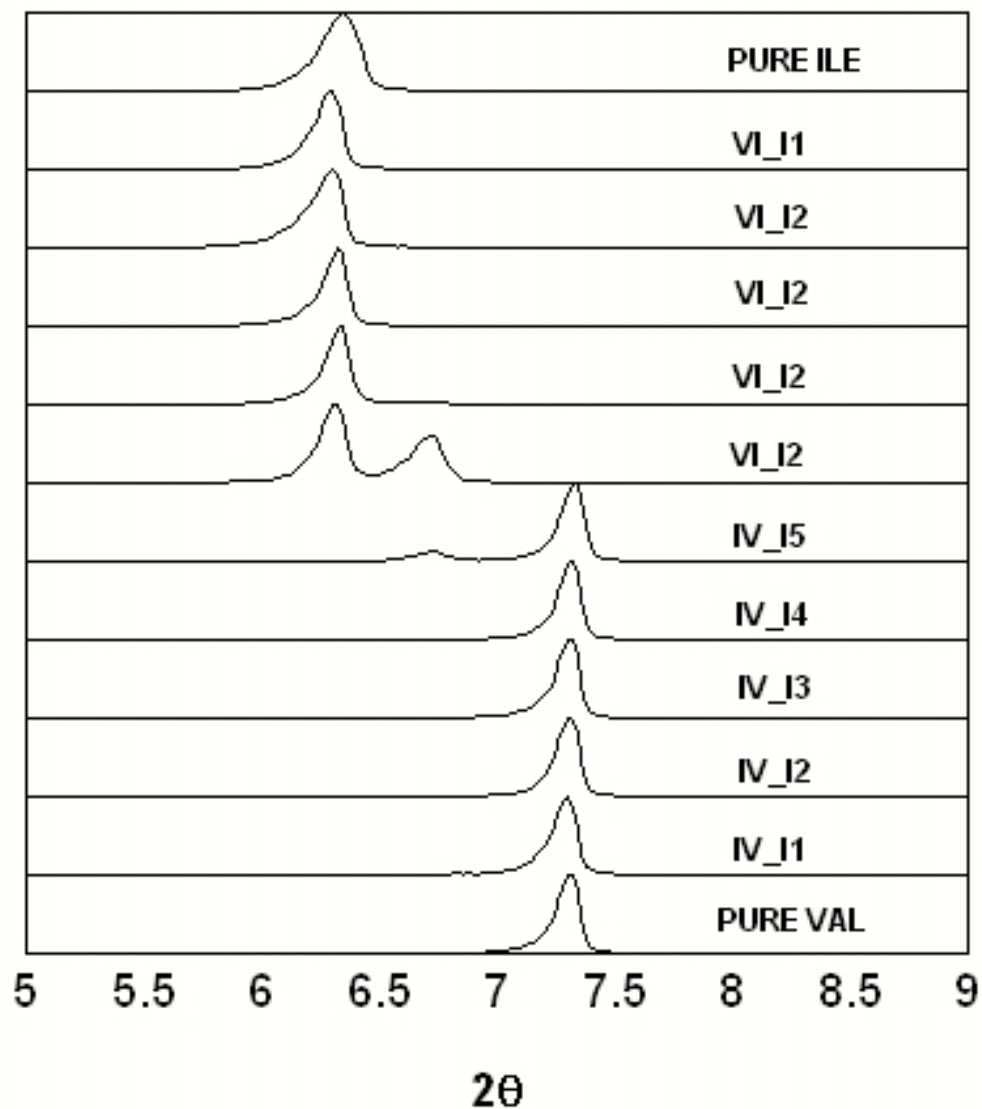
Figure 4-16 Powder XRD patterns of the crystals of L-ILE + L-VAL + water systems obtained by the isothermal method (VI_I# and IV_I# are the sample name). The liquid- and solid-phase compositions of the corresponding samples are tabulated in Table 4-4.
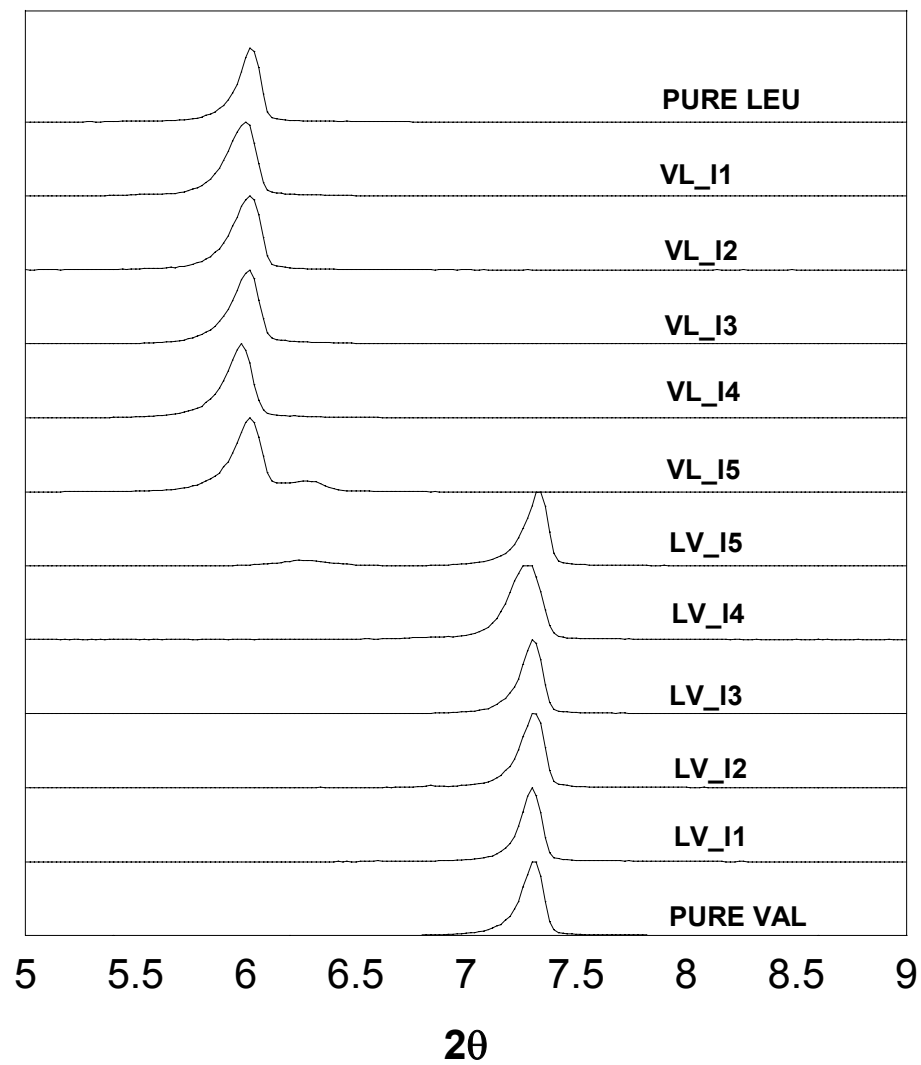
Figure 4-17 Powder XRD patterns of the crystals of L-LEU + L-VAL + water systems obtained by the isothermal method (VL_I# and LV_I# are the sample name). The liquid- and solid-phase compositions of the corresponding samples are tabulated in Table 4-6.

Table 4-12 The peak position, FWHM, and calculated d-spacing of the crystals of L-ILE + L-VAL + water systems obtained by the isothermal method with the equilibrium concentration of amino acids in liquid phase.

	2 Theta [θ]	d [Å]	Area	FWHM [θ]	L-VAL in Liquid [mol/mol] × 10³	L-ILE in Liquid [mol/mol] × 10³
Pure L-ILE	6.35	13.91	256793	0.16	0	4.54
VI_I1	6.3	14.03	136990	0.14	1.68	4.46
VI_I2	6.3	14.01	72078	0.14	3.23	4.26
VI_I3	6.32	13.97	128978	0.12	4.86	4.03
VI_I4	6.33	13.95	113241	0.12	6.59	3.81
VI_I5	6.31	13.99	66059	0.12	7.46	3.53
	6.72	13.14	54231	0.16		
IV_I5	6.73	13.13	11928	0.12	7.13	3.86
	7.33	12.06	102355	0.12		
IV_I4	7.31	12.08	137495	0.12	7.56	3.37
IV_I3	7.31	12.09	105872	0.12	7.73	2.57
IV_I2	7.31	12.09	180756	0.12	7.8	1.7
IV_I1	7.3	12.11	92177	0.12	8.33	0.91
Pure L-VAL	7.31	12.09	104121	0.12	9.13	0

Table 4-13 The peak position, FWHM, and calculated d-spacing of the crystals of L-LEU + L-VAL + water systems obtained by the isothermal method with the equilibrium concentration of amino acids in liquid phase.

	2 Theta [θ]	d (A) [Å]	Area	FWHM [θ]	L-VAL in Liquid [mol/mol] × 10³	L-LEU in Liquid [mol/mol] × 10³
Pure L-LEU	6.02	14.66	146894	0.12	0	2.96
VL_I1	6.01	14.7	140152	0.14	1.73	3
VL_I2	6.02	14.66	135405	0.16	3.57	3.06
VL_I3	6.02	14.68	120301	0.12	5.27	3.05
VL_I4	5.98	14.77	143153	0.14	6.85	3.06
VL_I5	6.02	14.67	121608	0.14	8.69	2.92
	6.3	14.01	16945	0.14		
LV_I5	6.23	14.19	14877	0.2	8.54	2.92
	7.33	12.05	111160	0.12		
LV_I4	7.3	12.11	128058	0.18	8.81	2.66
LV_I3	7.3	12.1	130468	0.12	8.86	2.11
LV_I2	7.31	12.08	92870	0.12	8.68	1.46
LV_I1	7.3	12.1	144694	0.12	8.71	0.87
Pure L-VAL	7.31	12.09	104121	0.12	9.13	0
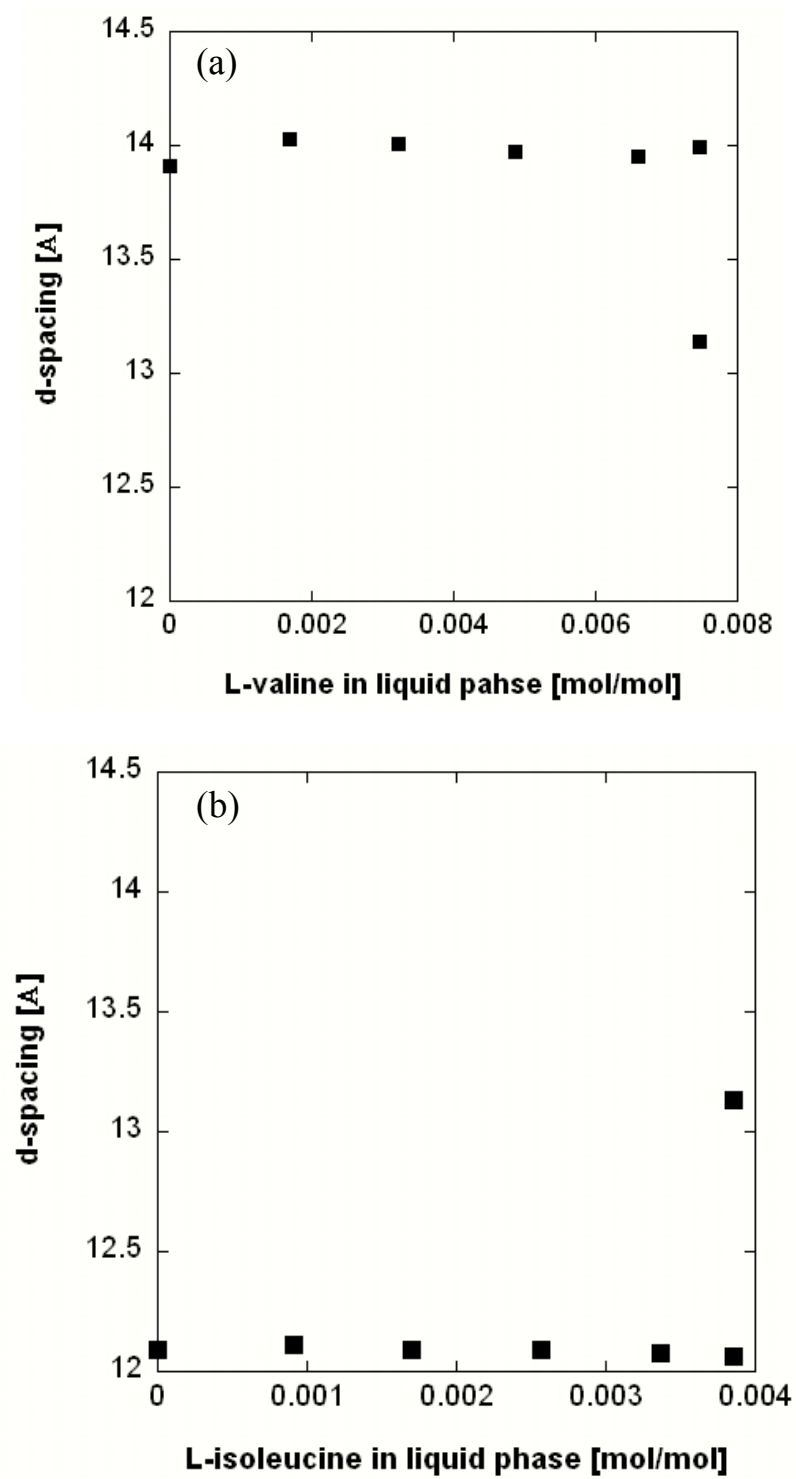
Figure 4-18 Peak positions with the concentration of minor amino acid in liquid phase. (a) with L-ILE seed crystals (b) with L-VAL seed crystals.
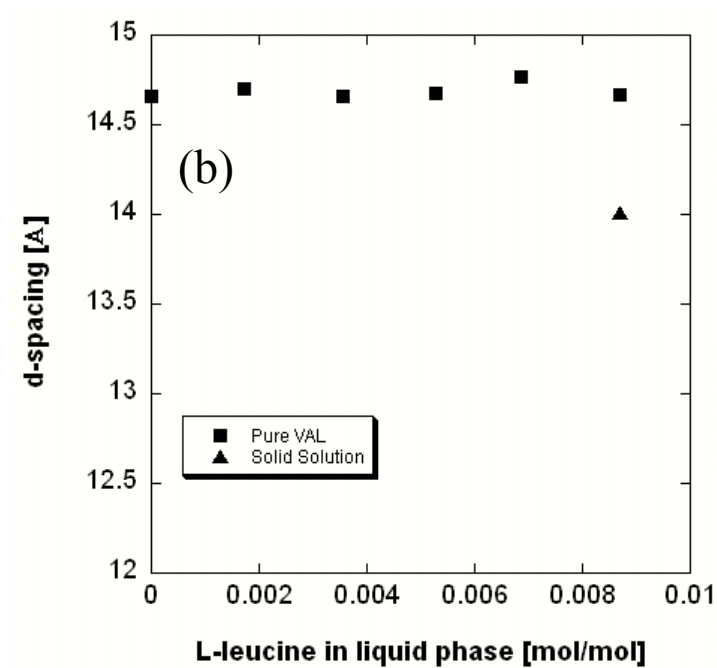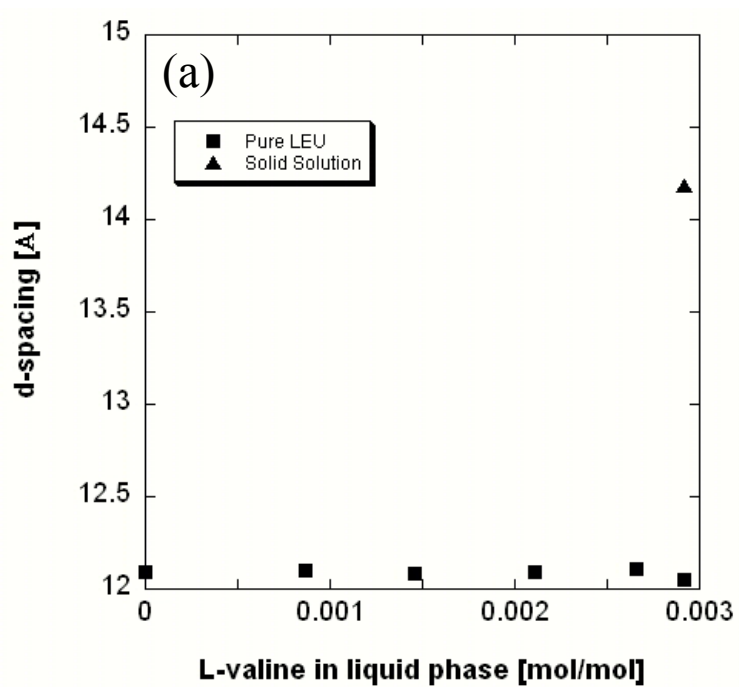
Figure 4-19 Peak positions with the concentration of minor amino acid in liquid phase. (a) with L-LEU seed crystals (b) with L-VAL seed crystals.

CHAPTER 5

THERMODYNAMIC MODELING

In this chapter, thermodynamic relationships are developed for solid-liquid equilibrium in aqueous systems containing dissolved amino acids. As discussed in Chapter 4, it is necessary to account for non-ideality in both phases when describing solid-liquid equilibrium in such systems. A modified UNIFAC approach to obtain liquid-phase nonideality is reviewed briefly in Section 5-1. In Section 5-2, the prediction of the solubility of two amino acids in water using the UNIFAC model is described, and comparisons with experimental data are presented. The calculation of solid-phase activity coefficients is outlined in Section 5-3. Finally in Section 5-4, a relationship between crystal purity and equilibrium liquid composition is investigated in order to develop a predictive model for ternary systems of two amino acids in water.

5.1 **The UNIFAC-Kuramochi liquid-phase activity coefficient model**

Nonidealities in the liquid phase are generally adequately described by activity coefficient expressions such as the Wilson equation (Coutinho *et al*., 1996b), or the NRTL equation (Chen and Zhu, 1989). However, experimental phase equilibrium data are required to obtain parameters in these models. Since solid-liquid equilibrium data for

amino acid solutions are not common, it is necessary to use predictive models such as the

UNIFAC group-contribution model of Kuramochi *et al.* (1996) to describe nonidealities

in the liquid phase in such systems. The Kuramochi *et al.* model is based on the Larsen et

al. (1987) version of the UNIFAC model and extends this model to aliphatic amino acids

and homopeptides. In the original UNIFAC model (Fredenslund *et al.*, 1977), the excess

molar Gibbs energy g^E is partitioned into two contributions as follows:

$$g^E = g_c^E + g_r^E \qquad (5\text{-}1)$$

where g_c^E and g_r^E are the combinatorial and residual contributions to the excess Gibbs

energy of the solution. Differentiation of g^E with respect to moles of molecule i leads to

the following expression for the activity coefficient:

$$\ln\gamma_i = \ln\gamma_i^c + \ln\gamma_i^r \qquad (5\text{-}2)$$

The combinatorial contribution is obtained from the Flory-Huggins theory:

$$\ln\gamma_i^c = \ln\left(\frac{\phi_i}{x_i}\right) + 1 - \frac{\phi_i}{x_i} - \frac{z}{2}q_i\left(\ln\left(\frac{\phi_i}{\theta_i}\right) + 1 - \frac{\phi_i}{\theta_i}\right) \qquad (5\text{-}3)$$

where ϕ_i, z, θ_i are molecular volume fraction, lattice coordination number, and surface

area fraction for i in mixture, respectively. The molecular volume fraction and the surface

area fraction are defined as follows:

$$\phi_i = \frac{x_i r_i}{\sum_j x_j r_j} \qquad (5\text{-}4)$$

$$\theta_i = \frac{x_i \frac{z}{2} q_i}{\sum_j x_j \frac{z}{2} q_j} \qquad (5\text{-}5)$$

where r and (z/2)q are segment number and contact number, respectively. The segment number is defined as:

$$r_i = \sum_k \nu_{ki} R_k \qquad (5\text{-}6)$$

where ν_i is the number of groups of type k in molecule i, and R_k is a volume parameter for the group k, respectively. R_k is calculated using:

$$R_k = V_{W,k} / 15.17 \qquad (5\text{-}7)$$

where $V_{W,k}$ is the van der Waals volume of the group k.

On the other hand, in Larsen's version of UNIFAC, the combinatorial contribution is obtained as follows:

$$\ln \gamma_i^c = \ln\left(\frac{\omega_i}{x_i}\right) + 1 - \frac{\omega_i}{x_i}$$

$$\text{where } \omega_i = \frac{x_i r_i^{2/3}}{\sum_j x_j r_j^{2/3}} \qquad (5\text{-}8)$$

The modified combinatorial term provides a much better description of VLE of alkane mixtures (Larsen, 1987). The residual contribution is expressed as:

$$\ln \gamma_i^r = \sum_k \nu_{ki} (\ln \Gamma_k - \ln \Gamma_k^i) \qquad (5\text{-}9)$$

$$\ln \Gamma_k = \frac{z}{2} Q_k \left[-\ln\left(\sum_m \theta_m \tau_{mk}\right) + 1 - \sum_i \frac{\theta_i \tau_{ki}}{\sum_j \theta_j \tau_{ji}} \right] \qquad (5\text{-}10)$$

$$\theta_k = \frac{n_k \frac{z}{2} Q_k}{\sum_m n_m \frac{z}{2} Q_m} \qquad (5\text{-}11)$$

$$\tau_{mk} = \exp(-a_{mk} / T) \qquad (5\text{-}12)$$

101

$$\frac{z}{2}Q_k = A_W /(2.5 \times 10^9)$$

<div align="right">(5-13)</div>

where n_k represents the total number of groups of type k in the mixture, A_W is the van der Waals surface area of group k, and a_{mk} is a group-interaction parameter between groups m and k. Group interaction parameters for 21 different main groups have been assigned using VLE (Gmehling and Onken, 1977), LLE (Sorensen and Arlt, 1979), and H^E data (Christensen *et al.*, 1984).

Kuramochi *et al.* (1996) introduced two additional groups, α-CH, and sc-CH$_2$ (side chain-CH$_2$) into Larsen's model. Interaction parameters for the new groups were determined from osmotic coefficient data for aliphatic amino acids such as glycine (Ellerton et al., 1964), DL-serine and DL-threonine (Smith and Smith, 1940a), DL-valine, DL-alanine, DL-α-amino-n-butyric acid, and DL- α -amino-n-valeric acid (Smith and Smith, 1937), and of homopeptides such as glycylglycine, DL-alanyl-DL-alanine, and triglycine (Smith and Smith, 1940b).

Experimental data points and the curves of calculated activity coefficients of DL-valine, DL-serine, glycine, and DL-alanine in aqueous solutions are shown in Figure 5-1. It should be added that Kuramochi's model yields activity coefficients that are symmetric with respect to the Lewis and Randall standard state, whereas literature values are usually reported using the unsymmetric convention and an infinite dilution standard state. Furthermore, UNIFAC calculations use a mole fraction basis whereas literature values are reported on a molal basis (see Appendix D). Therefore, the calculated (UNIFAC-Kuramochi) values were converted to unsymmetric activity coefficients using the following expression:

$$\gamma_{i,m}^* = \frac{\gamma_i(1-x_i)}{\gamma_i^\infty} \hspace{4cm} (5\text{-}14)$$

where $\gamma_{i,m}^*$, γ_i, and γ_i^∞ are the unsymmetric, symmetric, and infinite dilution activity

coefficients, respectively. Infinite dilution activity coefficients were calculated using the

Kuramochi model with $x_i = 10^{-10}$. The amino acid data shown in Figure 5-1 were used to

obtain UNIFAC-Kuramochi group interaction parameters and the model provides good

agreement with the data.

Figure 5-2 shows experimental (Smith and Smith, 1940a) and calculated liquid-

phase activity coefficients for DL-proline, L-serine and DL-serine in water. The

calculation for DL-proline and L-serine is a prediction using UNIFAC-Kuramochi model.

It can be seen that the model predicts these activity coefficients in excellent agreement

with the experimental results. The results also show that the activity coefficients of L-

serine can also be predicted using the parameters obtained from the experimental data of

DL-serine. As mentioned in Chapter 2, a racemate behaves as an ideal mixture in the gas

or liquid states, and its physical and chemical properties are indistinguishable from those

of individual enantiomers (Mitchell, 1998). It is therefore likely that the model will work

well for calculating activity coefficients in the *liquid* phase of other optical isomers such

as the L- amino acids investigated in this work.
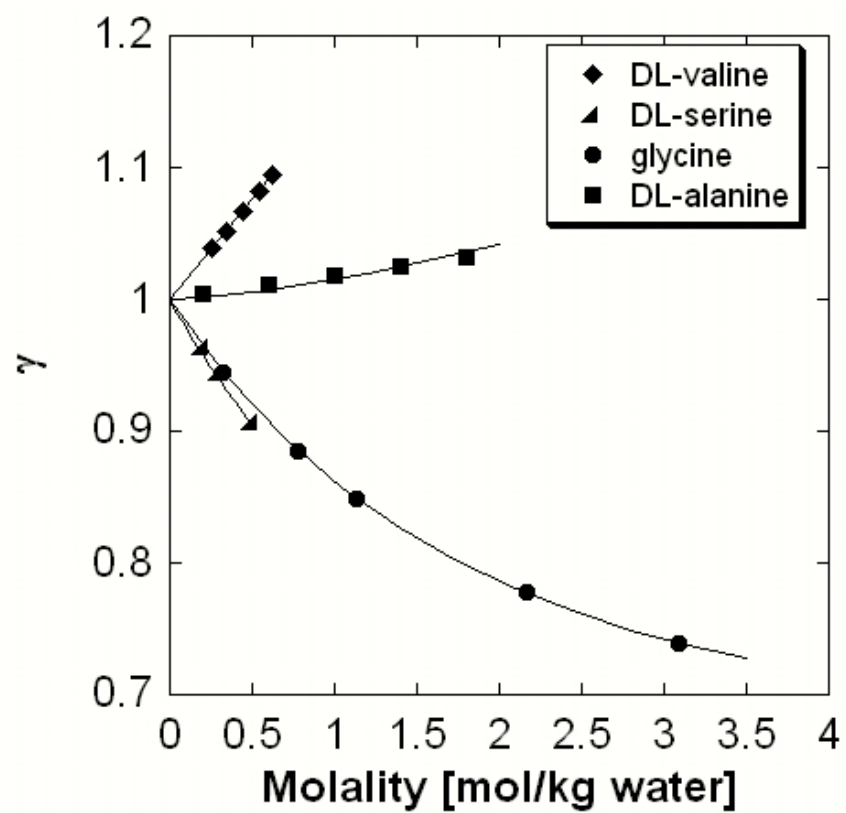
Figure 5-1. Correlation of activity coefficients of amino acids in water using the UNIFAC-Kuramochi model.
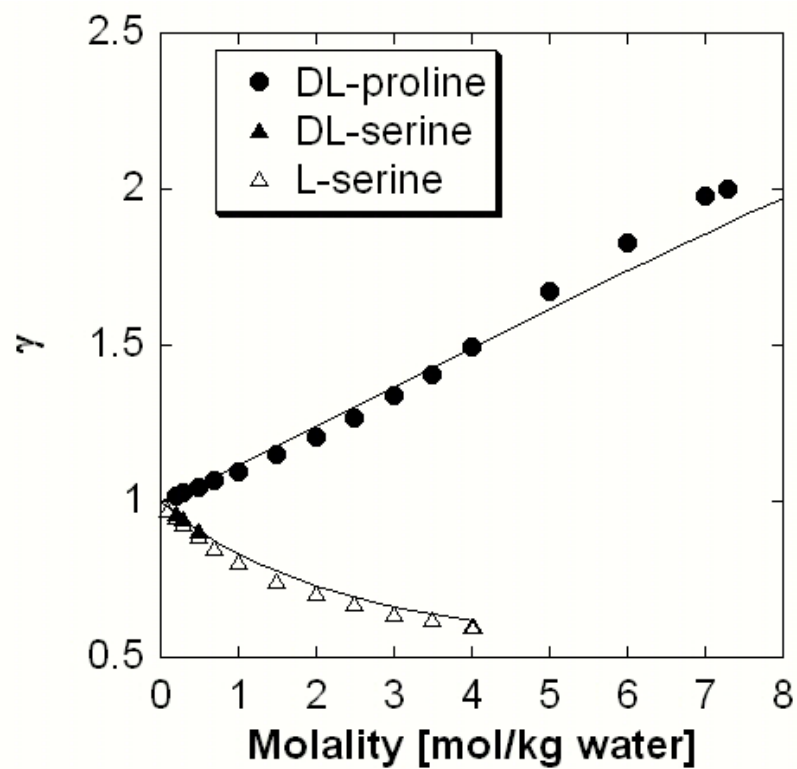
Figure 5-2. Prediction of activity coefficients of amino acids using the UNIFAC-Kuramochi model.

5.2 **Solubility calculations assuming pure solids in equilibrium with liquid solutions**

Solubilities of amino acids in ternary systems have been calculated by assuming the solid phase is pure (Kuramochi *et al.* 1996, Jin and Chao, 1992). In this section, this pure crystal assumption is tested using the results obtained from isothermal and cooling experiments.

If pure solid i is in equilibrium with a binary solution containing component i (e.g. a solution a single amino acid in water), we may write:

$$\mathbf{f_i^{\circ,S}} = \mathbf{f_i^{bin,L}} \tag{5-15}$$

where $f_i^{\circ,S}$ is the fugacity of pure solid i and $f_i^{bin,L}$ is the fugacity of i in the (binary) liquid solution. If pure solid i is in equilibrium with a ternary solution containing component i (e.g. a solution of two amino acids in water), we may write:

$$\mathbf{f_i^{\circ,S}} = \mathbf{f_i^{tern,L}} \tag{5-16}$$

where $f_i^{ter,L}$ is the fugacity of i in the ternary liquid solution. Thus:

$$\mathbf{f_i^{\circ,S}} = \mathbf{f_i^{bin,L}} = \mathbf{f_i^{tern,L}} \tag{5-17}$$

The fugacity of the component i in the liquid phase can be expressed as follows:

$$\mathbf{f_i^{bin,L}} = \mathbf{\gamma_i^{bin} x_i^{bin} f_i^{\circ,L}} \tag{5-18}$$

$$\mathbf{f_i^{tern,L}} = \mathbf{\gamma_i^{tern} x_i^{tern} f_i^{\circ,L}} \tag{5-19}$$

where x_i is a mole fraction of i, γ_i is the activity coefficient of i, and $f_i^{\circ,L}$ is the fugacity of pure subcooled liquid i (Prausnitz et al., 1999). Since component i is saturated in these solutions, x_i is its solubility. By substituting equations (5-18) and (5-19) into equation (5-17), the ternary solubility can be related to the binary solubility by:

106

$$x_i^{tern} \cdot \gamma_i^{tern} = x_i^{bin} \cdot \gamma_i^{bin} = \frac{f_i^{\circ,S}}{f_i^{\circ,L}} = \text{constant} \qquad (5\text{-}20)$$

Equation (5-20) indicates that x_i in a ternary system can be calculated from binary

solubility data if the activity coefficients are known or if they can be predicted from a

model such as UNIFAC. Binary solubility data for L-LEU, L-ILE, and L-VAL in water

obtained in this work were used with activity coefficients predicted using the UNIFAC-

Kuramochi model to calculate the (ternary) solubility behavior of two amino acids in

water (see Appendix E). The results are presented in Figure 5-3 together with

experimental data from isothermal and cooling experiments. The calculated values are

generally in poor agreement with experimental data, with the exception of the data

obtained in isothermal experiments in the case of L-LEU +L-VAL + water. This is

probably fortuitous since XRD analysis (Chapter 4) has shown that all these systems

form solid solutions. It may therefore be concluded that the assumption that the solid

phase is in pure form cannot be used in the case of isomorphous or near-isomorphous

amino acids such as L-LEU, L-ILE, and L-VAL. This is likely to be true of other

isomorphous and near-isomorphous compounds (Makarov, 1972).
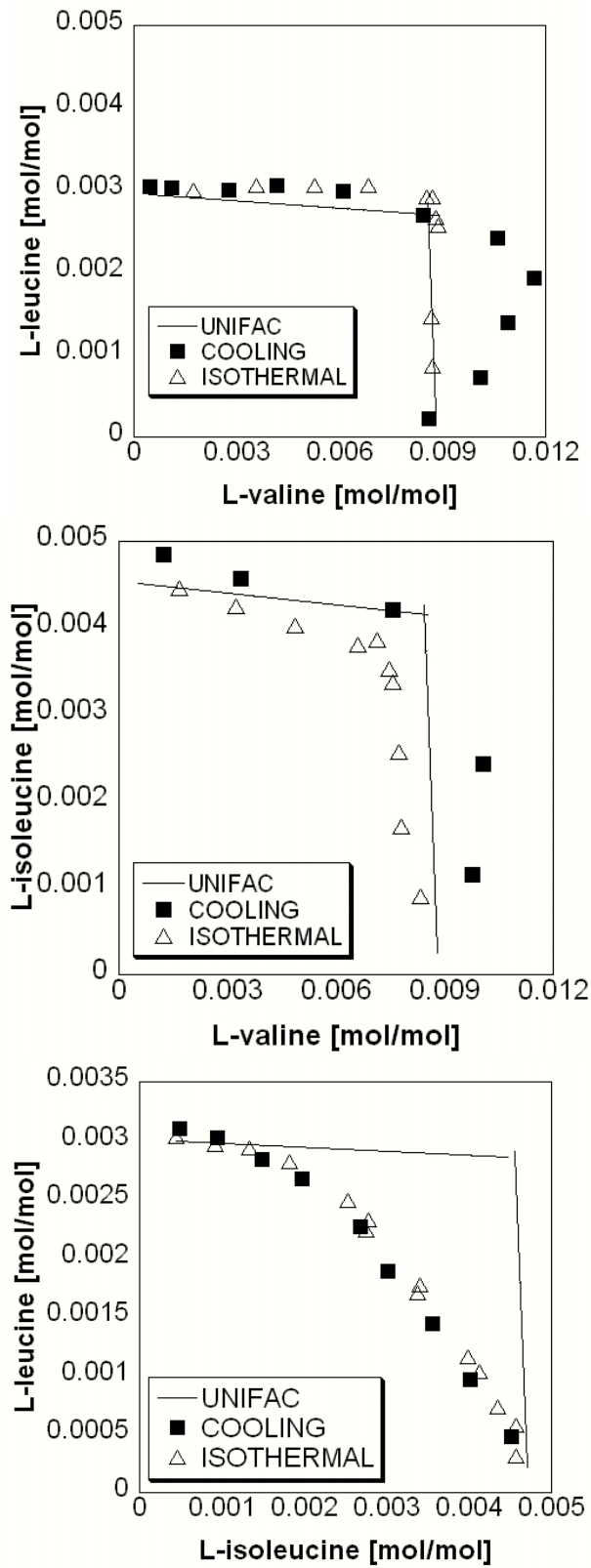
Figure 5-3. Prediction of the solubility in (a) L-VAL + L-LEU + water, (b) L-VAL + L-ILE + water, and (c) L-ILE + L-LEU + water systems using the pure crystal assumption.

5.3   Solubility calculations involving solid solutions in equilibrium with liquid solutions

The above discussion (and XRD information) suggests that the presence of a solid solution must be considered in solubility calculations involving two amino acids in water. In addition, non-ideality in the solid phase must also be considered and cannot be neglected *a priori*. In this section, therefore, activity coefficients in the solid phase are estimated using the measured binary and ternary solubilities and liquid-phase activity coefficients based on the UNIFAC- Kuramochi model.

As described previously, equilibrium between a pure solid i and its solution in water can be described by:

$$f_i^{0,S} = \gamma_i^{bin} x_i^{bin} f_i^{\circ,L} \tag{5-21}$$

In the case of a solid solution of i and j in equilibrium with a (ternary) solution containing both i and j, we may write:

$$z_i^{tern} \Gamma_i^{tern} f_i^{0,S} = x_i^{tern} \gamma_i^{tern} f_i^{0,L} \tag{5-22}$$

where z_i is the mole fraction of i and Γ_i is the activity coefficient of i in the solid phase. Substituting equation (5-21) into equation (5-22), and rearranging as follows:

$$\Gamma_i^{tern} = \frac{x_i^{tern} \gamma_i^{tern}}{z_i^{tern}} \cdot \frac{f_i^{0,L}}{f_i^{0,S}} = \frac{1}{z_i^{tern}} \cdot \frac{\gamma_i^{tern}}{x_i^{bin} \gamma_i^{bin}} \cdot x_i^{tern} \tag{5-23}$$

Solid-phase activity coefficients were obtained using experimental binary and ternary solubilities, and liquid-phase activity coefficients from the UNIFAC-Kuramochi model. The results are listed in Table 5-1 and plotted as a function of the solid composition in Figure 5-4, 5-5, and 5-6. The trends exhibited appear to be reasonable and in good agreement with the size differences between the molecules (L-LEU > L-ILE > L-VAL along the c-axis). The unit cell constant along the c-axis, which corresponds to the length of the aliphatic side-groups in the amino acid, is 14.62 Å, 14.12 Å, and 12.06 Å for L-LEU, L-ILE and L-VAL, respectively. The ratio of the unit-cell constants is 1.04, 1.17, 1.21 for L-LEU:L-ILE, L-ILE:L-VAL, and L-LEU:L-VAL, respectively. These ratios can be correlated with the ratios of the solid activity coefficients at infinite dilution, so that lattice constants may be used to infer the nonideality in the solid phase in these systems.

In order to correlate the structural and compositional data, the change in d-spacing of the first peak is considered. As explained in Section 3.2.2, the d-spacing of the first peak corresponds to the c-axis length in a unit cell as follows:

$$\frac{1}{d^2} = \frac{1}{\sin^2 \beta} \frac{l^2}{c^2} \propto \frac{l^2}{c^2} \qquad (3\text{-}21)$$

The L-LEU, L-ILE, and L-VAL molecules differ only in the length of the aliphatic side-groups, which corresponds to the c-axis length. Therefore, the c-axis length represents the lattice volume of the solid solution. Figure 5-7, 5-8, and 5-9 show the variation of the d-spacing of the first peak with the solid composition. In L-ILE + L-LEU and L-LEU + L-VAL systems, the d-spacing shifts continuously with the composition, which is characteristic of solid solutions as described in the literature (Blasdale, 1927; Yoshimura *et al.*, 1997; Abel *et al.*, 1999; Chae *et al.*, 2003, Suda, *et al.*, 2002). In the L-ILE + L-

VAL system, on the other hand, it can be seen that there are two peaks in Figure 4-12 (see Appendix C for details). One of the peaks may correspond to solid solutions due to the continuous shift of d-spacing with the solid composition. The other d-spacing corresponding to the second peak at 13.0 Å, which is close to the average value of pure L-ILE and pure L-VAL crystals (12.99 Å). It suggests that not only solid solutions but also equimolar compound crystals of L-ILE and L-VAL are formed in this system. However, no quantitative information on such compound crystals was obtained in this work.

In all systems, the d-spacing increases nonlinearly with the solid composition. It indicates that the nonideality of the solid phase may require a more sophisticated model that considers molecular configuration of each crystal lattice than a simple thermodynamic model such as regular solution theory.

Table 5-1. Activity coefficients in the liquid and solid phases in (a) L-VAL + L-LEU + water, (b) L-VAL + L-ILE + water, and (c) L-ILE + L-LEU + water systems.

(a) L-VAL + L-LEU + water

x [mol/mol] x 10³		z [mol/mol]		γ x 10²		Γ	
L-VAL	L-LEU	L-VAL	L-LEU	L-VAL	L-LEU	L-VAL	L-LEU
10.90	1.40	0.87	0.13	9.92	7.62	1.44	3.94
11.70	1.90	0.72	0.28	10.05	7.73	1.89	2.52
10.60	2.40	0.45	0.55	10.00	7.69	2.73	1.61
8.40	2.70	0.23	0.77	9.83	7.54	4.16	1.27
6.10	3.00	0.15	0.85	9.66	7.38	4.55	1.25
4.20	3.10	0.08	0.92	9.51	7.24	5.78	1.17
2.80	3.00	0.05	0.95	9.38	7.12	6.08	1.08
1.10	3.00	0.02	0.98	9.23	6.99	5.88	1.03
0.50	3.00	0.01	0.99	9.18	6.95	5.31	1.01

(b) L-VAL + L-ILE + water

x [mol/mol] x 10³		z [mol/mol]		γ x 10²		Γ	
L-VAL	L-ILE	L-VAL	L-ILE	L-VAL	L-ILE	L-VAL	L-ILE
9.80	1.10	0.89	0.11	9.79	7.50	1.25	2.36
10.00	2.40	0.72	0.28	9.95	7.64	1.60	2.06
7.50	4.20	0.42	0.58	9.91	7.60	2.05	1.73
3.40	4.60	0.11	0.89	9.59	7.31	3.43	1.19
1.20	4.80	0.05	0.95	9.43	7.16	2.62	1.14

(c) L-ILE + L-LEU + water

x [mol/mol] x 10³		z [mol/mol]		γ x 10²		Γ	
L-ILE	L-LEU	L-ILE	L-LEU	L-ILE	L-LEU	L-ILE	L-LEU
0.95	3.02	0.09	0.91	6.99	6.99	2.32	1.11
1.49	2.84	0.15	0.85	7.02	7.02	2.20	1.13
1.97	2.67	0.23	0.77	7.05	7.05	1.90	1.17
2.68	2.27	0.4	0.6	7.08	7.08	1.49	1.29
3.01	1.89	0.54	0.46	7.07	7.07	1.24	1.40
3.55	1.44	0.66	0.34	7.08	7.08	1.20	1.44
4.02	0.96	0.77	0.23	7.08	7.08	1.16	1.42
4.52	0.48	0.86	0.14	7.08	7.08	1.17	1.17
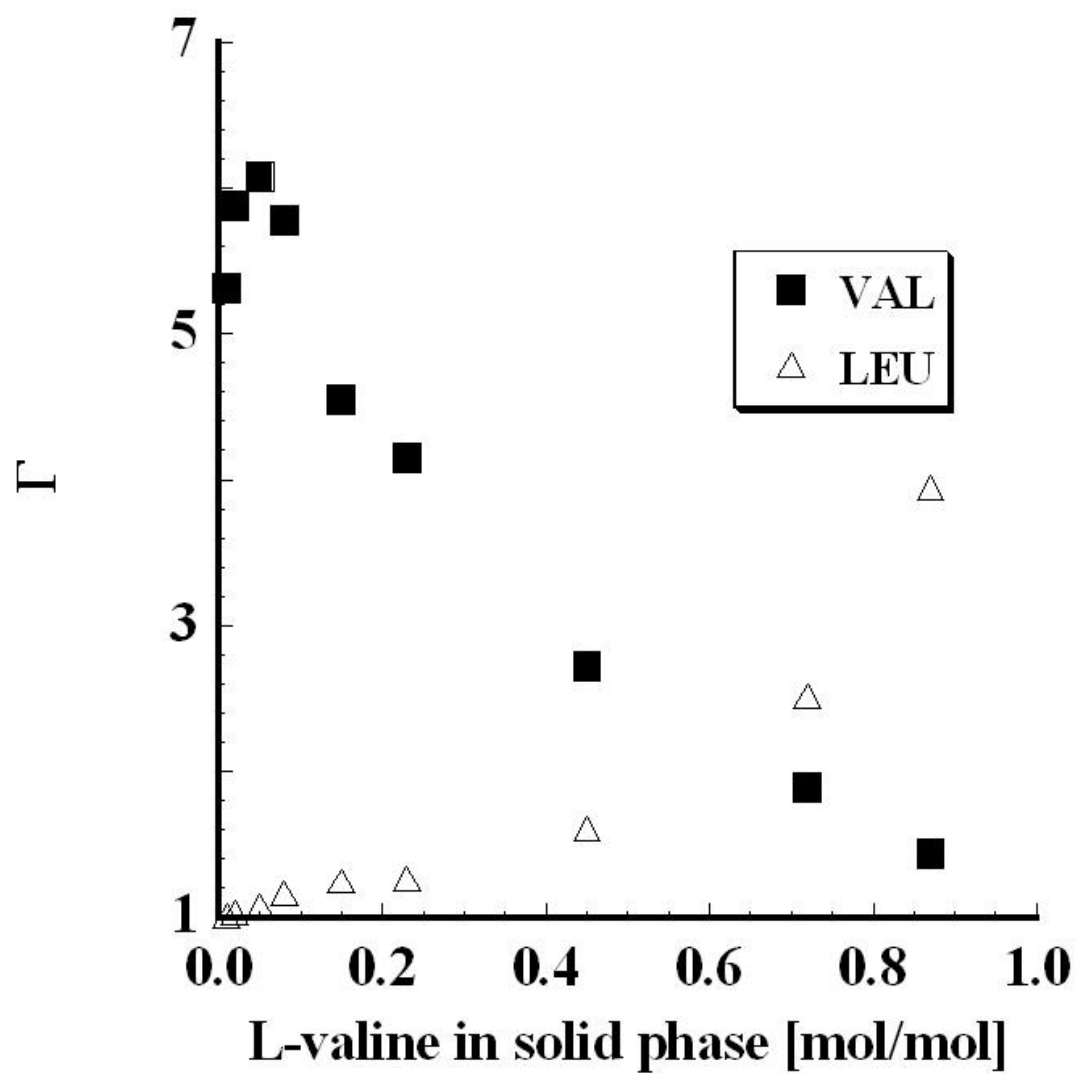
Figure 5-4 Activity coefficients in the solid phase in L-VAL + L-LEU + water.
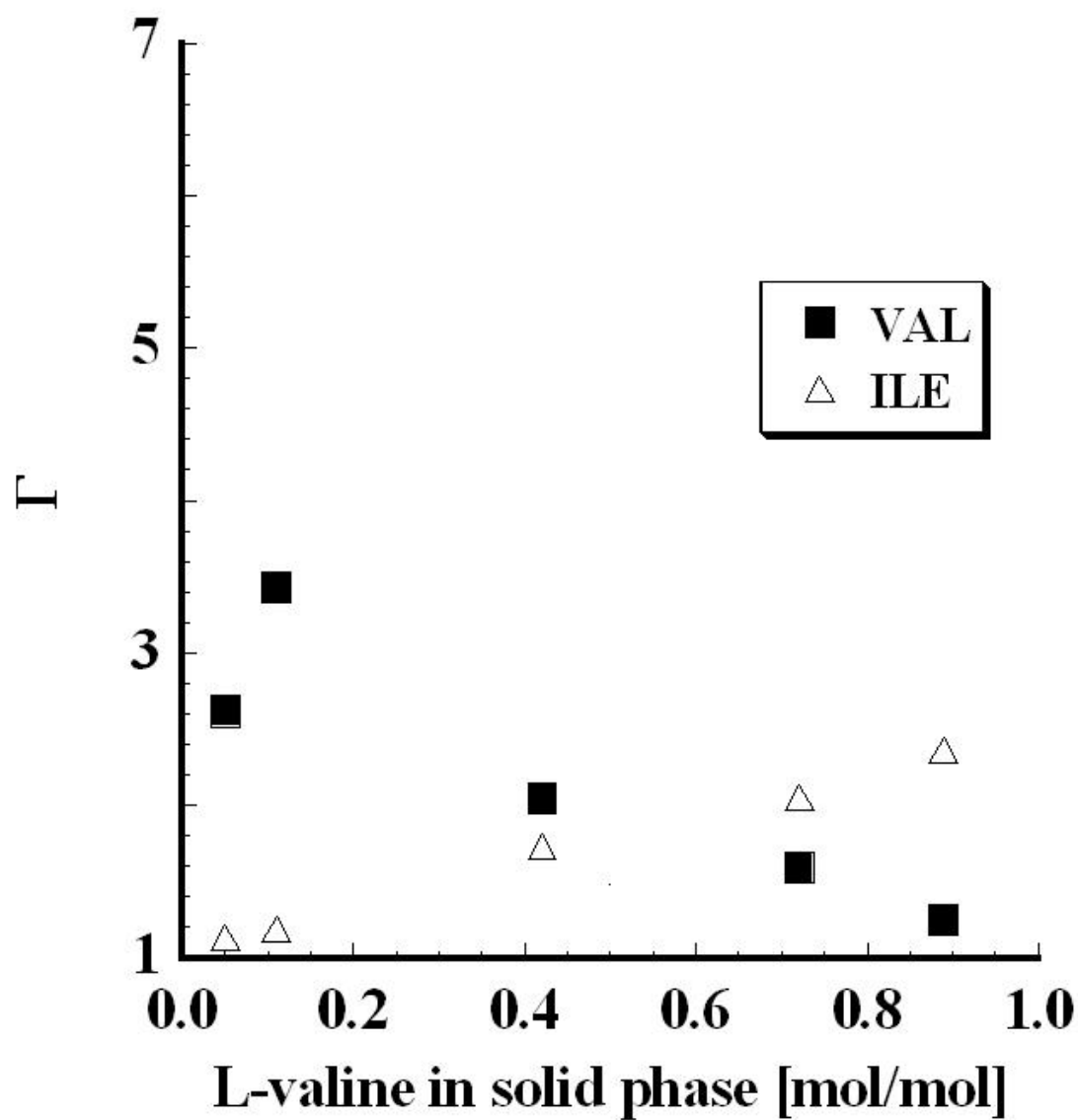
Figure 5-5 Activity coefficients in the solid phase in L-VAL + L-ILE + water.
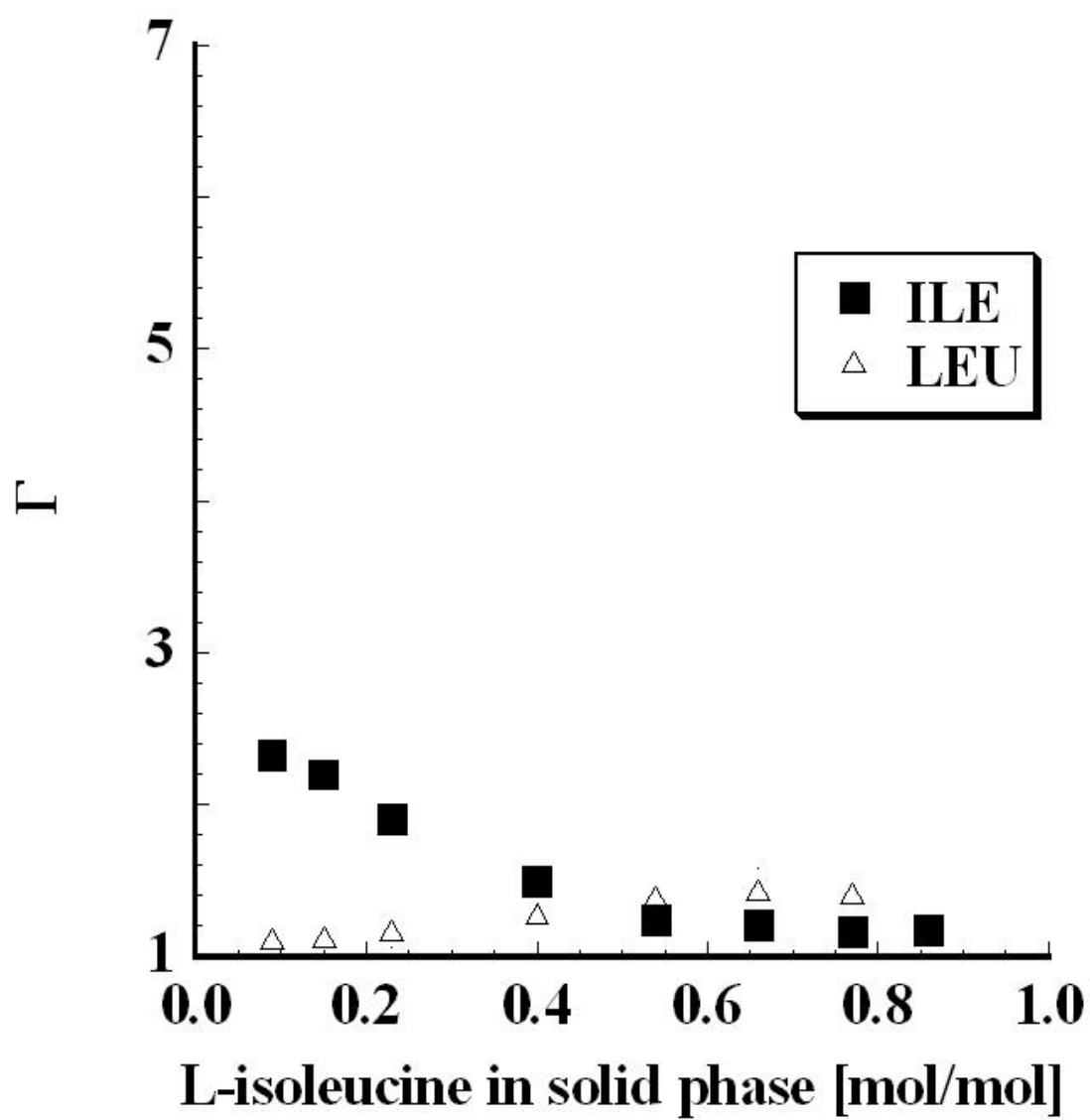
Figure 5-6. Activity coefficients in the solid phase in L-ILE + L-LEU + water.
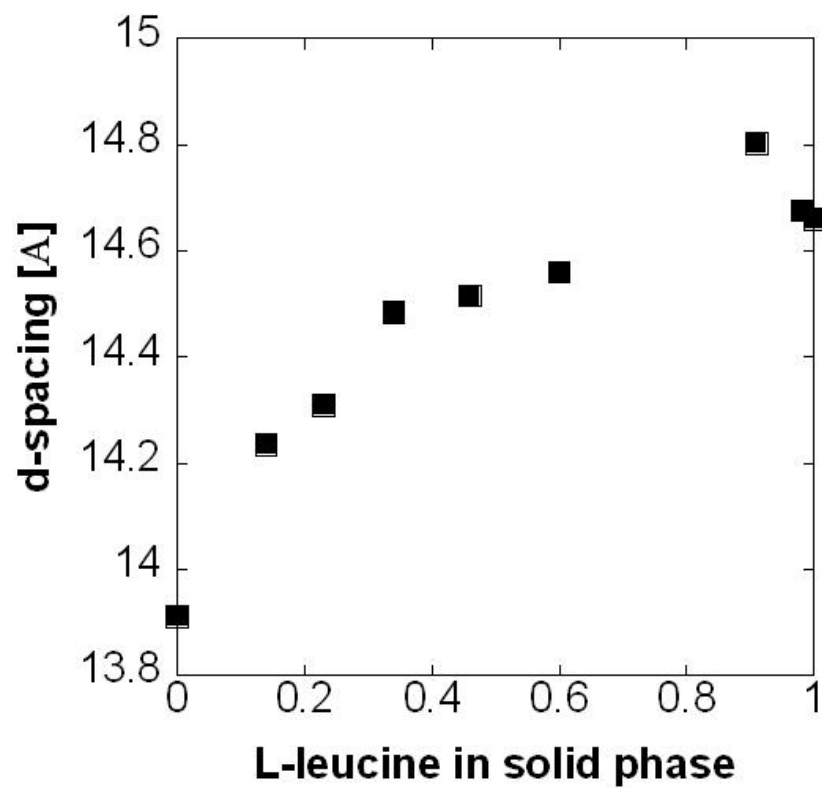
Figure 5-7 d-spacing of crystals of L-ILE + L-LEU + water versus L-LEU composition in the solid phase.
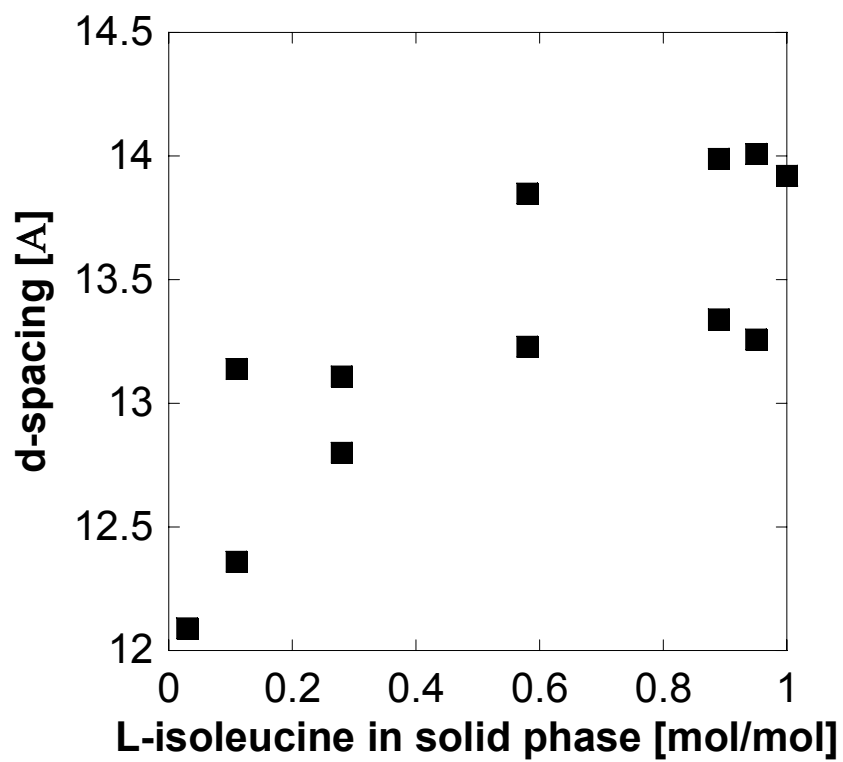
Figure 5-8 d-spacing of the crystals of L-ILE + L-VAL + water versus L-LEU composition in the solid phase.
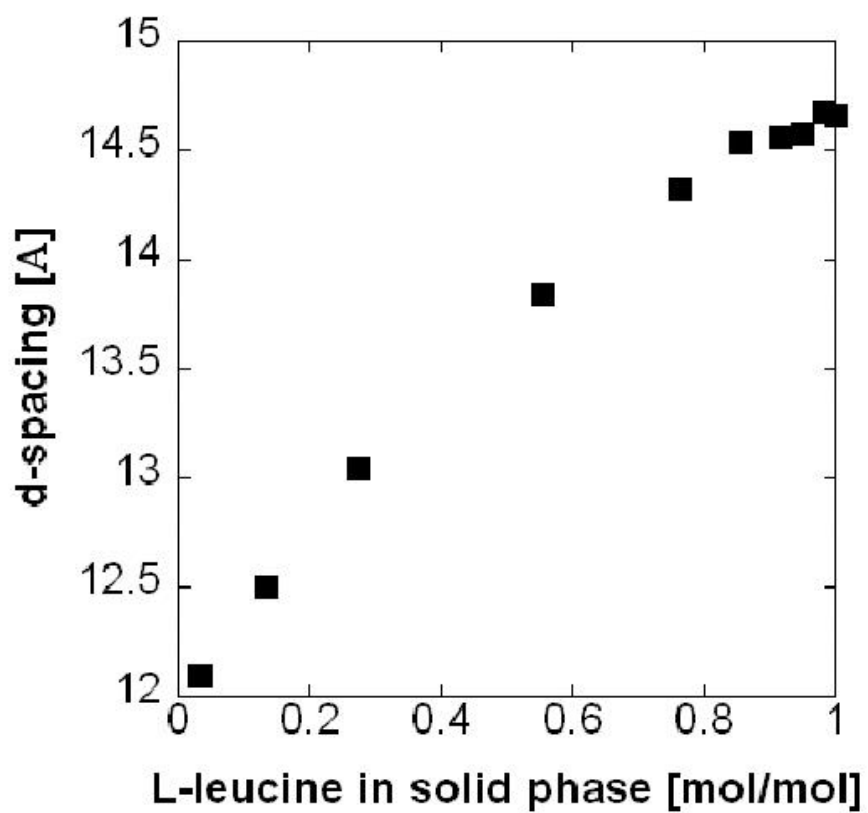
Figure 5-9 d-spacing of the crystals of L-LEU + L-VAL + water versus L-LEU composition in the solid phase.

The significant nonideality exhibited by the solid phases is quite surprising, although such nonideality has also been reported in carbon dioxide + nitrous oxide + oxygen systems (De Stefani *et al.*, 2003). The activity coefficients in the liquid phase, on the other hand, were almost constant in the whole range of concentrations studied (Table 5-1), although it must be added that the solutions were quite dilute.

As a result of the behavior exhibited by the liquid-phase activity coefficients, it is possible to make the following assumption:

$$\gamma_i^{tern} = \gamma_i^{bin} = \gamma_i^{\infty} \tag{5-24}$$

Solid-phase activity coefficients were recalculated by substituting equation (5-24) into (5-23):

$$\Gamma_i^{tern} = \frac{1}{z_i^{tern}} \cdot \frac{\gamma_i^{tern} x_i^{tern}}{\gamma_i^{bin} x_i^{bin}} = \frac{1}{z_i^{tern}} \cdot \frac{x_i^{tern}}{x_i^{bin}} \tag{5-25}$$

and compared with the previous results. The comparison is shown in Figure 5-10, 5-11, and 5-12 for L-VAL + L-LEU + water, L-VAL + L-ILE + water, and L-ILE + L-LEU + water systems, respectively. The results obtained from equation (5-25) are almost the same as the results obtained using equation (5-23). This means that solid activity coefficients can be obtained from knowledge only of the composition of the solid phase and the binary and ternary solubilities.
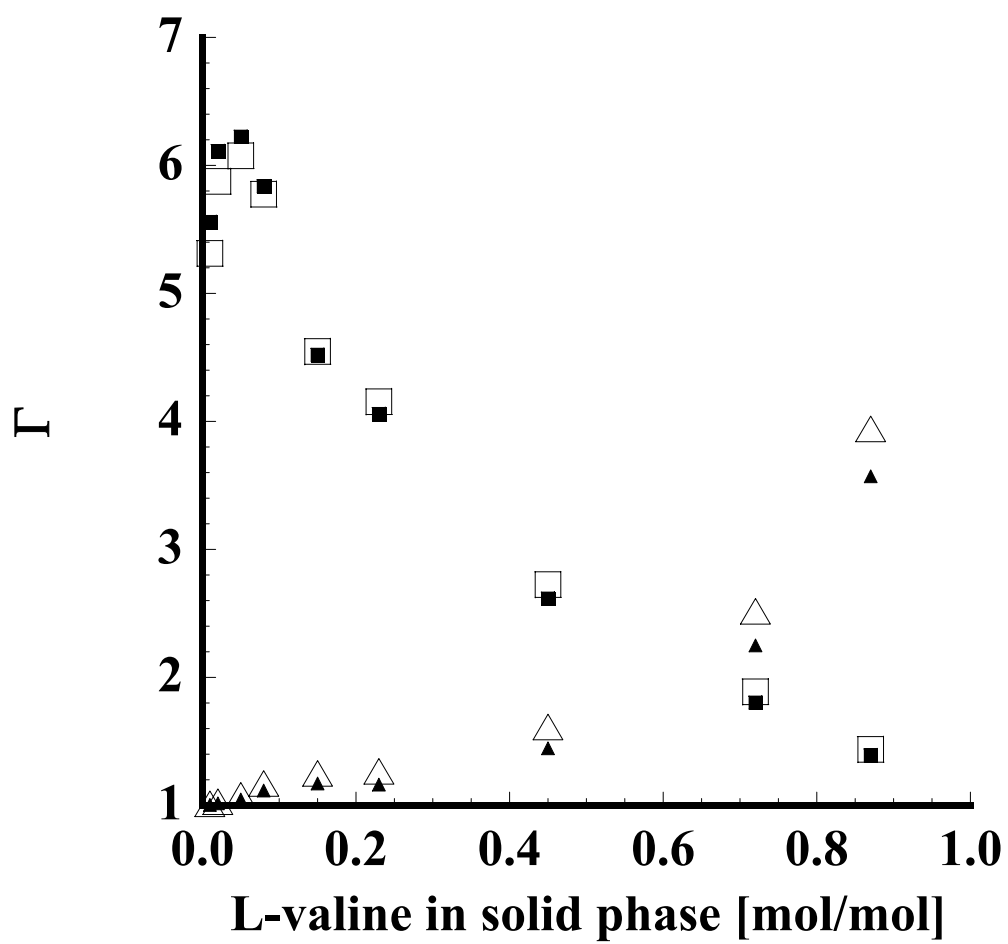
Figure 5-10. Activity coefficients in the solid phase in L-VAL + L-LEU + water systems: □ L-VAL and △ L-LEU obtained from equation (5-23), and ■ L-VAL and ▲ L-LEU obtained from equation (5-25).
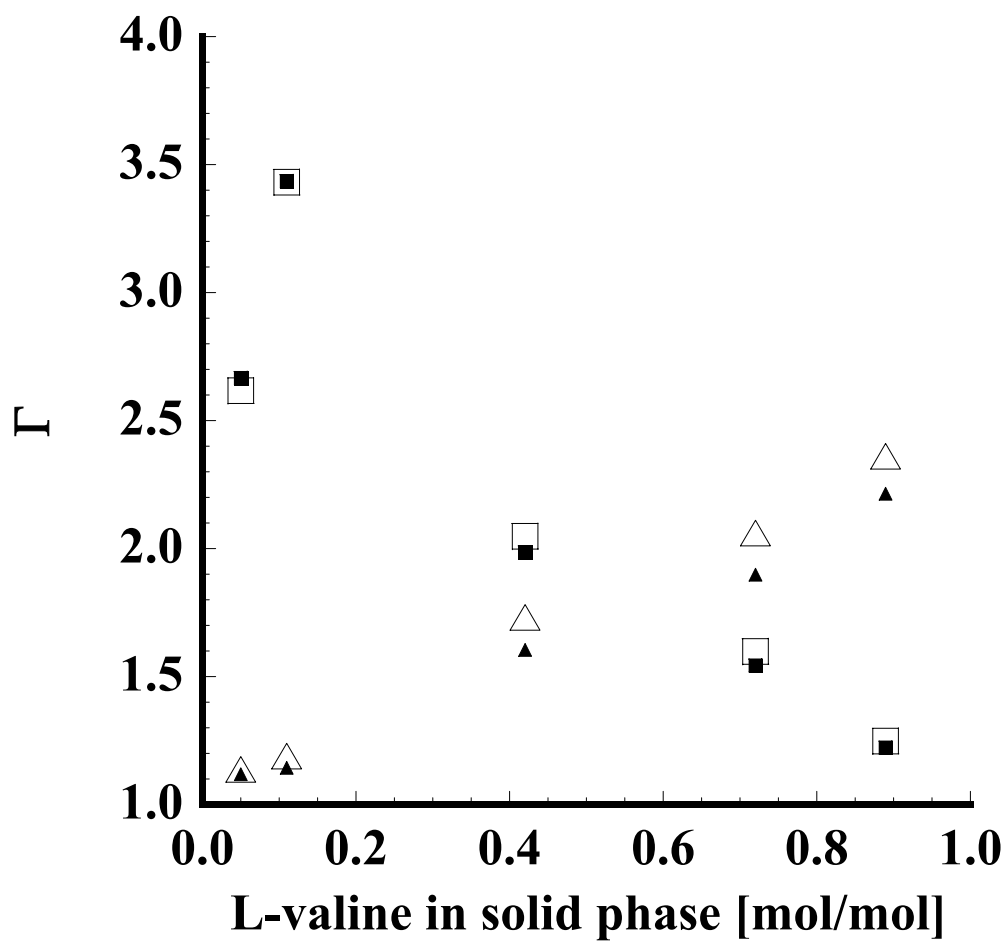
Figure 5-11. Activity coefficients in the solid phase in L-VAL + L-ILE + water systems: □ L-VAL and △ L-ILE obtained from equation (5-23), and ■ L-VAL and ▲ L-ILE obtained from equation (5-25).
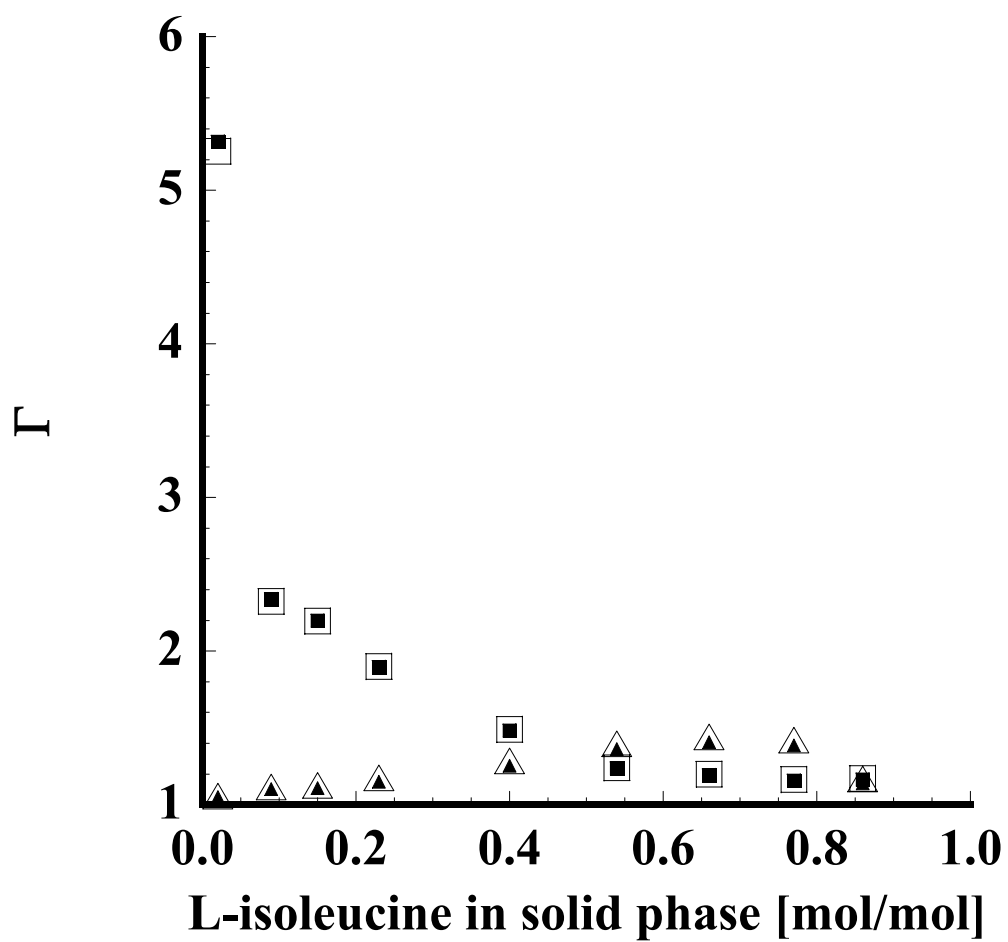
Figure 5-12. Activity coefficients in the solid phase in L-ILE + L-LEU + water systems: □ L-ILE and Δ L-LEU obtained from equation (5-23), and ■ L-ILE and ▲ L-LEU obtained from equation (5-25).

The same equation was also derived by Givand *et al*. (2002a). They wrote equation (5-22) for both components i and j and obtained the following:

$$\frac{z_i}{z_j} = \left(\frac{\gamma_i^{tern}/\gamma_i^{bin}}{\gamma_j^{tern}/\gamma_j^{bin}} \cdot \frac{\Gamma_j^{tern}}{\Gamma_i^{tern}} \right) \cdot \frac{x_j^{bin}}{x_i^{bin}} \cdot \frac{x_i^{tern}}{x_j^{tern}} = \xi \cdot \frac{x_j^{bin}}{x_i^{bin}} \cdot \frac{x_i^{tern}}{x_j^{tern}} \qquad (5\text{-}26)$$

where

$$\xi = \frac{\gamma_i^{tern}/\gamma_i^{bin}}{\gamma_j^{tern}/\gamma_j^{bin}} \cdot \frac{\Gamma_j^{tern}}{\Gamma_i^{tern}} \qquad (5\text{-}27)$$

Givand *et al*. further assumed that the amino acid solutions were dilute and therefore infinite dilution values could be substituted for the liquid-phase activity coefficients. As a result, the activity coefficient ratio ξ is approximately equal to the ratio of solid-phase activity coefficients Γ_i / Γ_j They also found that the solid mole fraction increases linearly with the liquid mole fraction, and concluded that the activity coefficient ratio, ξ, must be constant. However, their "purity" plots implicitly assume that the ratio of the mole fractions in the solid phase (z_i/z_j) can be replaced by the mole fraction of component i (z_i), and the ratio of the mole fractions in the liquid phase (x_i/x_j) can be replaced by the solvent-free mole fraction of component i {xi/(xi+xj)} in the plots. These assumptions are discussed below. Figure 5-13 and 5-14 show the difference between the plots of z_i/z_j vs x_i/x_j and z_i vs $x_i/(x_i+x_j)$ of L-VAL + L-LEU + water systems. It can be seen that the slopes of the two curves, which correspond to the activity coefficient ratio ξ, are different. Furthermore, the two curves are in agreement only at very low concentrations of i. It can therefore be concluded that the "purity" plots of Givand et al. are limiting cases of the more general correlations presented in this work.

By rearranging equation (5-26), the following equation can be obtained:

$$\xi = \left(\frac{z_i}{z_j} \right) \bigg/ \left(\frac{x_i^{tern}}{x_j^{tern}} \right) \cdot \frac{x_i^{bin}}{x_j^{bin}} \qquad\qquad (5\text{-}28)$$

The activity coefficient ratio, ξ, is plotted as a function of the solid phase composition in Figure 5-15, 5-16, and 5-17. From these figures, it is obvious that the activity coefficient ratio can be assumed to be constant only in the dilute region where Givand *et al.* (2002b) measured their purities. It is also obvious that both liquid and solid phase compositions are necessary to represent the phase behavior.

It should also be mentioned that the addition of co-solvents or co-solutes leads to changes in the activity coefficient ratio (see Appendix F), which is contrary to the idea of Givand (2000a). It indicates that the liquid-phase and/or solid-phase activity coefficients of the two amino acids depend on the type and concentration of additives. Since no activity coefficients are available in such systems, additional research is required to determine which phase contributes most to the change in the activity coefficient ratio.
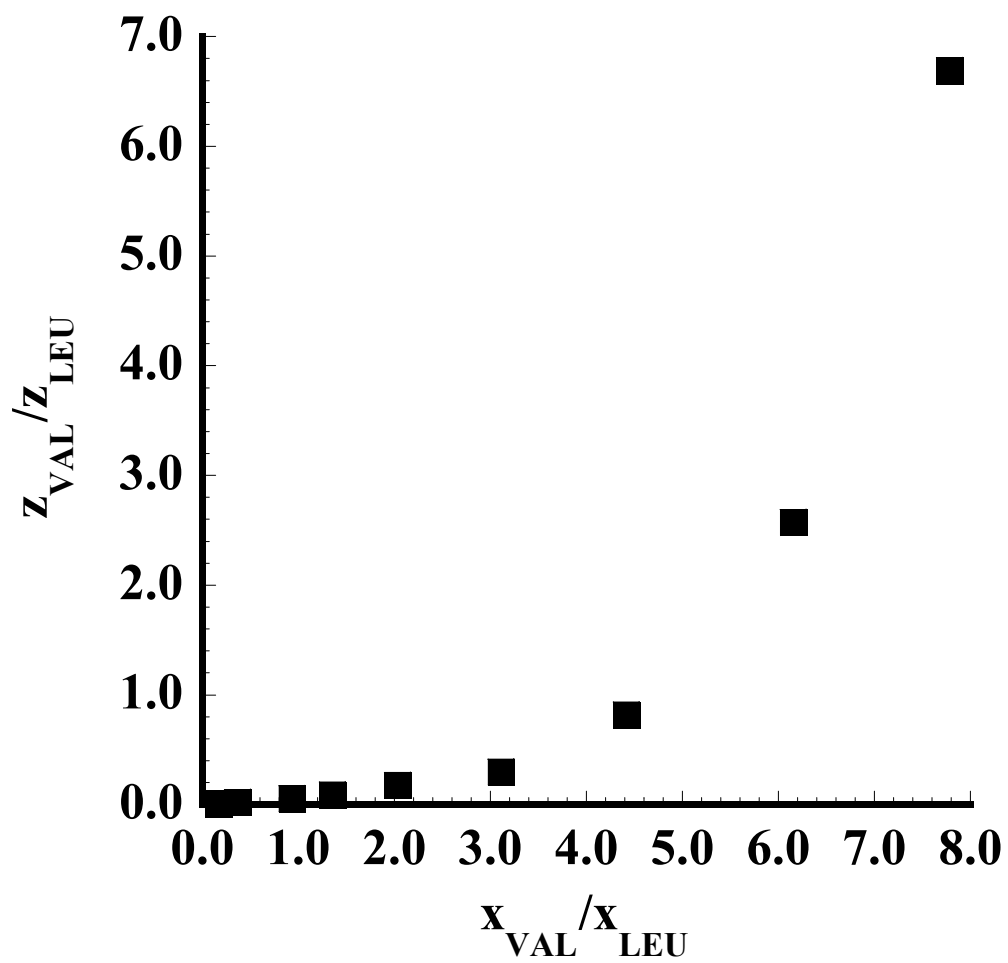
Figure 5-13 z_i/z_j versus x_i/x_j in the L-VAL + L-LEU + water system.
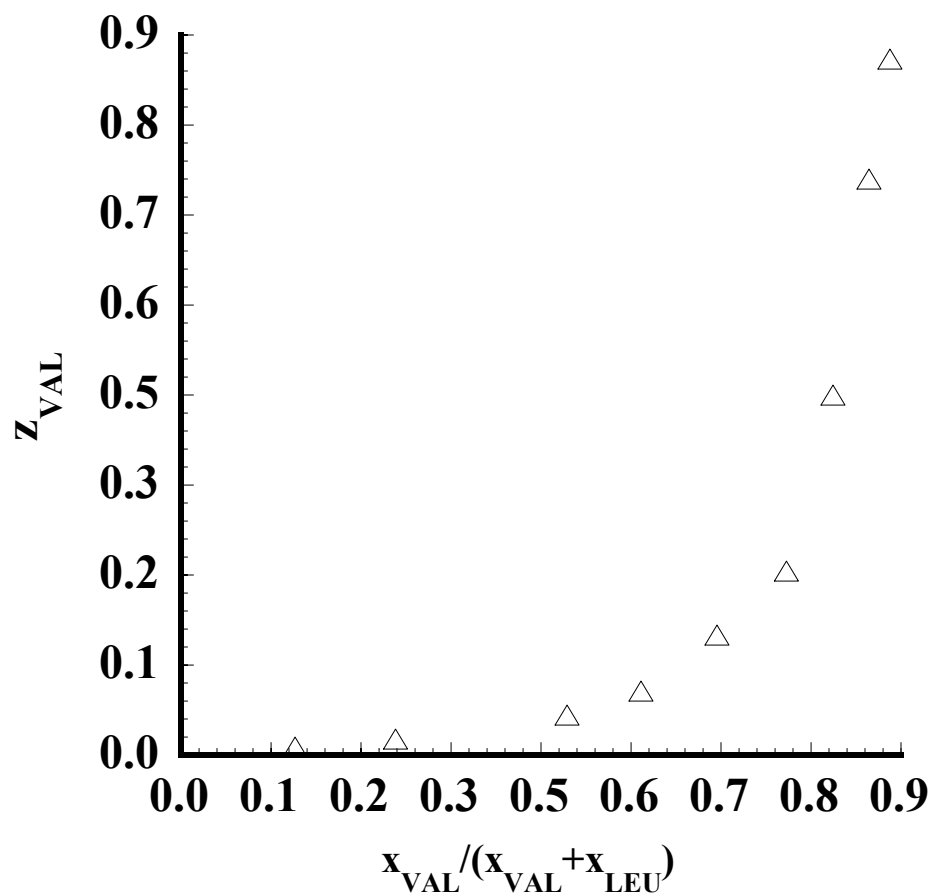
Figure 5-14 z_i versus $x_i/(x_i+x_j)$ in the L-VAL + L-LEU + water system.
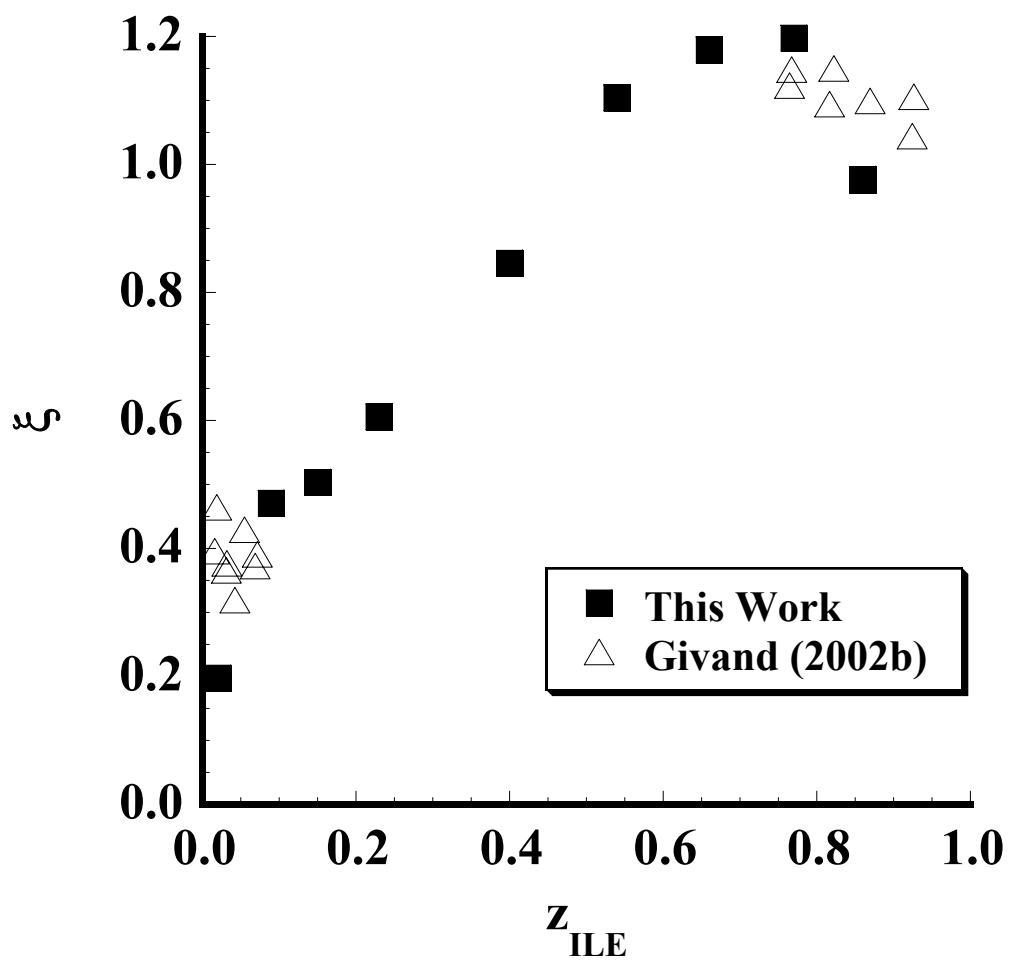
Figure 5-15 Activity coefficient ratio, ξ, versus the solid composition of L-ILE in the L-ILE + L-LEU + water system.
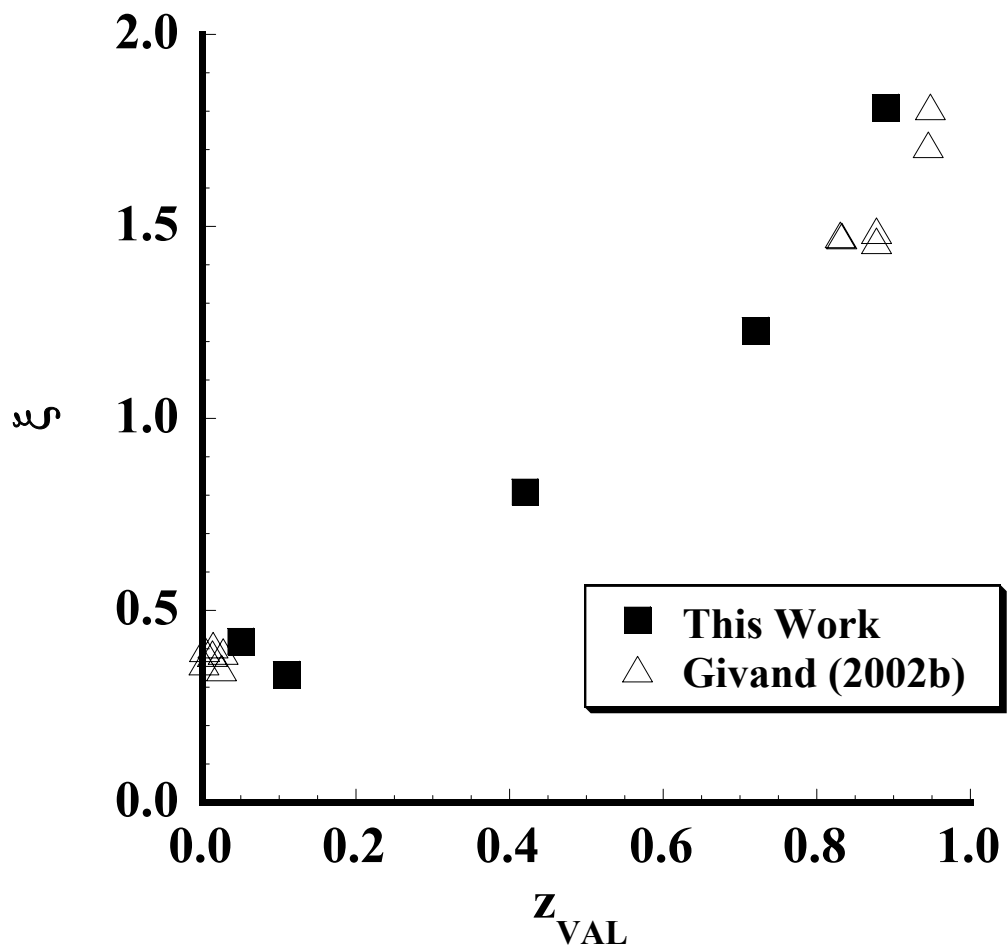
Figure 5-16 Activity coefficient ratio, ξ, versus the solid composition of L-VAL in the L-VAL + L-ILE + water system.
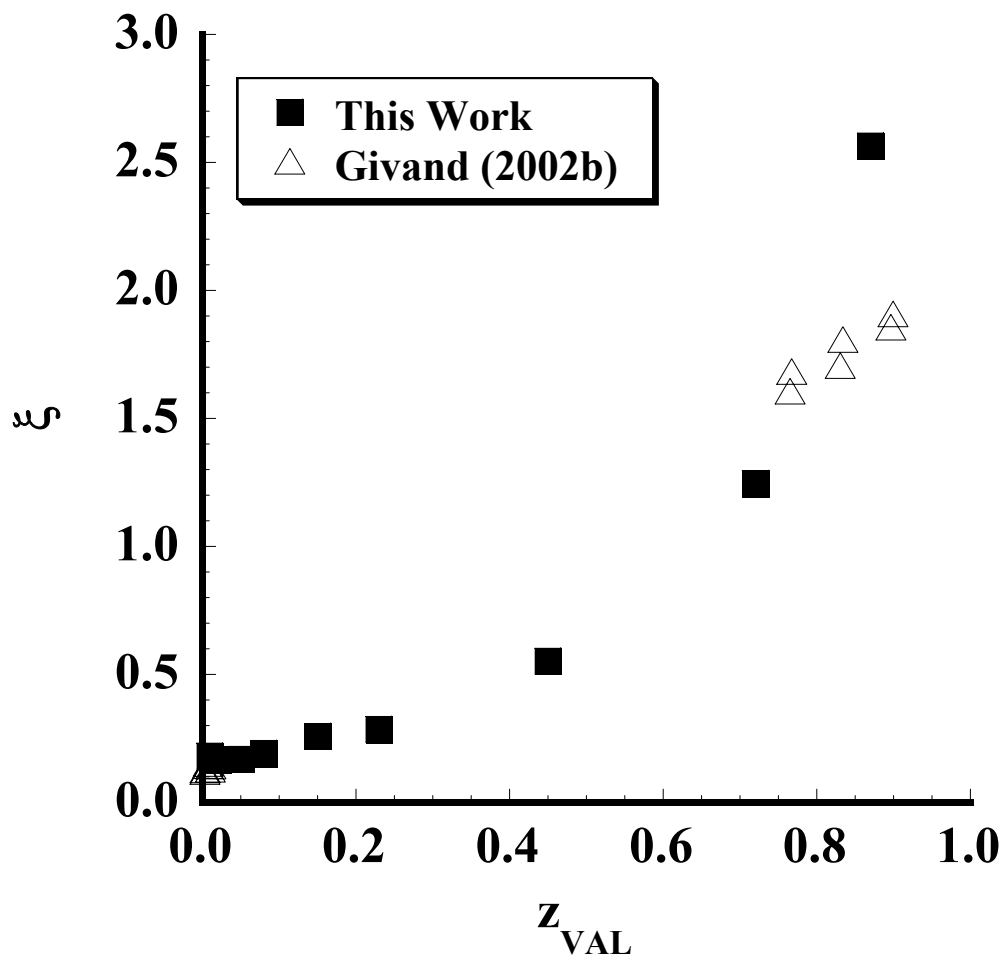
Figure 5-17 Activity coefficient ratio, ξ, versus the solid composition of L-VAL in the L-VAL + L-LEU + water system.

In order to check the applicability of equation (5-23) to other systems, solid-phase activity coefficients were calculated in the same manner for n-alkane mixtures (docosane (C22) and tetracosane (C24) in heptane (C7)). Flöter *et al.* (1997) reported that the solid phase in this system consists of C22 and C24 only. The composition of the solid phase was not reported, but assumed to be the same as the feed compositions of C22 and C24. Solid-phase activity coefficients were therefore estimated using equation (5-23) with liquid-phase activity coefficients from regular solution theory:

$$\ln\gamma_i = \frac{v_i(\bar{\delta} - \delta_i)^2}{RT} \qquad (5\text{-}29)$$

where

$$\bar{\delta} = \sum \phi_i \delta_i \qquad (5\text{-}30)$$

and

$$\phi_i = \frac{x_i v_i}{\sum x_i v_i} \qquad (5\text{-}31)$$

where v_i, ϕ_i, δ_i, $\bar{\delta}$ are molar volume, volume fraction, solubility parameter of component i, and average solubility parameter of the mixture, respectively. The results are shown in Figure 5-18. It can be seen that the solid-phase activity coefficients of both components increase monotonically with C22 composition, which is not realistic because these values do not satisfy the Gibbs-Duhem relationship:

$$d\ln a_i = -\frac{z_i}{z_j} d\ln a_j \qquad (5\text{-}32)$$

Lira-Galeana *et al.* (1996) predicted the solubility of each component in the liquid phase by assuming mixed pure crystals in the solid phase and by applying the regular solution theory for the calculation of activity coefficients in the liquid phase. However, the

assumption of mixed pure crystals is not valid because the liquid composition should be fixed at a eutonic point if both C22 and C24 exist as pure crystals. The experiments conducted by Flöter *et al.* show that this is not the case.

Whether the solid phase of n-alkane mixtures is composed of pure mixed crystals or of solid solution is yet to be resolved (Hansen *et al*., 1988; Pedersen *et al*., 1991; Erickson *et al.*, 1993; Snyder *et al.*, 1994, Lira-Galeana *et al.*, 1996). The analysis presented in this work shows that C22 and C24 crystals probably form solid solutions and the compositions of both the solid solution and the liquid solution must be reported for the data to be meaningful.
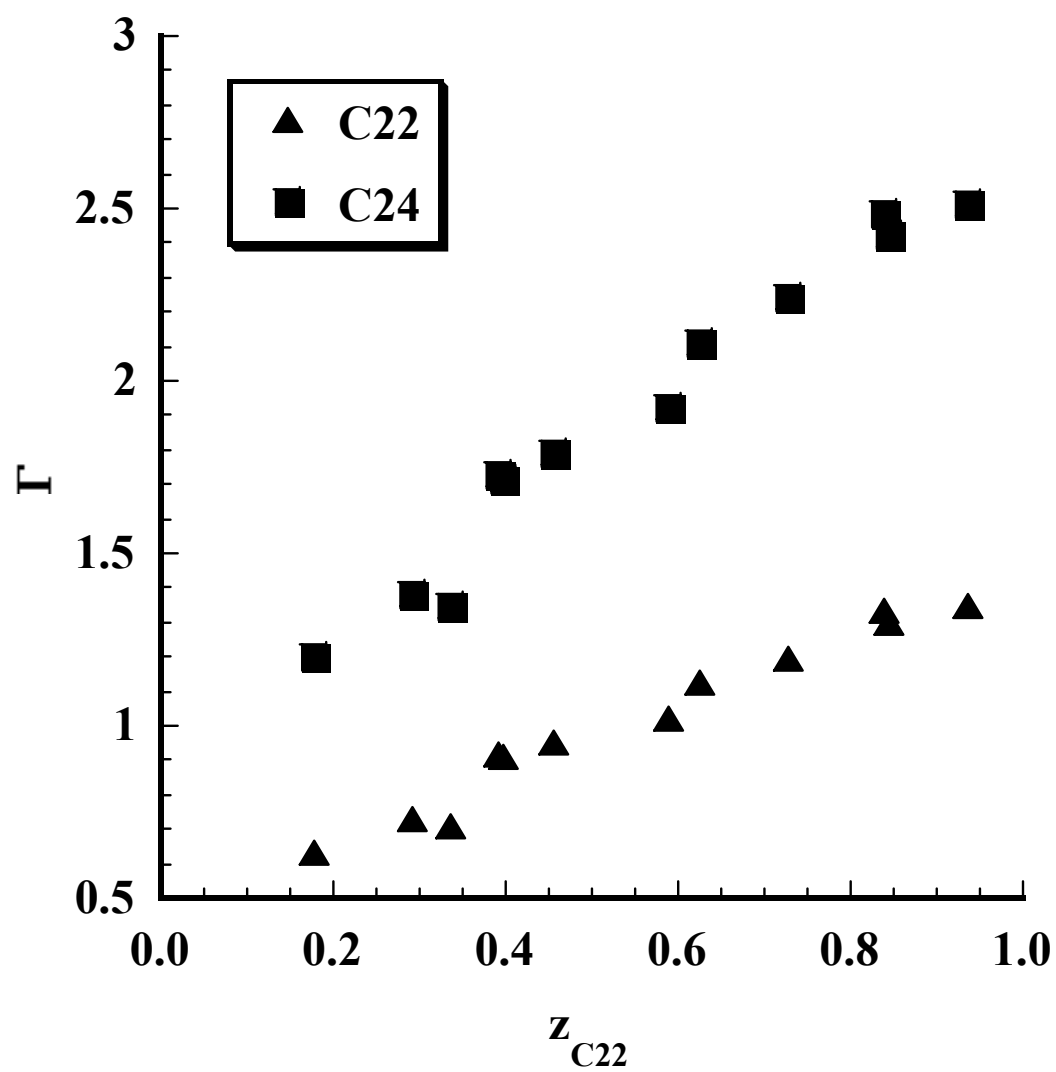
Figure 5-18. Activity coefficients of docosane (C22) and tetracosane (C24) in the solid phase.

Solid- phase activity coefficients of the amino acids tabulated in Table 5-1 were
fitted to the Margules model:

$$\ln\Gamma_1 = (2A_{12} - A_{21})z_2^2 + 2(A_{21} - A_{12})z_2^3 \tag{5-33}$$

$$\ln\Gamma_2 = (2A_{21} - A_{12})z_1^2 + 2(A_{12} - A_{21})z_1^3 \tag{5-34}$$

The regression results are shown as solid curves in Figures 5-19, 5-20, and 5-21 for L-
VAL + L-LEU + water, L-VAL + L-ILE + water, and L-ILE + L-LEU + water systems,
respectively. The parameters determined by least-square fitting are tabulated in Table 5-2.
The correlation works reasonably well for all the systems studied in this work in the
whole range of the composition, although the R^2 values are not very close to 1. However,
given the errors inherent in the liquid-phase activity coefficients and also in the
experiments, this may be considered to be satisfactory.

In order to explore the possibility of using the Margules model to predict the
parameters for ternary systems, the two fitting parameter were correlated using the binary
solubility of each amino acid in water, x^*_i. The results are shown in Figure 5-22, which
shows that the parameters have a linear relationship with the binary solubility ratio as
follows:

$$A_{ij} = a \cdot \frac{x^*_i}{x^*_i + x^*_j} + b \tag{5-35}$$

The constants a and b for each system are listed in Table 5-3. The success of the
correlation suggests that the activity coefficients of the solid phase in solid solutions may
be estimated with a set of binary solubility data of each component in a solvent.
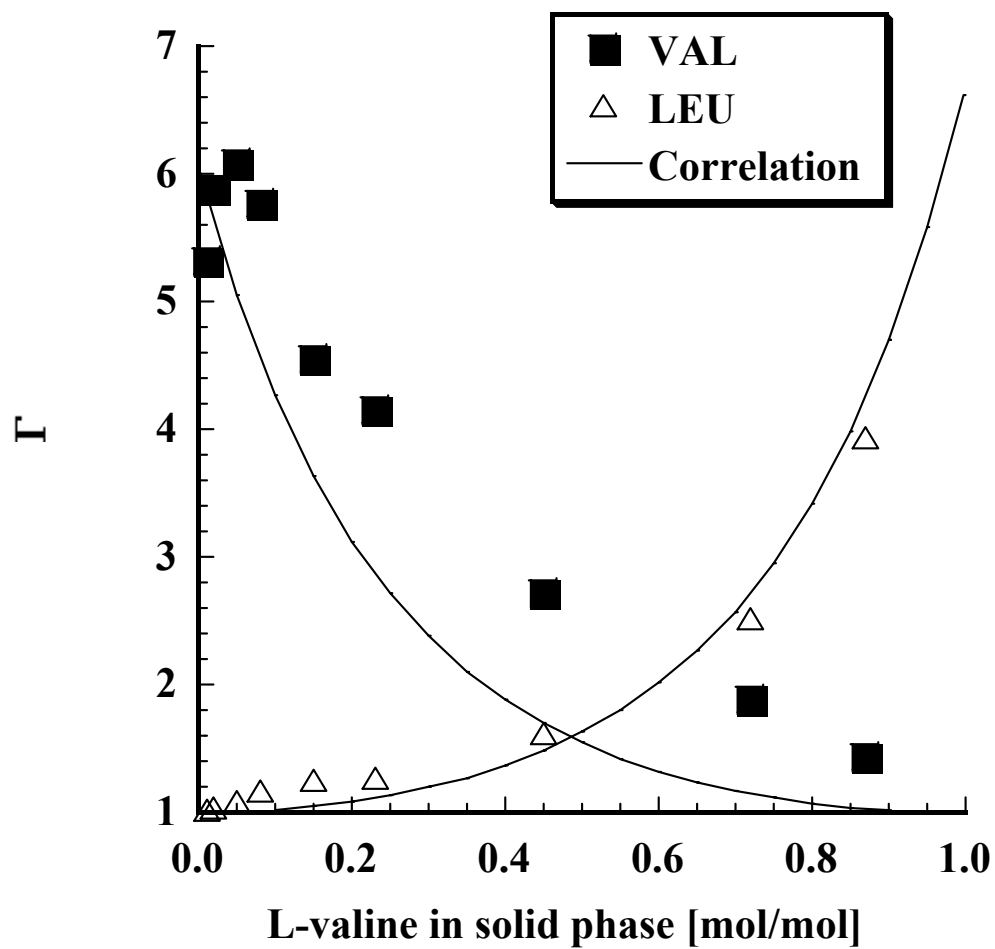
Figure 5-19. Correlation of activity coefficients in the solid phase in VAL + LEU + water systems.
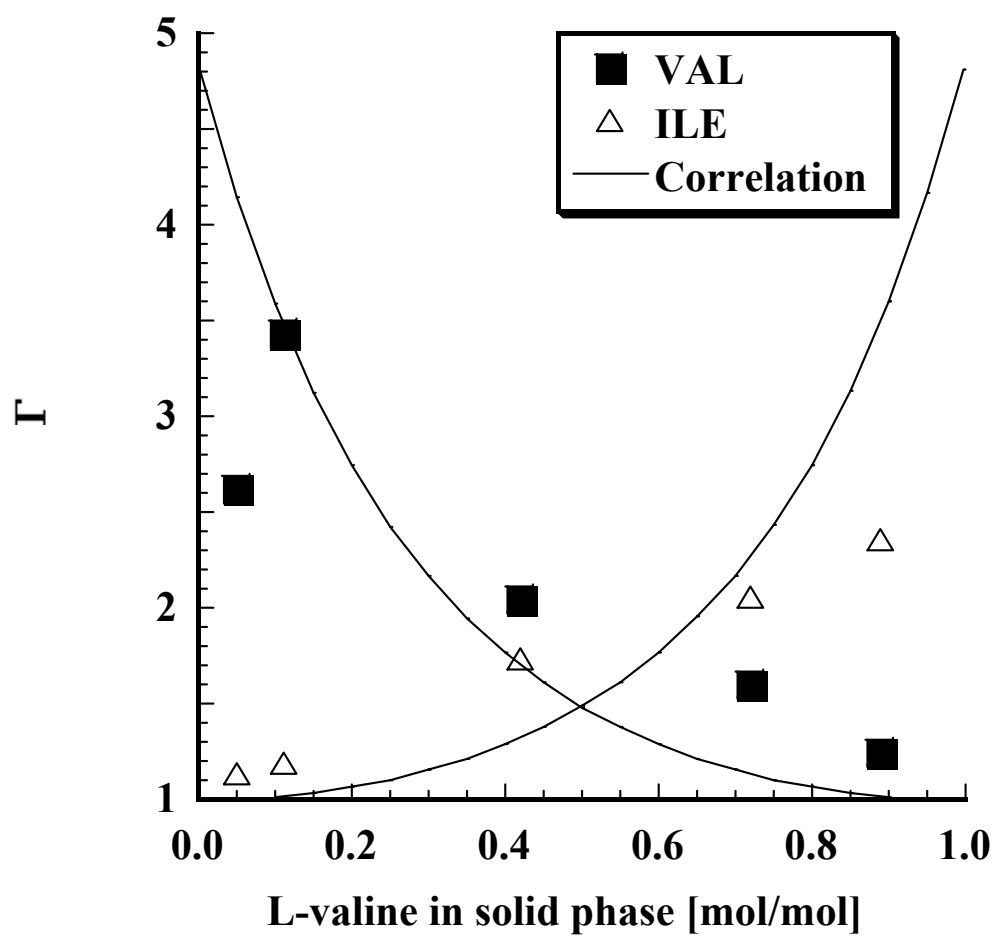
Figure 5-20. Correlation of activity coefficients in the solid phase in L-VAL + L-ILE + water systems.
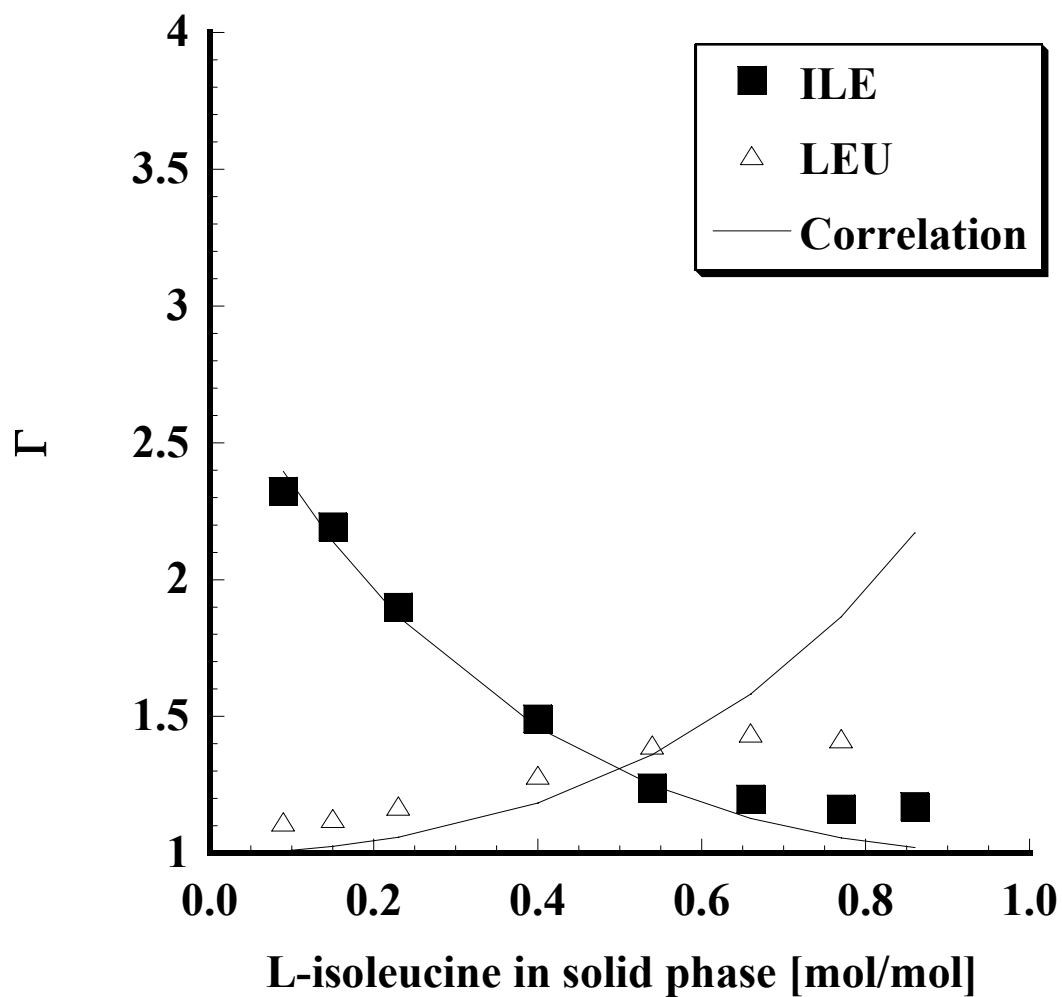
Figure 5-21. Correlation of activity coefficients in the solid phase in L-ILE + L-LEU + water systems.

Table 5-2. Fitting parameters for Margules equation.

	$x_1/(x_1+x_2)$	A_{12}	A_{21}	R^2
L-VAL(1) + L-LEU(2)	0.75	1.90	1.90	0.86
L-VAL(1) + L-ILE(2)	0.67	1.58	1.58	0.77
L-ILE(1) + L-LEU(2)	0.60	1.06	1.04	0.63
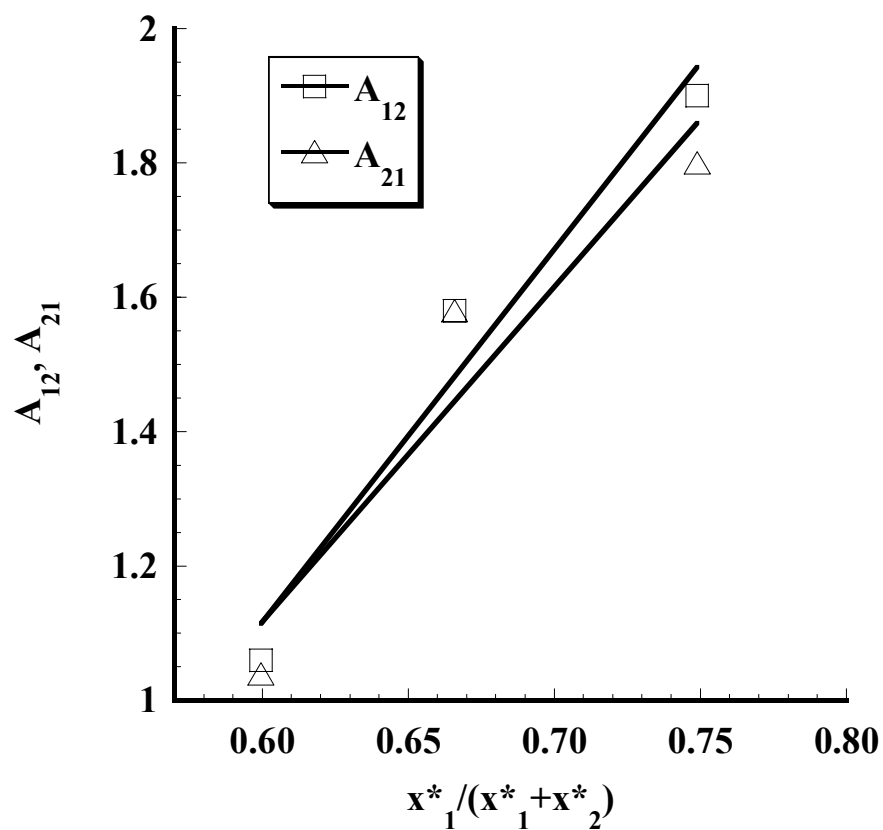
Figure 5-22. Fitting parameters for Margules equation as a function of the binary solubilities.

Table 5-3. Fitting parameters for the linear equation (5-35).

	a	b	R^2
A_{12}	5.55	-2.21	0.96
A_{21}	4.99	-1.87	0.95

5.4   An empirical correlation for crystal purity as a function of liquid composition

It was shown in the previous section that the solid phase in equilibrium with an aqueous solution of two amino acids is quite nonideal and that the solubilities in the ternary systems can be estimated using binary solubility data. In this section, an alternative empirical correlation is proposed for crystal purity (or solid composition) as a function of the liquid composition.

Solid- and liquid-phase mole fractions (on a solvent-free basis) of the less soluble amino acids at equilibrium are plotted in Figure 5-23. It can be seen that the experimental data lie above the diagonal line, indicating that a less-soluble component is preferentially partitioned into the solid phase. Moreover, the data apparently follow sigmoid behavior above the diagonal. We may therefore write:

$$z_i = \frac{1}{1 + \exp\left(-a_{ij}\left(x_i - b_{ij}\right)\right)} \tag{5-36}$$

where a and b are system-dependent parameters. The results of fitting experimental data to equation (5-36) are shown as solid curves in Figure 5-23. The parameters determined by least-squares fit of the data are tabulated in Table 5-4. A similar function is used for modeling populations of bacterial colonies (Hajmeer and Basheer, 2003).

By analogy with bacterial growth, consider the case where a pair of chemical species in a solvent is precipitated independently. When the number of crystals of each species i and j increases geometrically at different rates, the total number of each species in the solids, y, can be described as follows:

$$y_i \equiv \alpha_i^x \cdot \beta_i \tag{5-37}$$

$$y_j \equiv \alpha_j^x \cdot \beta_j \qquad (5\text{-}38)$$

where α is an increment coefficient, β is an initial number, and x is a constant. The fraction of species i, z_i, is then expressed by:

$$z_i \equiv \frac{y_i}{y_i + y_j} = \frac{\alpha_i^x \cdot \beta_i}{\alpha_i^x \cdot \beta_i + \alpha_j^x \cdot \beta_j} = \frac{1}{1 + (\beta_j / \beta_i) \cdot (\alpha_j / \alpha_i)^x} \qquad (5\text{-}39)$$

where

$$a_{ij} \equiv \ln(\alpha_i / \alpha_j) \qquad (5\text{-}40)$$

$$b_{ij} \equiv -\ln(\beta_i / \beta_j) / \ln(\alpha_i / \alpha_j) \qquad (5\text{-}41).$$

Since

$$(\alpha_j / \alpha_i) = \exp(-a_{ij}) \qquad (5\text{-}42)$$

$$(\beta_j / \beta_i) = \exp(a_{ij} b_{ij}) \qquad (5\text{-}43),$$

rearranging equation (5-39) yields

$$z_i = \frac{1}{1 + \exp(a_{ij} b_{ij}) \cdot (\exp(-a_{ij}))^x} = \frac{1}{1 + \exp(-a_{ij}(x - b_{ij}))} \qquad (5\text{-}44).$$

Note that this equation is equivalent to the logarithmic function used above when x is replaced by x_i. The formation of solid solutions therefore may be comparable to co-precipitation in which solutes with similar chemical structure are competitively recrystallized. Ease of recrystallization may be related to the relative (binary) solubility; therefore, this should be reflected in the values of the parameters. Note that in each system the parameter b, which corresponds to the liquid mole fraction of the less-soluble species at $z_i = 0.5$, is close to the value, $x^*_i/(x^*_i + x^*_j)$, depending only on binary solubility data. Furthermore, the product of a and b in each system is close to 2.5. These empirical

relationships may be used for the prediction of crystal purity in other systems forming solid solutions.

It should be added that the advantage of the logarithmic model is that extension to multi-component systems can be made using the following relationship:

$$z_i \equiv \frac{y_i}{\sum_{k=i,j,\dots} y_k} \tag{5-45}.$$

Therefore, solid-liquid equilibria of multi-component systems of more than two solutes may be predicted by the application of equation (5-45). A disadvantage of the model is, however, that the model does not yield the correct behavior when $x \approx 0$ or when $x \approx 1$. In the case of the bacterial growth, the value of z at $x=0$ represents the feed composition of the bacterial mixture (having a non-zero value). However, in the case of amino acid mixtures, z should be always zero at $x=0$ in the case of solid-liquid equilibrium. Note that the logarithmic model is used for this correlation not because the model can explain the behavior theoretically, but because the plots of solid- and liquid- compositions exhibit sigmoid curves. Therefore, in order to generalize this model, further analysis is required.
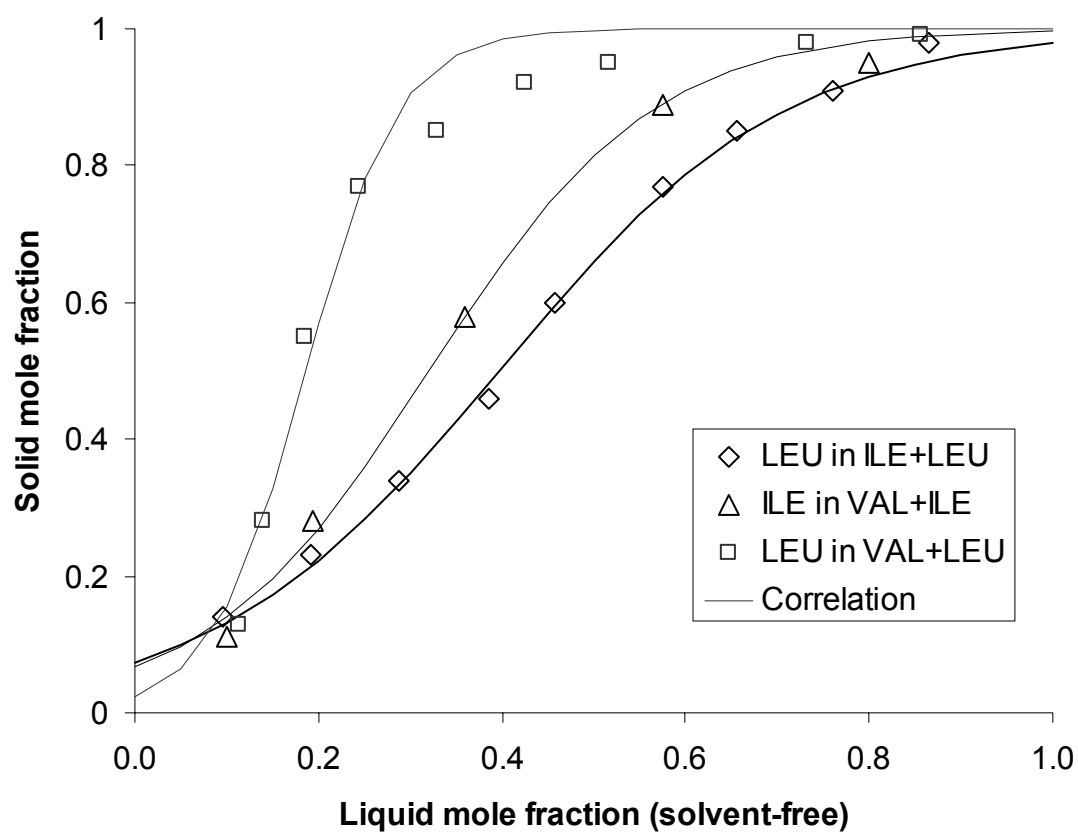
Figure 5-23. Solid and liquid-phase mole fractions (on a solvent-free basis) of amino acids at equilibrium.

Table 5-4. Fitting parameters and binary solubility data.

Solutes		a_{ij}	b_{ij}	$a_{ij}\,b_{ij}$	$\dfrac{x^*_i}{x^*_i + x^*_j}$	Solubility [mol/mol] $\times 10^3$	
i	j					x^*_i	x^*_j
L-LEU	L-ILE	6.38	0.396	2.53	0.394	2.96	4.54
L-ILE	L-VAL	8.26	0.321	2.65	0.332	4.54	9.13
L-LEU	L-VAL	19.8	0.186	3.69	0.245	2.96	9.13

CHAPTER 6

CONCLUSIONS AND RECOMMENDATIONS

6.1   Conclusions

Solid-liquid equilibrium in isomorphous amino acid systems has been investigated as a model for systems that form solid solutions. Solid- and liquid-phase compositions in L-valine + L-leucine + water, L-valine + L-isoleucine + water, and L-isoleucine + L-valine + water were measured over the entire range of solid compositions, and it was shown (from mass balance and phase rule considerations) that these systems form solid solutions. The solid phases resulting from isothermal and cooling crystallization experiments were also investigated using powder x-ray diffractometry, which showed that homogeneous solid solutions could only be obtained in cooling crystallization experiments, whereas isothermal experiments generally produced inhomogeneous solids. This suggests that the determination of SLE via isothermal experiments can lead to erroneous results when the solid phase consists of isomorphous or near-isomorphous compounds that are able to substitute easily into the crystal lattices and form solid solutions. This was found to be true in the case of L-LEU, L-Val, and L-ILE. Therefore, cooling experiments, combined with solid-phase composition and XRD analyses, should be used for determining SLE in systems that form solid solutions.

Solid-phase activity coefficients were estimated using binary and ternary equilibrium data and the UNIFAC-Kuramochi model to account for liquid-phase nonidealities. The solid phases in the three systems investigated exhibited significant nonidealities. The activity coefficients in the liquid phase, on the other hand, were almost constant in the whole range of concentrations. This suggests that the infinite dilution assumption may be valid for amino acid solutions. The data of Givand et al. (2002b) were replotted in terms of (z_i/z_j) and (x_i/x_j) and it was verified that the activity coefficient ratio, ξ, is approximately constant in the infinitely dilute region as suggested by Givand *et al.* (2002a). However, this is valid only in a very dilute region.

Solid-phase activity coefficients were correlated using the Margules model. The model parameters exhibited a linear relationship with the ratio of binary solubilities of the two solutes. Therefore, these activity coefficients may be predicted from knowledge of the relative solubilities of the pure amino acids in the solvent. This is in agreement with the qualitative observations of Givand *et al* (2002a).

An empirical correlation was also proposed for crystal purity as a function of the liquid composition. The data exhibited sigmoid behavior that can be described with a two-parameter logarithmic function. Moreover, the parameters of this empirical model also exhibited a simple relationship to the binary solubility ratio. These results may facilitate the prediction of crystal purity at an arbitrary liquid composition in other systems forming solid solutions since the parameters require only binary solubility data. Such simple relationship may be advantageous when solid-liquid equilibrium of thermally unstable solutes or components with unknown physical properties are crystallized.

6.2 **Recommendation**

In order to predict solid-liquid equilibrium in multi-component systems, accurate and reliable thermodynamic data are necessary. For example, if the concentration of the solution is not low, nonideality in the liquid phase may not be negligible. Besides, addition of co-solvent and/or co-solute may change the liquid-phase nonideality significantly, resulting in salting-out and/or salting-in behavior. Therefore, the liquid-phase activity coefficients of systems of interest should be obtained experimentally, and compared with those estimated by a model such as the UNIFAC-Kuramochi model for consistency. Liquid-phase activity coefficients may be obtained from osmotic coefficient measurements (Appendix D). Furthermore, solid-phase activity coefficient data are rarely reported in the literature; therefore, simultaneous measurements of both solid and liquid compositions should be carried out.

In this study, the temperature at equilibrium was fixed at 298 K although the processing temperature for crystallizing amino acids in industry may vary. Therefore, temperature dependence should be investigated to extend the model to practical applications. The extension of the model to other systems such as the alkanes should also be considered. Whether the solid phase of n-alkane mixtures is composed of pure mixed crystals or of solid solution is yet to be determined. To resolve this problem, the compositions of both solid and liquid solutions must be measured simultaneously.

The model in this study may be applicable to the study of hydrates whose solubility depends on solid-phase morphology (Grant and Higuchi, 1990). For hydrates, it is difficult to determine the crystal structure equilibrated with the solution attached in situ. Therefore, this model may be used to infer the composition of the solid phase

because in the model the nonideality in solid phase can be represented using the parameters obtained only from binary solubility data.

Molecular simulation could be combined with powder XRD analysis to provide information on physical properties of mixtures or crystal dimensions, and hence, Margules parameters.

APPENDIX A

TIME TO ATTAIN EQUILIBRIUM

The time required to attain equilibrium must be known in order to measure the equilibrium compositions of the solid and liquid. The variation in concentration with time in the case of the ILE + LEU + water system is presented in Table A5 and Figure A5. The system was cooled from 353 K to 298 K in about one hour. Both ILE and LEU concentrations in the liquid phase decreased during cooling, and leveled off after 24 hours of cooling. Other systems also reach equilibrium within 24 hours. Therefore, it was assumed that equilibrium is attained in all systems studied within 24 hours.

Table A-1 The change in concentration of ILE and LEU in the liquid phase with time during cooling.

TIME[hour]	ILE [g/kg water]	LEU [g/kg water]
0	31.21	21.14
3	23.55	14.55
17	23.28	14.62
27	23.18	14.62
49	23.23	15.11
65	22.89	14.51
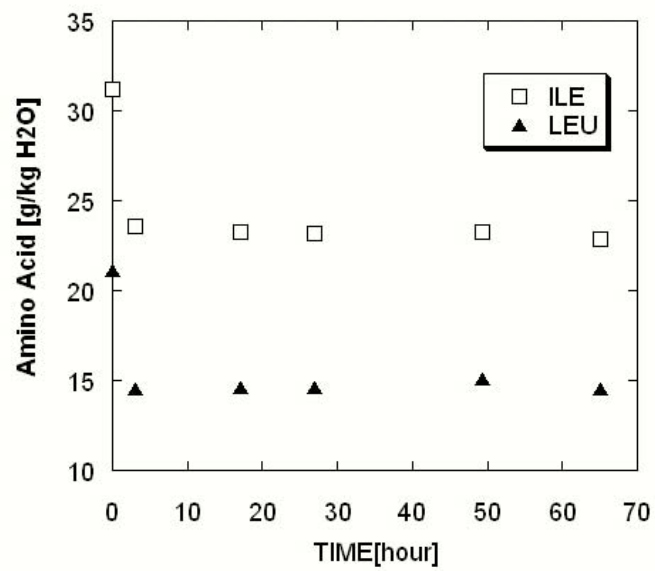
Figure A-1 Change of the concentrations of ILE and LEU with time during cooling.

APPENDIX B

SETTINGS FOR POWDER XRD MEASUREMENTS

Table B-1 Settings for powder XRD measurements.

Parameter	Value
Scan Angle	3-60 º
Scan Rate	2.5 º/min
Step Size	0.02 º
Number of Points	2851
Scan type	Normal
Current	15.0 mA
Voltage	45.0 kV

APPENDIX C

POWDER XRD PATTERNS
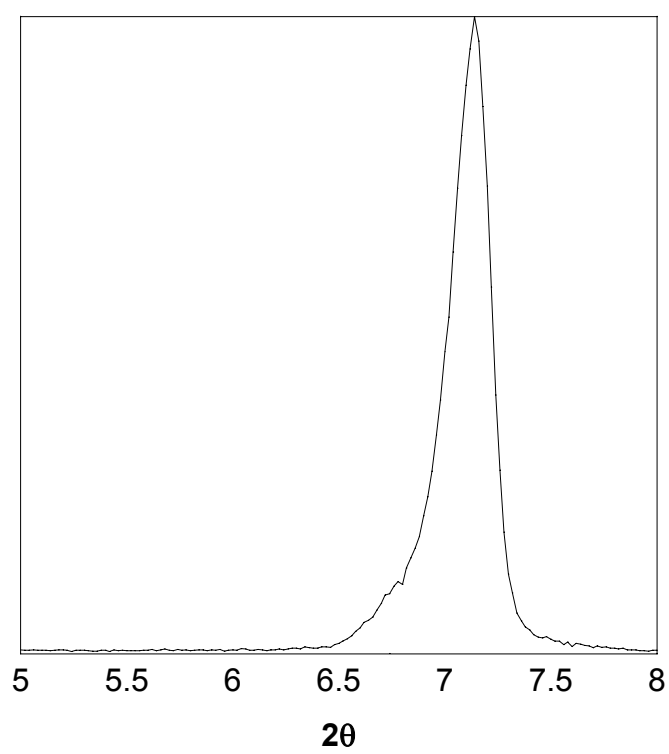
Figure C-1 Diffraction pattern of VI_C1.
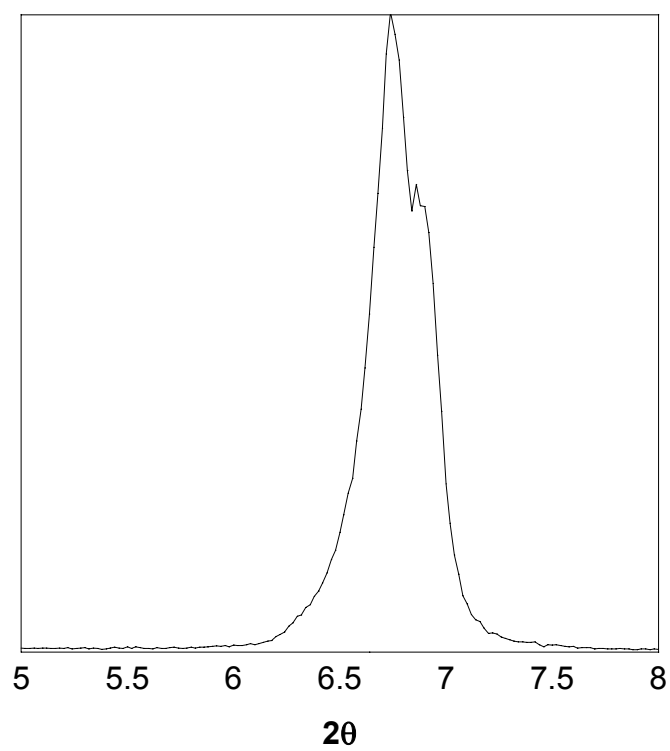
Figure C-2 Diffraction pattern of VI_C2.
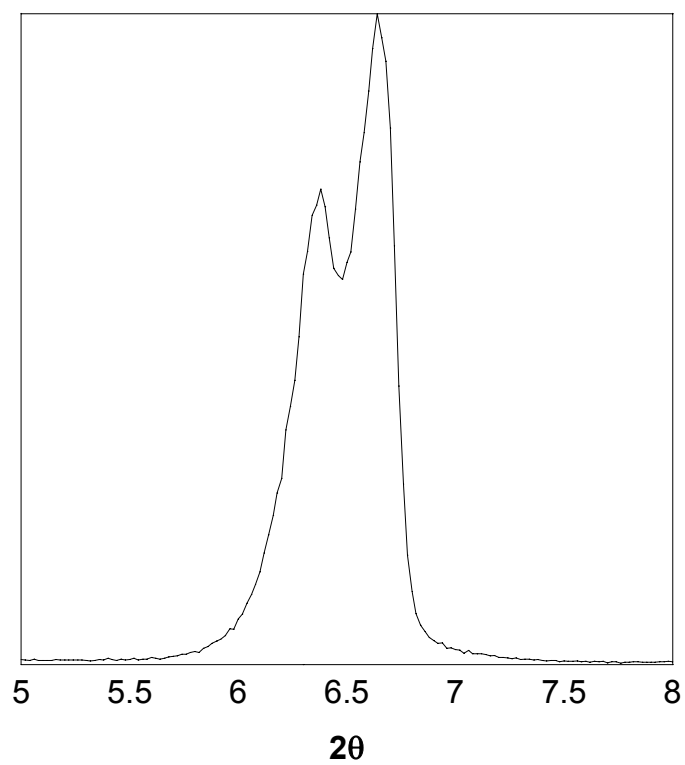
Figure C-3 Diffraction pattern of VI_C3.
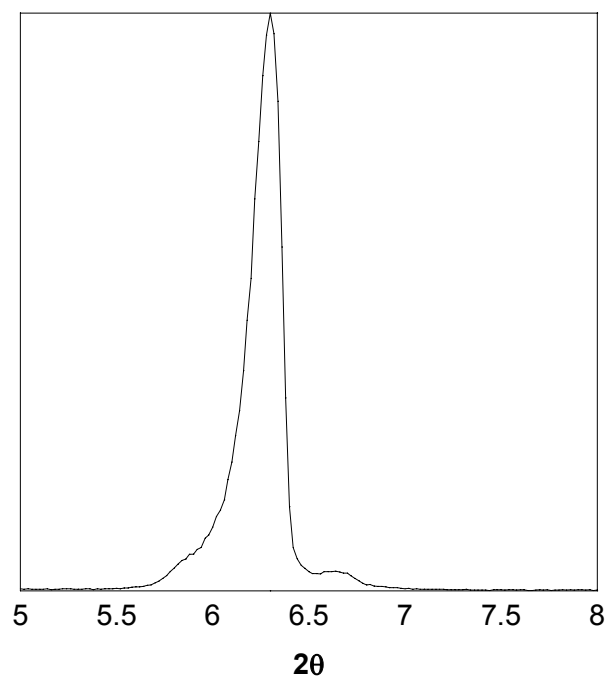
Figure C-4 Diffraction pattern of VI_C4.
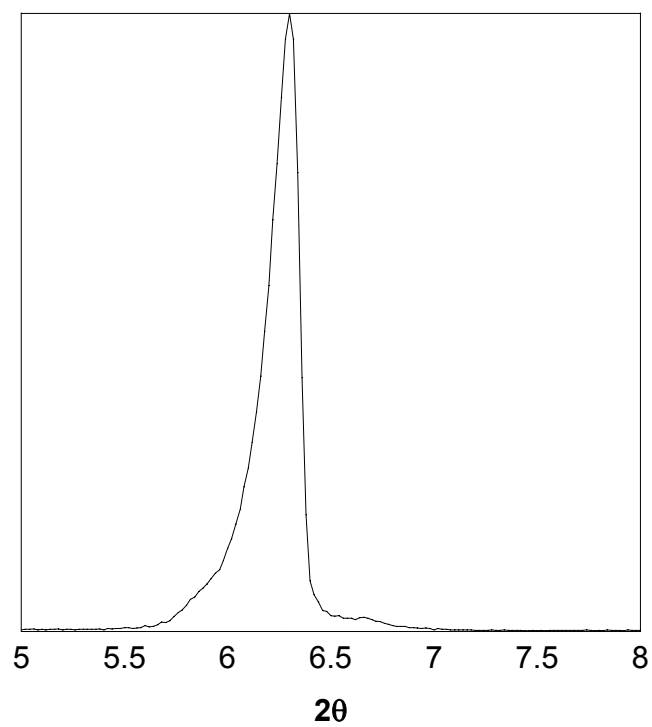
Figure C-5 Diffraction pattern of VI_C5.

APPENDIX D

ACTIVITY COEFFICIENT MEASUREMENTS

Activity coefficients of solutes in solutions can be obtained from a number of experiments such as measurements of vapor pressure, freezing-point depression, and boiling-point elevation. However, each method tends to suffer from experimental difficulties due to high sensitivity of the variables to interferences. For example, in the case of vapor pressure measurements, precise control of system temperature is required because the vapor pressure of the solvent is quite sensitive to a small temperature change. It is also hard to detect changes in solute concentration in dilute solutions. Furthermore, in the measurements of freezing-point depression and boiling-point elevation, additional thermodynamics data such as partial molar heat capacity are needed to calculate activity coefficients (Park et al., 1998).

Unlike the measurements above, the so-called isopiestic method has the ability to yield activity coefficients at arbitrary temperatures with less effort than the other methods (Lewis, 1923). Therefore, the isopiestic method was employed in this study to obtain liquid-phase activity coefficients of amino acids in water.

157

D.1 Calculation of activity coefficients in the isopiestic method

The activity of solute, a_1, in a binary solution is determined from activity of solvent, a_{sol}, using the Gibbs-Duhem equation:

$$d \ln a_1 = -\frac{x_1}{x_{sol}} d \ln a_{sol} \qquad \text{(D-1)}$$

where x_1 and x_{sol} denote the mole fraction of the solute and solvent, respectively. However, it is difficult to integrate equation (D-1) because the ratio x_1/x_{sol} approaches infinity for dilute solutions. Therefore, osmotic coefficient of the solvent in the solution, ϕ_1, has been used to overcome this problem, which for a single electrolyte dissociating into ν_1 ions per molecule on molality basis is defined by:

$$\phi_1 = -\frac{1000}{\nu_1 m_1 M_{sol}} \ln a_{sol} \qquad \text{(D-2)}$$

where m_1 denotes the molality of solute, and M_{sol} the molecular weight of the solvent. Substitution of equation (D-2) in equation (D-1) and integration from 0 to m_1 yields:

$$\ln \gamma_1 = (\phi_1 - 1) + \int_0^{m_1} \frac{(\phi_1 - 1)}{m'} dm' \qquad \text{(D-3)}$$

where γ_1 is the activity coefficient of the solute on molality basis. The equation (D-3) indicates that the calculation of activity coefficient at m_1 requires a set of osmotic data at concentrations from infinite dilution to m_1.

In the isopiestic method, a set of undersaturated solutions, of which initial solution masses and initial solute concentrations are known, is allowed to equilibrate in a closed

vessel at a constant temperature. When the sample solutions are in equilibrium with a reference solution, equation (D-2) yields:

$$\nu_i m_i \phi_i = \nu_r m_r \phi_r \tag{D-4}$$

where subscripts i and r denote solutions of component i and reference, respectively. Therefore, the activity coefficient of the solute in the sample solutions can be calculated from equations (D-3) and (D-4) if the osmotic coefficient in the reference solution is known. In this study, alkali chloride salts, potassium chloride (KCl) and sodium chloride (NaCl), were used to prepare the reference solutions since their osmotic coefficient data are available experimentally and analytically over a wide range of concentrations at 298 K (Hamer and Wu, 1972). The osmotic coefficients for the reference solutions have been expressed by the following equation (Hamer and Wu, 1972):

$$\phi_r = 1 - 2.302585 \cdot \{\frac{0.5108 \mid z_+ z_- \mid}{(B^*)^3 m_r}[(1 + B^* \sqrt{m_r}) - 4.60517 \, \log(1 + B^* \sqrt{m_r})$$
$$- 1/(1 + B^* \sqrt{m_r})] - \beta m_r / 2 - \frac{2}{3} C m_r^{\,2} - \frac{2}{3} D m_r^{\,3}\} \tag{D-5}$$

where z is ionic valency of the solute in the reference solutions. The constants for each solute in equation (D-5) are listed in Table D-1. In each experiment, a NaCl solution was used to determine the osmotic coefficients of samples whereas a KCl solution was used to confirm the reliability of the experiments and to calculate experimental errors (Park and Englezos, 1998).

In ternary systems, activity coefficients of amino acids in water have been calculated by analogy with electrolyte solutions. For example, Robinson and Stokes (1961) showed that the cross-differential relation pointed out by Guggenheim (1949) could be represented as follows:

159

$$\left(\frac{\partial \ln \gamma_1}{\partial m_2}\right)_{m_1} = \left(\frac{\partial \ln \gamma_2}{\partial m_1}\right)_{m_1} = -\frac{1}{v_1 m_1 v_2 m_2}\left(\frac{1000}{M_{sol}}\ln a_{sol} + v_1 m_1 \phi_1^{\circ} + v_2 m_2 \phi_2^{\circ}\right) \qquad (D\text{-}6)$$

where superscript ○ denotes a binary solution containing only one solute at the same

molality. The authors also used a linear combination of polynomial expressions for a

sucrose-mannitol-water system:

$$\left(\frac{\partial \ln \gamma_1}{\partial m_2}\right)_{m_1} = \left(\frac{\partial \ln \gamma_2}{\partial m_1}\right)_{m_1} = A + Bm_1 + Cm_1^2 + Dm_1^3 + Em_2 \qquad (D\text{-}7).$$

Integration of equation (D-7) gives for the activity coefficients of the solutes in the

mixture:

$$\ln \gamma_1 = \ln \gamma_1^{\circ} + m_2\left(A + Bm_1 + Cm_1^2 + Dm_1^3 + \frac{1}{2}Em_2\right) \qquad (D\text{-}8)$$

and

$$\ln \gamma_2 = \ln \gamma_2^{\circ} + m_1\left(A + \frac{B}{2}m_1 + \frac{C}{3}m_1^2 + \frac{D}{4}m_1^3 + Em_2\right) \qquad (D\text{-}9).$$

Therefore, activity coefficients of two amino acids in water can be calculated from a set

of binary and ternary osmotic data from infinite dilution to the molality of interest.

Table D-1 Constants for each component in equation (D-5).

	B^*	β	C	D
NaCl	1.4495	2.0442×10^{-2}	5.7927×10^{-3}	-2.8860×10^{-4}
KCl	1.295	7.0000×10^{-2}	3.5990×10^{-3}	-1.9540×10^{-4}

D.2 **Materials**

Water used in all the experiments was HPLC grade and obtained from Fisher Chemicals (catalog# W5SK-4, Fair Lawn, NJ). Sodium chloride (granular, AR, ACS grade, catalog # MK685804) and potassium chloride (crystal, ACS grade, catalog # EM-SX0420-11) were obtained from VWR International (West Chester, PA). L-isoleucine, L-leucine, and L-valine were supplied by Ajinomoto Company (Tokyo, Japan) and used as received. All of the samples were dried in oven at 353 K for at least one day before use.

D.3 **Procedure**

A predetermined amount of each solute was dissolved in 50 mL of water in each glass beaker as a stock solution. Sample vials were weighed before and after loading of the stock solutions. The sample vials were then placed in a vacuum flask, and the flask was evacuated by a vacuum pump to about 25 mmHg to remove air. The flask was sealed and kept at 298 K and placed on a motor-driven rocker through an angle of 12º and at the rate of 30 times a minute to stir the solutions. After a predetermined period of time, the flask was opened, and the vials were immediately capped and weighed. The concentrations of the samples were determined by the weight changes, which correspond to the amounts of water redistributed.

D.4 **Apparatus**

In this section, apparatus description and experimental results are presented to discuss the problems associated with apparatus designs.

D.4.1 **Four-neck flask**

a) Design

Design of the following apparatus was adapted from the literature (Park and Englezos, 1998) with some modification. Figure D-1 shows a schematic description of the apparatus. A four-neck flask contains a vacuum stopcock, and the four necks are connected to detachable 10-mL ground glass bottles containing sample and reference solutions. Each joint can be sealed with a reusable Teflon® joint sleeve (catalog# 56608-948, VWR international) wrapped around the neck.

In each run, the flask was kept at 298 K in a jacketed glass vessel. The temperature in the vessel was controlled to $\pm$ 0.01 K by a means of circulating water in the jacket from a programmable water bath (VWR Scientific Model 1157, VWR international, West Chester, PA). The vessel was placed on a rocking device described in Figure D-2 until the system reached isopiestic equilibrium. The rocking device was consisted of a motor (E650MG, Robbinson & Mayers Electrocraft/Servo products, Eden Prairie, MN), torque controller (Servodyne Controller, cat#4445-30, Cole-Parmer Instrument Co., Chicago, ILL), wooden board, pulley, and wheel. The rocking device was placed in an acrylic box to reduce temperature fluctuation.
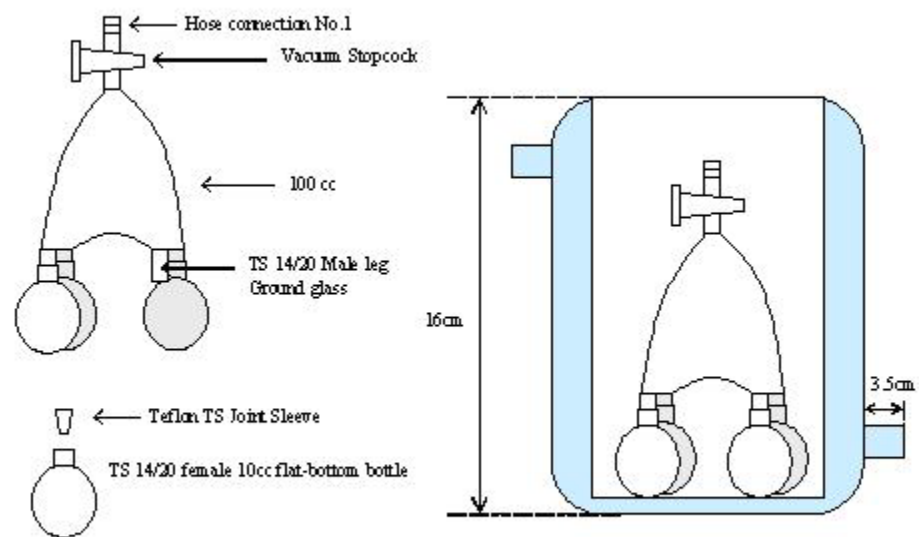
Figure D-1 Four-neck flask and glass jacketed vessel.
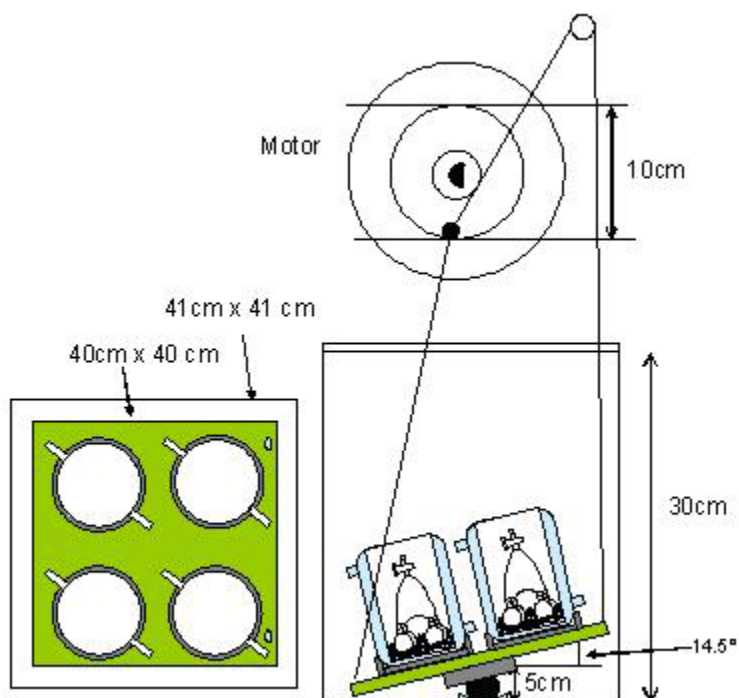
Figure D-2 Rocking device for isopiestic measurements.

b) Problems

After a run, water droplets were observed probably due to condensation of vapor on an inner wall near the stopcock. It seemed that the temperature at the upper side of the flask was lower than at the bottom part. Furthermore, a gap between joint and neck was found out. Instead of the sleeves, vacuum grease was applied to the surfaces on the joints although it could not hold a high vacuum for one week. Besides, the grease was thought to be a source of contamination and uncertainty in weight. To avoid these problems, a fast-freeze flask was employed as an alternative vacuum flask as discussed in the next section.

D.4.2 **Fast-freeze flask**

a) Design

The apparatus was consisted of 120-mL fast-freeze flasks (catalog # 75403-00, LABCONCO, Kansas City, MO), sample holder (aluminum foil), and jacketed glass vessels connected to the water bath. Figure D-3 shows the design of the flask and sample holder. The flask includes a rubber cap connected to a vacuum valve and a wide-mouth glass bottom designed to allow loading and removing samples easily. The sample holder was intended to maintain a uniform temperature distribution. Screw top vials were used as sample vials, which were also used in the solubility measurements described in Chapter 3.

In each run, the flask was placed on the jacketed glass vessel as in the previous design. In order to avoid any temperature non-uniformity, the flask and vessel were immersed in water as shown in Figure D-4. The rocking device in Figure D-2 was not used due to dimensional restriction.
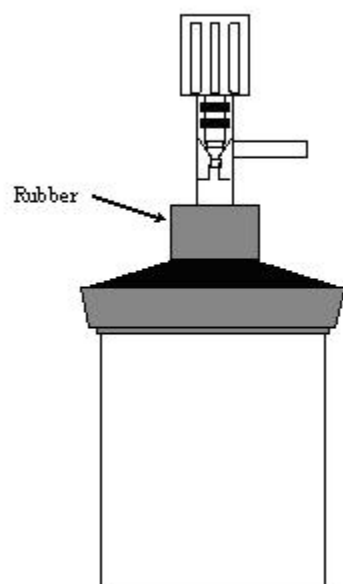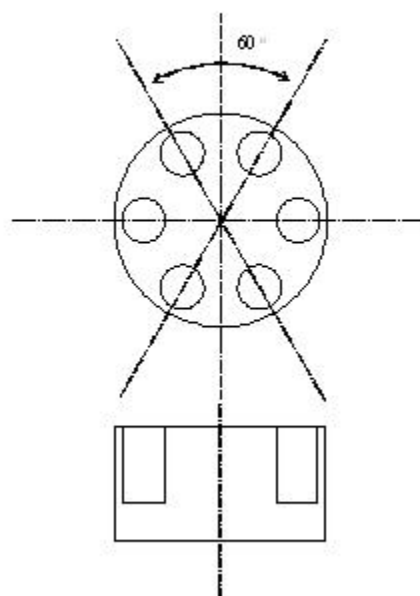
Figure D-3 Fast-freeze flask and sample holder.
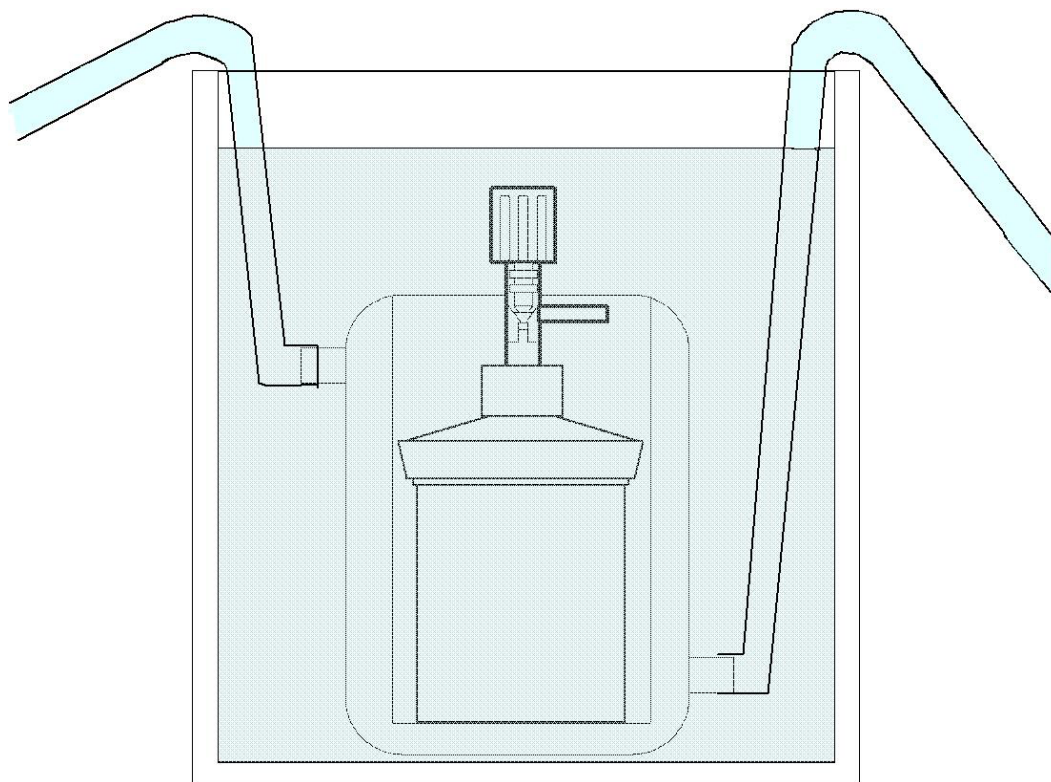
Figure D-4 Fast-freeze flask immersed into water.

b) Results and discussions

In order to validate the apparatus and experimental procedures, an experiment was carried out using potassium chloride solutions. About 0.8 mL of the solutions with different concentrations were poured in four sample vials, and left for 3 days for equilibration. At equilibrium, the solutions should exhibit the same concentration through redistributing water among the solutions. The initial and final concentrations and water increment in each vial are tabulated in Table D-2, compared with the literature data obtained by a similar set-up (Robinson and Sinclair, 1934). The table indicates that the solutions did not reach equilibrium in 3 days. In the literature, on the other hand, equilibrium was attained in 2 days even when the initial concentrations were much smaller. The authors used dishes with larger cross-section (14.44 cm^2) than those in this study (0.33 cm^2). Therefore, in another run, sample vials with larger cross-sectional area (6.88 cm^2) made of aluminum foil were used as alternative sample vials. The experimental procedures were repeated for potassium chloride and sodium chloride solutions, and the results were shown in Table D-3. It can be seen that amount of water redistributed among vials becomes larger than that in the first experiment. However, the final concentrations varied even after 6 days of equilibration period.

Table D-2 Initial and final concentration of the sample solutions and water increment in each vial.

(a) This study

Solute: KCl

Cross section of a sample vial: 0.33 [cm^2]

Vial	Initial con. [mol/kg H$_2$O]	Con. after 3 days [mol/kg H$_2$O]	Water increment [g]
1	2.63	2.37	0.08
2	1.92	1.86	0.02
3	1.25	1.53	-0.13
4	0.62	0.69	-0.07

(b) Robinson and Sinclair, 1934

Solute: KCl

Cross section of a sample vial: 14.44 [cm^2]

Vial	Initial con. [mol/kg H$_2$O]	Con. after 1 days [mol/kg H$_2$O]	Water increment [g]
1	4.09	2.18	1.75
2	3.10	2.18	0.85
3	1.73	2.18	-0.41
4	0.82	2.18	-1.24

Solute: KCl

Cross section of a sample vial: 14.44 [cm^2]

Vial	Initial con. [mol/kg H$_2$O]	Con. after 2 days [mol/kg H$_2$O]	Water increment [g]
1	0.25	0.22	0.32
2	0.25	0.22	0.32
3	0.22	0.22	0.04
4	0.22	0.22	0.04

Table D-3 Initial and final concentrations of sample solutions and water increment in larger sample vials.

Solute: KCl
Cross section of a sample vial: 6.13 [cm^2]

Vial	Initial con. [mol/kg H$_2$O]	Con. after 2 days [mol/kg H$_2$O]	Water increment [g]
1	3.98	3.21	0.41
2	2.88	2.81	0.05
3	1.85	1.94	-0.09
4	0.90	1.16	-0.43

Solute: NaCl
Cross section of a sample vial: 6.13 [cm^2]

Vial	Initial con. [mol/kg H$_2$O]	Con. after 6 days [mol/kg H$_2$O]	Water increment [g]
1	1.70	1.03	0.96
2	0.83	0.82	0.01
3	0.66	0.79	-0.31
4	0.41	0.81	-0.76

Solute: NaCl
Cross section of a sample vial: 6.13 [cm^2]

Vial	Initial con. [mol/kg H$_2$O]	Con. after 6 days [mol/kg H$_2$O]	Water increment [g]
1	1.70	1.30	0.47
2	1.26	1.07	0.27
3	0.84	1.01	-0.26
4	0.41	0.67	-0.58

D.5 Recommendations

From the observed results, 6 days are not long enough to reach equilibrium for the sodium chloride and potassium chloride solutions in the apparatuses tested. In the case of amino acids a solute, the period of time for equilibrium is estimated to be much longer because of low concentrations (< 0.5 mol/kg H_2O). In order to obtain isopiestic data in a practical period of time, sample vials should have a large cross-sectional area and devices for mechanical agitation should be installed inside the flask to enhance mass transfer.

APPENDIX E

VISUAL C++ PROGRAM

This program is composed of the following three files:

1) modifiedUNIFAC_main.c

2) modifiedUNIFAC_sub.c

3) modifiedUNIFAC_header.h

E.1 **modifiedUNIFAC_main.c**

```c
//***********************************************************************
//********************//
//
// A Program of The modified UNIFAC method
// Source: Kuramochi et al., Biotechnol. Prog. 1996, 12, 371-379
//
// The molal activity coefficients in the aqueous mixture with total NumGroup-groups in
water at T
// Water(0)-Solute(1) w/ m1 in binary / Water(0)-Solute(1)-Solute(2) w/ m1 and m2 in
ternary
//
// OR
//
// The prediction of solubility of Solute(1) w/ m2 of Solute(2) in Water(0)
// Using the product of activity coefficient and solubility w/ temperature / solubility only
//
//***********************************************************************
//********************//

#include <stdio.h>
#include <stdlib.h>
#include <string.h>
#include <math.h>
#include "modifiedUNIFAC_header.h"

const double T=298.15; // T:temperature at 25 C
int NumComp;          // # of components,
int NumGroup=0;       // total # of groups existed in the system

// ### Start Main() ###
int main(void)
{
        // Output file
        FILE *fp;
        char fname[MAXCHARS];

        // Auto variables
        int i,j,k, Option, NumIter;
        double Molmax1, Molmax2, xa, xb, xc, fa, fc, xgamma;

        // Variables allocated dinamically
        char **NameComp;
        int *NYU, *nyu, *NumCalc;
```

```c
double *Mw, *Q, *r, *psi, *Mol, *x, *lngammainf, *Moltemp, *lngamma;

// Option, NumComp
// Option=1 ==> Activity Coeff, Option=2 ==> Solubility
if(!(Option=f_Option_NumComp())) exit(1);

// ### MEMORY ALLOCATION ###
// char NameComp[NumComp][MAXCHARS]
// int NYU[NumComp][SUBGROUP]:# of every group in each component
NameComp=(char **)malloc(NumComp*sizeof(char *)); if(!NameComp)
_alloc_error("**NameComp.");
        for(i=0;i<NumComp;i++) {NameComp[i]=(char
*)malloc(MAXCHARS*sizeof(char)); if(!NameComp[i])
_alloc_error("*NameComp.");}
        NYU=(int *)malloc(NumComp*SUBGROUP*sizeof(int)); if(!NYU)
_alloc_error("*NYU.");
        NumCalc=(int *)malloc(NumComp*sizeof(int)); if(!NumCalc)
_alloc_error("*NumCalc.");

// NameComp, NYU, NumGroup
if(!(f_NameComp_NYU_NumGroup(NameComp,NYU))) exit(1);

// ### MEMORY ALLOCATION ###
// int nyu[NumComp*NumGroup]
// double Mw[NumComp], Q[NumGroup], r[NumComp],
psi[NumGroup][NumGroup]
// double Mol[NumComp], x[NumComp], lngamma[NumComp],
Moltemp[NumComp], lngamma[NumComp]
        nyu=(int *)malloc(NumComp*NumGroup*sizeof(int)); if(!nyu)
_alloc_error("*nyu.");
        Mw=(double *)malloc(NumComp*sizeof(double)); if(!Mw)
_alloc_error("*Mw.");
        Q=(double *)malloc(NumGroup*sizeof(double)); if(!Q) _alloc_error("*Q.");
        r=(double *)malloc(NumComp*sizeof(double)); if(!r) _alloc_error("*r.");
        psi=(double *)malloc(NumGroup*NumGroup*sizeof(double)); if(!psi)
_alloc_error("*psi.");
        Mol=(double *)malloc(NumComp*sizeof(double)); if(!Mol)
_alloc_error("*Mol.");
        x=(double *)malloc(NumComp*sizeof(double)); if(!x) _alloc_error("*x.");
        lngammainf=(double *)malloc(NumComp*sizeof(double)); if(!lngammainf)
_alloc_error("*lngammainf.");
        Moltemp=(double *)malloc(NumComp*sizeof(double)); if(!Moltemp)
_alloc_error("*Moltemp.");
        lngamma=(double *)malloc(NumComp*sizeof(double)); if(!lngamma)
_alloc_error("*lngamma.");
```

```
        // nyu, Mw, Q, r, psi
        if(!(f_nyu_Mw_Q_r_psi(NYU,nyu,Mw,Q,r,psi))) exit(1);

        // ### INPUT ###
        // NumCalc: # of calc, Mol: Max Molalities
        if(!(f_NumCalc_Mol(NumCalc,Mol,Option,NameComp,Mw))) exit(1);

        // xgamma for solubility
        if(Option==2) {if(!(f_xgamma(NYU,&xgamma))) exit(1);}

        // ### FILE OUTPUT ###
        printf("Input the file name (< %d characters):", MAXCHARS);
        scanf("%s",fname); fflush(stdin);

        // OPEN THE OUTPUT FILE
        if(!(fp=fopen(fname,"w"))){printf("\nCan't open the file %s \n",fname);exit(1);}

        // ### OUTPUT & CALCULATION ###
        // Solubility
        if(Option==2)
        {
                printf("\nWater(0)-%s(1,Mw=%.1f)-%s(2,Mw=%.1f) at %.2f
[K]\n",NameComp[1],Mw[1],NameComp[2],Mw[2],T);
                puts("solubility[1]\tmolality[2]");
                fprintf(fp,"Water(0)-%s(1,Mw=%.1f)-%s(2,Mw=%.1f) at %.2f [K],
x*gamma=%e\n",NameComp[1],Mw[1],NameComp[2],Mw[2],T,xgamma);

        fprintf(fp,"solubility[1]\tmolality[2]\tx[1]\tx[2]\tgamma[%s]\tgamma[%s]\n",Nam
eComp[1],NameComp[2]);

                // Molmax2=Max molality
                Molmax2=Mol[2];

                // FIND Mol[1] BY THE BISEC METHOD
                // NumIter: # OF ITERATION
                NumIter=(int)(log(1.0/EPSILON)/log(2.0)+1.0);

                for(i=0;i<NumCalc[2];i++)
                {
                        // range of x[1]: xa<x[1]<xb
                        xa=XINF;xb=1.0-xa;

                        // Mol[2]
                        Mol[2]=(double)(i+1)*Molmax2/(double)(NumCalc[2]);

                        // Mol[1], x[2], x[0] at x[1]=xa
```

```c
                x[1]=xa;
                if(!(f_x_Mol(x,Mol))) exit(1);

                // ln(gamma) and fa
                if(!(f_lngamma(x,nyu,Q,r,psi,lngamma))) exit(1);
                fa=xa*exp(lngamma[1])-xgamma;

                for(j=0;j<NumIter;j++)
                {
                        xc=(xa+xb)*0.5; // bisection:xc

                        // Mol[1], x[2], x[0] at x[1]=xc
                        x[1]=xc;
                        if(!(f_x_Mol(x,Mol))) exit(1);

                        // ln(gamma) and fc
                        if(!(f_lngamma(x,nyu,Q,r,psi,lngamma))) exit(1);
                        fc=xc*exp(lngamma[1])-xgamma;


        if(((fa>0.0)&&(fc>0.0))||((fa<0.0)&&(fc<0.0))){xa=xc;fa=fc;} else xb=xc;
                }

                printf("%f\t%f\n",Mol[1],Mol[2]);

        fprintf(fp,"%f\t%f\t%e\t%e\t%f\t%f\n",Mol[1],Mol[2],x[1],x[2],exp(lngamma[1])
,exp(lngamma[2]));
                }
        }
        // Activity Coefficient in binary
        else if(NumComp==BINARY)
        {
                printf("\nWater(0)-%s(1,Mw=%.1f) at %.2f
[K]\n",NameComp[1],Mw[1],T);
                puts("molality[1]\tx[1]\t\ngamma[1](sym)\ngamma[1](unsym)");
                fprintf(fp,"Water(0)-%s(1,Mw=%.1f) at %.2f
[K]\n",NameComp[1],Mw[1],T);

        fprintf(fp,"molality[1]\tx[1]\tgamma[1](sym)\tgamma[%s](unsym)\n",NameComp[1]);

                // Molmax1=Max molality
                Molmax1=Mol[1];

                for(i=0;i<NumCalc[1]+1;i++)
                {
```

```
                // Mol[1] & x
                Mol[1]=(double)(i)*Molmax1/(double)(NumCalc[1]);
                if(!i) Mol[1]=MOLINF; // Infinite dilution
                if(!(f_Mol_x(Mol,x))) exit(1);

                // ln(gamma)
                if(!(f_lngamma(x,nyu,Q,r,psi,lngamma))) exit(1);
                if(!i) lngammainf[1]=lngamma[1];


        printf("%e\t%e\t%f\t%f\n",Mol[1],x[1],exp(lngamma[1]),exp(lngamma[1])/exp(lngammainf[1])*x[0]);

        fprintf(fp,"%e\t%e\t%f\t%f\n",Mol[1],x[1],exp(lngamma[1]),exp(lngamma[1])/exp(lngammainf[1])*x[0]);
                }
        }
        // Activity Coefficient in ternary
        else
        {
                printf("\nWater(0)-%s(1,Mw=%.1f)-%s(2,Mw=%.1f) at %.2f [K]\n",NameComp[1],Mw[1],NameComp[2],Mw[2],T);
                puts("molality[1]\tmolality[2]\tgamma,m[1]\tgamma,m[2]");
                fprintf(fp,"Water(0)-%s(1,Mw=%.1f)-%s(2,Mw=%.1f) at %.2f [K]\n",NameComp[1],Mw[1],NameComp[2],Mw[2],T);

        fprintf(fp,"molality[1]\tmolality[2]\tx[1]\tx[2]\tgamma[1]\tgamma[2]\tgamma,m[%s]\tgamma,m[%s]\n",NameComp[1],NameComp[2]);

                // Molmax1,Molmax2=Max molality
                Molmax1=Mol[1]; Molmax2=Mol[2];

                for(i=0;i<NumCalc[1];i++)
                {
                        // Mol[1]
                        Mol[1]=(double)(i+1)*Molmax1/(double)(NumCalc[1]);

                        for(j=0;j<NumCalc[2]+1;j++)
                        {
                                Mol[2]=(double)(j)*Molmax2/(double)(NumCalc[2]);

                                if(!j) // lngammainf
                                {
                                        for(k=1;k<TERNARY;k++)
                                        {
                                                Moltemp[k]=Mol[k]; Mol[k]=MOLINF;
```

```c
                                                  if(!(f_Mol_x(Mol,x))) exit(1);

                                                  if(!(f_lngamma(x,nyu,Q,r,psi,lngamma)))
exit(1);

                                                  lngammainf[k]=lngamma[k];

Mol[k]=Moltemp[k];
                                     }
                                     continue;
                          }

                          // x
                          if(!(f_Mol_x(Mol,x))) exit(1);

                          // ln(gamma)
                          if(!(f_lngamma(x,nyu,Q,r,psi,lngamma))) exit(1);


          printf("%f\t%f\t%f\t%f\n",Mol[1],Mol[2],exp(lngamma[1])/exp(lngammainf[1])*
x[0],exp(lngamma[2])/exp(lngammainf[2])*x[0]);

          fprintf(fp,"%f\t%f\t%e\t%e\t%f\t%f\t%f\t%f\n",Mol[1],Mol[2],x[1],x[2],exp(lnga
mma[1]),exp(lngamma[2]),exp(lngamma[1])/exp(lngammainf[1])*x[0],exp(lngamma[2])
/exp(lngammainf[2])*x[0]);
                    }
               }
          }

          // CLOSE THE OUTPUT FILE
          fclose(fp);
          printf ("Output the datafile = %s \n\n",fname);

          // FREE THE DYNAMICALLY ALLOCATED MEMORY
          free(lngamma);free(Moltemp);free(lngammainf);free(x);free(Mol);
          free(psi);free(r);free(Q);free(Mw);free(NumCalc);free(nyu);free(NYU);
          for(i=0;i<NumComp;i++) free(NameComp[i]);
          free(NameComp);

          return(0);
}
// ### End Main() ###
// EOF
```

E.2 modified UNIFAC_sub.c

```c
// Header files
#include <stdio.h>
#include <stdlib.h>
#include <string.h>
#include <math.h>
#include "modifiedUNIFAC_header.h"

//
// Subroutine functions
//
int f_Option_NumComp()
{
	int i, Option;

	// ### INPUT ###
	for(i=0;i<OUT;i++)
	{
		// Which to be calculated, Option
		printf("Activity Coefficient(%d) or Solubility(%d)? (0 to exit)",1,2);
		scanf("%d",&Option); fflush(stdin);

		if(!Option) exit(1);
		else if(Option==1)
		{
			puts("==> Activity Coefficient");
			// # of components in the system, NumComp
			printf("Binary(%d) or Ternary(%d)?",BINARY,TERNARY);
			scanf("%d",&NumComp); fflush(stdin);
		}
		else if(Option==2){puts("==> Solubility of Component 1");
NumComp=3; break;}
		else{puts("TYPE 0, 1 or 2!");continue;}

		if(NumComp==BINARY) {puts("==> Binary"); break;}
		else if(NumComp==TERNARY){puts("==> Ternary"); break;}
		else{puts("TYPE 2 or 3!"); continue;}
	}
	if(i==OUT) exit(1);

	return Option;
}
//
```

```c
int f_NameComp_NYU_NumGroup(char **NameComp,int *NYU)
{
        int i, j, IdComp; // IdComp:ID # of the selected component in NameCompList
        // Name of components+none
        const char *NameCompList[LIST]={"None","Water","Glycine","DL-
Alanine","DL-Valine","DL-(iso)Leucine"};
        // # of each sub-group in each component
        const int NumSubgroupList[LIST][SUBGROUP]={{0,0,0,0,0,0,0,0,0,0,0}
// None
        // {"H2O","a-CH2","a-CH","sc-CH3","sc-CH2","sc-
CH","OH","NH2","NH","COOH","CONH"}
        ,{   1,   0,   0,   0,   0,   0, 0,   0, 0,   0,   0} // Water
        ,{   0,   1,   0,   0,   0,   0, 0,   1, 0,   1,   0} // Glycine
        ,{   0,   0,   1,   1,   0,   0, 0,   1, 0,   1,   0} // Alanine
        ,{   0,   0,   1,   2,   0,   1, 0,   1, 0,   1,   0} // Valine
        ,{   0,   0,   1,   2,   1,   1, 0,   1, 0,   1,   0} // (iso)Leucine
              };
        // Name of each sub-group
        const char *NameSubgroupList[SUBGROUP]={"H2O","a-CH2","a-CH","sc-
CH3","sc-CH2","sc-CH","OH","NH2","NH","COOH","CONH"};

        // ### INPUT ###
        for(i=0;i<NumComp;i++)
        {
                if(!i) // i==0
                {
                        // Water in NameCompList
                        printf("\nthe component[0]:1 (Water).\n\n");
                        IdComp=1;

                        // List the available sets of components
                        puts("Available components:");
                        puts("######################");
                        for(j=0;j<LIST;j++) printf("%d\t%s\n",j,NameCompList[j]);
                        puts("######################");
                        puts("");
                }
                else
                {
                        printf("Select the number of the component[%d](-1 to exit):",i);
                        scanf("%d",&IdComp); fflush(stdin);
                        if(IdComp==-1) exit(1);
                }

                // Copy the data according to the selection
                if(IdComp) // IdComp!=0
```

```c
                {
                        strcpy(NameComp[i],NameCompList[IdComp]);
                        for(j=0;j<SUBGROUP;j++)
NYU[i*SUBGROUP+j]=NumSubgroupList[IdComp][j];
                }
                else      // IdComp==0
                {
                        // Name of the component
                        printf("Name the component:");  // Name
                        scanf("%s",NameComp[i]); fflush(stdin);

                        // # of the goups in the solute
                        puts("Assign the number of each group in the component:");
                        for(j=0;j<SUBGROUP;j++)
                        {
                                printf("%s:",NameSubgroupList[j]);
                                scanf("%d",&NYU[i*SUBGROUP+j]); fflush(stdin);
                        }
                }
        }

        // total # of groups existed in the system, NumGroup
        for(i=0;i<SUBGROUP;i++)for(j=0;j<NumComp;j++){if(NYU[j*SUBGROUP+i]
){NumGroup++;break;}}

        return(1);
}
//
int f_nyu_Mw_Q_r_psi(int *NYU,int *nyu,double *Mw,double *Q,double *r,double
*psi)
{
        // The main-group number corresponding to each sub-group
        const int MainSubgroupList[SUBGROUP]={0,1,1,2,2,2,3,4,4,5,6};
        // Interaction Parameters of each main-group
        const double InterParamList[MAINGROUP][MAINGROUP]={
        {   0.0 ,-1385.0,  85.70, -47.15, -66.39,   8.62, -16.87}, // 0 H2O
        {-401.4 ,    0.0, -167.3 ,-983.1 ,-960.5 ,-573.2 ,-812.1 }, // 1 a-CH2
        {  49.97, -896.5,   0.0 , 707.2 ,1554.0 , 218.6 ,-114.7 }, // 2 sc-CH3
        { 155.6 ,-1936.0, 1674.0 ,   0.0 ,-176.5 ,  61.78,   0.0 }, // 3 OH
        {-244.5 , -603.4, 3085.0 ,-173.7 ,   0.0 ,-489.0 ,-193.7 }, // 4 NH2
        {  86.44,  921.8, 1360.0 , -92.21, 867.7 ,   0.0 , -85.28}, // 5 COOH
        {  16.71, -249.0, 45.50 ,   0.0 , -33.16, 189.8 ,   0.0 }};// 6 CONH
        // Size Parameters(R,Q) and Molecular Weight(Mw) of each sub-group
        const double SizeParamList[SUBGROUP][SIZE]={
        {0.9200, 1.400, 18.0}, // 0 H2O
        {0.6744, 0.540, 14.0}, // 1 a-CH2
```

```
{0.4469, 0.228, 13.0},   // 2 a-CH
{0.9011, 0.848, 15.0},   // 3 sc-CH3
{0.6744, 0.540, 14.0},   // 4 sc-CH2
{0.4469, 0.228, 13.0},   // 5 sc-CH
{1.0000, 1.200, 17.0},   // 6 OH
{0.6948, 1.150, 16.0},   // 7 NH2
{0.5326, 1.150, 15.0},   // 8 NH
{1.3013, 1.224, 45.0},   // 9 COOH
{1.3039, 1.036, 43.0}};  //10 CONH

int i,j,k=0, *id;
double *R, *a;

// Memory allocation
// int id[NumGroup]; // id: # of the groups in the component
// a[NumGroup][NumGroup]:group-interaction parameter, R[NumGroup]:volume
// double psi[NumGroup][NumGroup]=exp(-a[NumGroup][NumGroup]/T)
// double Q[NumGroup]:surface area
id=(int *)malloc(NumGroup*sizeof(int)); if(!id) _alloc_error("*id.");
R=(double *)malloc(NumGroup*sizeof(double)); if(!R) _alloc_error("*R.");
a=(double *)malloc(NumGroup*NumGroup*sizeof(double)); if(!a)
_alloc_error("*a.");

// IDENTIFY THE GROUPS IN THE MIXTURE
for(i=0;i<SUBGROUP;i++)
for(j=0;j<NumComp;j++){if(NYU[j*SUBGROUP+i]){id[k++]=i;break;}} // Input
Group Number

// EXTRACT THE DATA USING THE ID'S
for(i=0;i<NumComp;i++)
{
        Mw[i]=0.0;
        for(j=0;j<NumGroup;j++)
        {
                nyu[i*NumGroup+j]=NYU[i*SUBGROUP+id[j]];        //
nyu[NumComp][NumGroup]
                Mw[i]+=nyu[i*NumGroup+j]*SizeParamList[id[j]][2]; // Mw in
SizeParamList[i][2]
        }
}
for(i=0;i<NumGroup;i++)
{
        R[i]=SizeParamList[id[i]][0]; // R in SizeParamList[i][0]
        Q[i]=SizeParamList[id[i]][1]; // Q in SizeParamList[i][1]
        // a in InterParamList[i][j]
```

```c
                for(j=0;j<NumGroup;j++)
a[i*NumGroup+j]=InterParamList[MainSubgroupList[id[i]]][MainSubgroupList[id[j]]];
        }

        // r[NumComp]
        for(i=0;i<NumComp;i++)
        {
                r[i]=0.0;
                for(j=0;j<NumGroup;j++) r[i]+=nyu[i*NumGroup+j]*R[j];
        }

        // psi[NumGroup][NumGroup]
        for(i=0;i<NumGroup;i++) for(j=0;j<NumGroup;j++) psi[i*NumGroup+j]=exp(-
a[i*NumGroup+j]/T);

        // Free allocated memory
        free(a);free(R);free(id);

        return(1);
}
//
int f_NumCalc_Mol(int *NumCalc,double *Mol,int Option,char **NameComp,double
*Mw)
{
        NumCalc[0]=1;

        // Molality-->Water
        Mol[0]=1000.0/Mw[0];

        // Molality-->Component[1]
        if(Option==1) // Activity Coefficient
        {
                printf("%s: Maximum Molality [mole/kg of water]:",NameComp[1]);
                scanf("%lf",&Mol[1]); fflush(stdin);
                printf("How many points of calculation:"); // # of calculation
                scanf("%d",&NumCalc[1]); fflush(stdin);
        }

        // Molality-->Component[2]
        if(NumComp==TERNARY) // if ternary
        {
                printf("%s: Maximum Molality [mole/kg of water]:",NameComp[2]);
                scanf("%lf",&Mol[2]); fflush(stdin);
                printf("How many points of calculation:"); // # of calculation
                scanf("%d",&NumCalc[2]); fflush(stdin);
        }
```

```
        return(1);
}
//
int f_xgamma(int *NYU,double *xgamma)
{
        // Correlated Constants for the Solubility of Amino Acids in Water (Binary vs T)
        const char *NameSolubList[SOLUBILITY]={"None","Glycine","DL-
Serine","DL-Valine(WRONG)","DL-Alanine","DL-Isoleucine"
                ,"DL-alpha-amino-n-butyric acid(NODATA)","L-alanine","L-serine","L-
valine","L-leucine","L-isoleucine"};
        const double ParamSolubList[SOLUBILITY][ABC]={{0.,0.,0.} // None
        ,{   2.2990, 2105.5,  0.0000} // Glycine
        ,{ -28.939,  -318.35, 4.0617}  // DL-Serine
        ,{-5236.3,   -5236.3, 17.455 } // DL-Valine ###WRONG!####
        ,{ -77.052, -2668.6, 11.082 }  // DL-Alanine
        ,{ -170.70, -7290.6, 24.183 }  // DL-Isoleucine
        ,{   0.,      0.,  0.   }  // DL-alpha-amino-n-butyric acid ###NODATA####
        ,{ -62.345, -2143.4,  8.8091}  // L-alanine
        ,{   46.558, 3150.1, -6.8443}  // L-serine
        ,{ -88.243, -3929.1, 11.933 }  // L-valine
        ,{ -140.42, -6369.1, 19.426 }  // L-leucine
        ,{ -68.815, -3149.7,  8.8183}};// L-isoleucine

        int i,j, ID1, ID2, *NumGrouptemp, *NYUsat, *nyusat;
        double S[ABC], *xsat, *lngammasat, *Mwsat, *Qsat, *rsat, *psisat;

        // List the available sets of components
        puts("Available components for the constants of A,B,C");
        puts("######################");
        for(i=0;i<SOLUBILITY;i++) printf("%d\t%s\n",i,NameSolubList[i]);
        puts("######################");
        puts("");

        // Values of constants for the solubility
        printf("Enter the corresponding # of Component[1]:");
        scanf("%d",&ID1); fflush(stdin);

        if(!ID1)
        {
                printf("Do you have the binary solubility(0) or the constants in ln
(x*gamma)=A-B/T+ClnT(1):");
                scanf("%d",&ID2); fflush(stdin);

                if(!ID2)
                {
```

```c
                // CONVERT INTO BINARY
                NumComp=BINARY;
                NumGrouptemp=(int *)malloc(sizeof(int)); if(!NumGrouptemp)
_alloc_error("*NumGrouptemp.");
                NYUsat=(int *)malloc(NumComp*SUBGROUP*sizeof(int));
if(!NYUsat) _alloc_error("*NYUsat.");

                *NumGrouptemp=NumGroup; NumGroup=0;

        for(i=0;i<NumComp;i++){for(j=0;j<SUBGROUP;j++){NYUsat[i*SUBGROUP+
j]=NYU[i*SUBGROUP+j];}}

        for(i=0;i<SUBGROUP;i++){for(j=0;j<NumComp;j++){if(NYUsat[j*SUBGROU
P+i]){NumGroup++;break;}}}

                nyusat=(int *)malloc(NumComp*NumGroup*sizeof(int));
if(!nyusat) _alloc_error("*nyusat.");
                Mwsat=(double *)malloc(NumComp*sizeof(double)); if(!Mwsat)
_alloc_error("*Mwsat.");
                Qsat=(double *)malloc(NumGroup*sizeof(double)); if(!Qsat)
_alloc_error("*Qsat.");
                rsat=(double *)malloc(NumComp*sizeof(double)); if(!rsat)
_alloc_error("*rsat.");
                psisat=(double *)malloc(NumGroup*NumGroup*sizeof(double));
if(!psisat) _alloc_error("*psisat.");
                xsat=(double *)malloc(NumComp*sizeof(double)); if(!xsat)
_alloc_error("*xsat.");
                lngammasat=(double *)malloc(NumComp*sizeof(double));
if(!lngammasat) _alloc_error("*lngammasat.");

                if(!(f_nyu_Mw_Q_r_psi(NYUsat,nyusat,Mwsat,Qsat,rsat,psisat)))
exit(1);

                printf("Input the solubility[mol/kg-water]:");
                scanf("%lf",&xsat[1]); fflush(stdin);
                xsat[1]=xsat[1]/(xsat[1]+1000.0/Mwsat[0]); xsat[0]=1.0-xsat[1];

                if(!(f_lngamma(xsat,nyusat,Qsat,rsat,psisat,lngammasat))) exit(1);

                // RETURN TO TERNARY
                NumComp=TERNARY; NumGroup=*NumGrouptemp;

                *xgamma=xsat[1]*exp(lngammasat[1]);
```

```c
                free(NumGrouptemp);free(NYUsat);free(xsat);free(lngammasat);free(Mwsat);fre
e(rsat);
                        free(nyusat);free(Qsat);free(psisat);

                        return(1);
                }
                else if(ID2==1)
                {
                        // Values of constants for the solubility
                        puts("Enter the constants for the solubility in the component.");
                        printf("%s:","A,B, and C");
                        scanf("%lf %lf %lf",&S[0],&S[1],&S[2]); fflush(stdin);
                }
                else exit(1);
        }
        else if((ID1>0)&&(ID1<SOLUBILITY)) {for(i=0;i<ABC;i++)
S[i]=ParamSolubList[ID1][i];}
        else exit(1);

        // ln (x*gamma)=A-B/T+ClnT
        *xgamma=exp(S[0]-S[1]/T+S[2]*log(T));
        return(1);
}
//
int f_x_Mol(double *x,double *Mol)
{
        int i;
        double Moldenom=0.0;

        // Mol[1] at x[1]
        Mol[1]=x[1]/(1.0-x[1])*(Mol[0]+Mol[2]);
        for(i=0;i<NumComp;i++) Moldenom+=Mol[i];

        // x[2], x[0]
        x[2]=Mol[2]/Moldenom;
        x[0]=1.0-x[1]-x[2];

        return(1);
}
//
int f_Mol_x(double *Mol,double *x)
{
        int i;
        double Moldenom=0.0;
```

```c
        // x
        for(i=0;i<NumComp;i++) Moldenom+=Mol[i];
        for(i=0;i<NumComp;i++) x[i]=Mol[i]/Moldenom;

        return(1);
}
//
int f_lngamma_Com(double *x,double *r,double *lngamma_Com)
{
        int i;
        double omegadenom=0.0, *omega;

        // Memory allocation
        omega=(double *)malloc(NumComp*sizeof(double)); if(!omega)
_alloc_error("*omega.");

        for(i=0;i<NumComp;i++) omegadenom+=x[i]*pow(r[i],2.0/3.0);
        for(i=0;i<NumComp;i++)
        {
                omega[i]=x[i]*pow(r[i],2.0/3.0)/omegadenom;
                lngamma_Com[i]=log(omega[i]/x[i])+1.0-omega[i]/x[i];
        }

        // Free allocated memory
        free(omega);

        return(1);
}
//
int f_lnGAMMA_ResP(int *nyu,double *Q,double *psi,double *lnGAMMA_ResP)
{
        int i,j,k,m;
        double **XP, **thetaRP, **s1P, **s2P, **s2Pdenom, *XPdenom,
*thetaRPdenom;

        // Memory allocation
        XP=(double **)malloc(NumComp*sizeof(double *)); if(!XP)
_alloc_error("**XP.");
        thetaRP=(double **)malloc(NumComp*sizeof(double *)); if(!thetaRP)
_alloc_error("**thetaRP.");
        s1P=(double **)malloc(NumComp*sizeof(double *)); if(!s1P)
_alloc_error("**s1P.");
        s2P=(double **)malloc(NumComp*sizeof(double *)); if(!s2P)
_alloc_error("**s2P.");
        s2Pdenom=(double **)malloc(NumComp*sizeof(double *)); if(!s2Pdenom)
_alloc_error("**s2Pdenom.");
```

```c
	for(i=0;i<NumComp;i++)
	{
		XP[i]=(double *)malloc(NumGroup*sizeof(double)); if(!XP)
_alloc_error("*XP.");
		thetaRP[i]=(double *)malloc(NumGroup*sizeof(double)); if(!thetaRP)
_alloc_error("*thetaRP.");
		s1P[i]=(double *)malloc(NumGroup*sizeof(double)); if(!s1P)
_alloc_error("*s1P.");
		s2P[i]=(double *)malloc(NumGroup*sizeof(double)); if(!s2P)
_alloc_error("*s2P.");
		s2Pdenom[i]=(double *)malloc(NumGroup*sizeof(double));
if(!s2Pdenom) _alloc_error("*s2Pdenom.");
	}
	XPdenom=(double *)malloc(NumComp*sizeof(double)); if(!XPdenom)
_alloc_error("*XPdenom.");
	thetaRPdenom=(double *)malloc(NumComp*sizeof(double)); if(!thetaRPdenom)
_alloc_error("*thetaRPdenom.");

	for(i=0;i<NumComp;i++)
	{
		XPdenom[i]=0.0;
		for(j=0;j<NumGroup;j++) XPdenom[i]+=nyu[i*NumGroup+j]; //
denominator of XP[I][K]
		for(j=0;j<NumGroup;j++) XP[i][j]=nyu[i*NumGroup+j]/XPdenom[i];

		thetaRPdenom[i]=0.0;
		for(j=0;j<NumGroup;j++) thetaRPdenom[i]+=Q[j]*XP[i][j]; //
denominator of thetaRP[I][K]
		for(j=0;j<NumGroup;j++) thetaRP[i][j]=Q[j]*XP[i][j]/thetaRPdenom[i];

		for(j=0;j<NumGroup;j++)
		{
			s1P[i][j]=0.0; s2P[i][j]=0.0;
			for(k=0;k<NumGroup;k++)
			{
				s1P[i][j]+=thetaRP[i][k]*psi[k*NumGroup+j];
				s2Pdenom[i][k]=0.0;
				for(m=0;m<NumGroup;m++)
s2Pdenom[i][k]+=thetaRP[i][m]*psi[m*NumGroup+k];

	s2P[i][j]+=thetaRP[i][k]*psi[j*NumGroup+k]/s2Pdenom[i][k];
			}
			lnGAMMA_ResP[i*NumGroup+j]=Q[j]*(1.0-log(s1P[i][j])-
s2P[i][j]);
		}
	}
```

```
        // Free allocated memory
        for(i=0;i<NumComp;i++)
{free(XP[i]);free(thetaRP[i]);free(s1P[i]);free(s2P[i]);free(s2Pdenom[i]);}
        free(XP);free(thetaRP);free(s1P);free(s2P);free(s2Pdenom);
        free(XPdenom);free(thetaRPdenom);

        return(1);
}
//
int f_lnGAMMA_ResM(double *x,int *nyu,double *Q,double *psi,double
*lnGAMMA_ResM)
{

        int i,j,k;
        double XMdenom=0.0, thetaRMdenom=0.0;
        double *XM, *thetaRM, *s1M, *s2M, *s2Mdenom;

        // Memory allocation
        XM=(double *)malloc(NumGroup*sizeof(double)); if(!XM)
_alloc_error("*XM.");
        thetaRM=(double *)malloc(NumGroup*sizeof(double)); if(!thetaRM)
_alloc_error("*thetaRM.");
        s1M=(double *)malloc(NumGroup*sizeof(double)); if(!s1M)
_alloc_error("*s1M.");
        s2M=(double *)malloc(NumGroup*sizeof(double)); if(!s2M)
_alloc_error("*s2M.");
        s2Mdenom=(double *)malloc(NumGroup*sizeof(double)); if(!s2Mdenom)
_alloc_error("*s2Mdenom.");

        for(i=0;i<NumComp;i++)
for(j=0;j<NumGroup;j++){XMdenom+=nyu[i*NumGroup+j]*x[i];} // denominator of
XM[K]

        for(i=0;i<NumGroup;i++)
        {
                XM[i]=0.0;
                for(j=0;j<NumComp;j++) XM[i]+=nyu[j*NumGroup+i]*x[j]/XMdenom;
                thetaRMdenom+=Q[i]*XM[i]; // denominator of thetaRM[K]
        }

        for(i=0;i<NumGroup;i++) thetaRM[i]=Q[i]*XM[i]/thetaRMdenom;
        for(i=0;i<NumGroup;i++)
        {
                s1M[i]=0.0; s2M[i]=0.0;
                for(j=0;j<NumGroup;j++)
```

```
                {
                        s1M[i]+=thetaRM[j]*psi[j*NumGroup+i];
                        s2Mdenom[j]=0.0;
                        for(k=0;k<NumGroup;k++)
s2Mdenom[j]+=thetaRM[k]*psi[k*NumGroup+j];
                        s2M[i]+=thetaRM[j]*psi[i*NumGroup+j]/s2Mdenom[j];
                }
                lnGAMMA_ResM[i]=Q[i]*(1.0-log(s1M[i])-s2M[i]);
        }

        // Free allocated memory
        free(XM);free(thetaRM);free(s1M);free(s2M);free(s2Mdenom);

        return(1);
}
//
int f_lngamma(double *x,int *nyu,double *Q,double *r,double *psi,double *lngamma)
{
        int i,j;
        double *lngamma_Com, *lnGAMMA_ResP, *lnGAMMA_ResM,
*lngamma_Res;

        // Memory allocation
        lngamma_Com=(double *)malloc(NumComp*sizeof(double));
if(!lngamma_Com) _alloc_error("*lngamma_Com.");
        lnGAMMA_ResP=(double *)malloc(NumComp*NumGroup*sizeof(double));
if(!lnGAMMA_ResP) _alloc_error("*lnGAMMA_ResP.");
        lnGAMMA_ResM=(double *)malloc(NumGroup*sizeof(double));
if(!lnGAMMA_ResM) _alloc_error("*lnGAMMA_ResM.");
        lngamma_Res=(double *)malloc(NumComp*sizeof(double)); if(!lngamma_Res)
_alloc_error("*lngamma_Res.");

        if(!(f_lngamma_Com(x,r,lngamma_Com))) exit(1);
        if(!(f_lnGAMMA_ResP(nyu,Q,psi,lnGAMMA_ResP))) exit(1);
        if(!(f_lnGAMMA_ResM(x,nyu,Q,psi,lnGAMMA_ResM))) exit(1);

        for(i=0;i<NumComp;i++)
        {
                lngamma_Res[i]=0.0;
                for(j=0;j<NumGroup;j++)
lngamma_Res[i]+=nyu[i*NumGroup+j]*(lnGAMMA_ResM[j]-
lnGAMMA_ResP[i*NumGroup+j]);
                lngamma[i]=lngamma_Com[i]+lngamma_Res[i];
        }

        // Free allocated memory
```

```
        free(lngamma_Com);free(lnGAMMA_ResP);free(lnGAMMA_ResM);free(lngam
ma_Res);

        return(1);
}
//
void _alloc_error(char *last_will)
{
        printf("*** ERROR *** Memory allocation failed at %s\n", last_will); exit(1);
}
//EOF
```

E.3 **modifiedUNIFAC_header.h**

```c
// header.h
#if defined( header_h )
#else
#define header_h

// Symbolic constants
#define BINARY      2
#define TERNARY     3
#define OUT         3       // Three Out
#define MAXCHARS   21       // Max # of Characters in Name
#define MAINGROUP   7       // # of Main-groups
#define SUBGROUP   11       // # of Sub-groups
#define SIZE        3       // # of Size Parameters:R, Q, Mw
#define LIST        6       // # of available components in List
#define SOLUBILITY 12       // # of available Solubility Constants Data
#define ABC         3       // # of Constants:A, B, C
#define MOLINF      1.0e-8  // Molality at Infinit Dilution
#define XINF        1.0e-10 // Infinitesimal Mole fraction
#define EPSILON     1.0e-10 // Allowable error


// Global Variables
extern const double T; // T:temperature
extern int NumComp;    // # of components,
extern int NumGroup;   // total # of groups existed in the system

// Function prototype
void _alloc_error(char *last_will); // Memory allocation error report function
int f_Option_NumComp();             // Return the value of int Option
int f_NameComp_NYU_NumGroup(char **NameComp,int *NYU);
int f_nyu_Mw_Q_r_psi(int *NYU,int *nyu,double *Mw,double *Q,double *r,double
*psi);
int f_NumCalc_Mol(int *NumCalc,double *Mol,int Option,char **NameComp,double
*Mw);
int f_xgamma(int *NYU,double *xgamma);
int f_x_Mol(double *x,double *Mol);
int f_Mol_x(double *Mol,double *x);
int f_lngamma_Com(double *x,double *r,double *lngamma_Com);
int f_lnGAMMA_ResP(int *nyu,double *Q,double *psi,double *lnGAMMA_ResP);
int f_lnGAMMA_ResM(double *x,int *nyu,double *Q,double *psi,double
*lnGAMMA_ResM);
int f_lngamma(double *x,int *nyu,double *Q,double *r,double *psi,double *lngamma);
```

```
#endif
// EOF of header.h
```

ACTIVITY COEFFICIENT RATIO AND CRYSTAL PURITY IN DIFFERENT

SOLVENTS
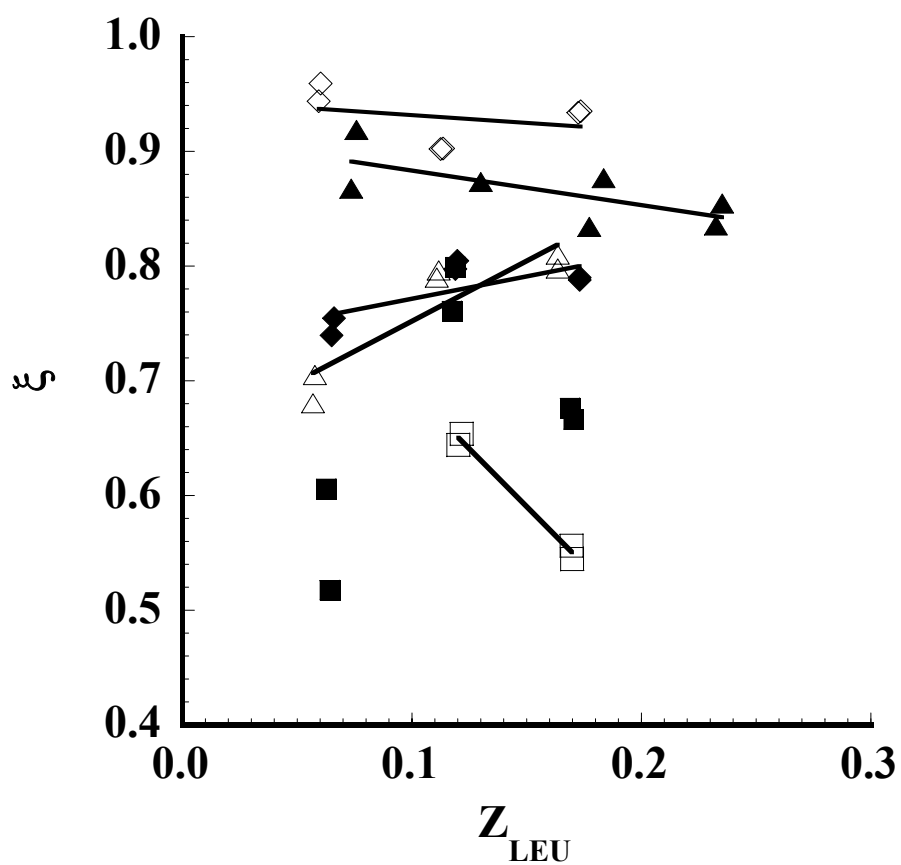
Figure F-1 Activity coefficient ratio, ξ, versus the solid composition of L-LEU in the L-ILE + L-LEU in aqueous solutions (Givand, 1999a): ▲ pure water, △ 20 % DMSO + CaCl$_2$ (I=3.0), ■ 8 % Butanol, □ 15 % Butanol, ♦ (NH$_4$)$_2$SO$_4$ (I=1.6), and ◊ 20 % Ethylene Glycol. Solid lines are for guide.

REFERENCES

Abel, Y; Kakegawa, K.; Sasaki, Y. A new method for the preparation of compositionally homogeneous and pyrochlore-free solid solution of $Pb(Mg_{1/3}Ta_{2/3})O_3$-$Pb(Yb_{1/2}Ta_{1/2})O_3$ system. *Materials Research Bulletin*, **1999**, *34(10/11)*, 1673-1682.

Back J. F.; Oakenfull, D.; Smith, M. B. Increased thermal-stability of proteins in the presence of sugars and polyols. *Biochemistry* **1979**, *18(23)*, 5191-5196.

Beckmann, W. Seeding the desired polymorph: background, possibilities, limitations, and case studies. *Organic Process Research & Development* **2000**, *4*, 372-383.

Blasdale, W.C. *Equilibria in saturated salt solutions.* Chemical Catalog Company, NY, 1927.

Brückner, H.; Westhauser, T.; Godel, H. Liquid chromatographic determination of D- and L-amino acids by derivatization with o-phthaldialdehyde and N-isobutyryl-L-cysteine. Applications with reference to the analysis of peptidic antibiotics, toxins, drugs and pharmaceutically used amino acids. *J. Chromatogr. A* **1995**, *711*, 201-215.

Budavari, S., The Merck Index, 11th ed., Merck & Co., Inc., Rahway, NJ, 1989.

Campbell-Roberts, S. N.; Williams, A. C.; Grimsey, I. M.; Booth, S. W. Quantitative analysis of mannitol polymorphs. X-ray powder diffractometry – exploring preferred orientation effects. *Journal of Pharmaceutical and Biomedical Analysis* **2002**, *28*, 1149-1159.

Carta, R.; Tola, G. Solubilities of L-cystine, L-tyrosine, L-leucine, and glycine in aqueous solutions at various pHs and NaCl concentrations. *J. Chem. Eng. Data* **1996**, *41*, 414-417.

Carta, R. Solubility of L-cystine, L-tyrosine, L-leucine, and glycine in their water solutions. *J. Chem. Eng. Data* **1999**, *44*, 563-567.

Chae, W. –S.; Kim, Y. –R.; Jung, J. –S. Structural confinement effects of ternary chalcogenide in mesoporous AIMCM-41 of different pore diameters. *J. Phys. Chem. B* **2003**, *107*, 1585-1591.

Chen, C.; Zhu Y.; Evans, L. B. Phase partitioning of biomolecules: solubilities of amino acids. *Biotechnology Progress* **1989**, *5(3),* 111-118.

Charmolue, H.; Rousseau, R. W. L-serine Obtained by Methanol Addition in Batch Crystallization. *AIChE Journal* **1991**, *37(8)*, 1121-1128.

Christensen, C.; Gmehling, J.; Rasmussen, P.; Weidlich, U. DECHEMA chemistry Data Series; DECHEMA; Frankfurt/M., 1984; Vol. III, Parts 1 and 2.

Cohn, E. J.; Mcmeekin, T. L.; Edsall, J. T.; Weare, J. H. Studies in the physical chemistry of amino acids, peptides and related substances. II. The solubility of α-amino acids in water and in alcohol-water mixtures. *J. Amer. Chem. Soc.* **1934**, *56*, 2270-2282.

Cottin, X.; Monson, P.A. Substitutionally ordered solid solutions of hard spheres. *J. Chem. Phys.* **1995**, *102(8)*, 3354-3360.

Cottin, X.; Monson, P. A. An application of classical thermodynamics to solid-fluid equilibrium in hard sphere mixtures. *J. Chem. Phys.* **1997**, *107(17)*, 6855-6858.

Coutinho, J. A. P.; Andersen, S. I.; Stenby, E. H. Evaluation of activity coefficient models in prediction of alkane solid-liquid equilibria. *Fluid Phase Equilib.* **1995**, *103*, 23-29.

Coutinho, J. A. P.; Stenby, E. H. Predictive local composition models for solid/liquid equilibrium in n-alkane systems: Wilson equation for multicomponent systems. *Ind. Eng. Chem. Res.* **1996a**, *35(3)*, 918-925.

Coutinho, J. A. P.; Knudsen, K.; Andersen, S. I.; Stenby, E. H. A local composition model for paraffinic solid solutions. *Chem. Eng. Sci.* **1996b**, *51(12)*, 3273-3282.

Coutinho, J. A. P. Predictive UNIQUAC: A new model for the description of multiphase solid-liquid equilibria in complex hydrocarbon mixtures. *Ind. Eng. Chem. Res.* **1998**, *37*, 4870-4875.

Dalton, J. B and Schmidt, C. L. A. Solubilities of Certain Amino Acids in Water, the Densities of Their Solutions at Twenty-Five Degrees, and the Calculated Heats of Solution and Partial Molal Volumes. *Journal of Biological Chemistry* **1933,** *103(2)*, 549-578.

Dalton, J. B; Schmidt, C. L. A. The solubilities of certain amino acids and related compounds in water, the densities of their solutions at twenty five degrees, and the calculated heats of solution and partial molar volumes. II. *J. Biol. Chem.* **1935**, 109, 241-248.

De Stefani, V.; Baba-Ahmed, A.; Richon, D.; Experimental determination of carbon dioxide and nitrous oxide co-solubility in liquid oxygen. *Fluid Phase Equilibria* **2003**, *207*, 131-142.

Douglas, T. B. *J. Chem. Phys.* **1966**, *45*, 4571.

Dunn, M. S.; Ross, F. J. Quantitative investigations of amino acids and peptides. IV. The solubilities of the amino acids in water-ethyl alcohol mixtures. *J. Biol. Chem.* **1938**, *125*, 309-332.

Ellerton, H.; Reinfelds, G.; Mulcahy, D. E.; Dunlop, P. J. Activity, density, and relative viscosity data for several amino acids, lactamide, and raffinose in aqueous solution at 25º. *J. Phys. Chem.* **1964**, *68(2)*, 398.

Erickson, D. D.; Niesen, V. G.; Brown, T. S. Thermodynamic measurement and prediction of paraffin precipitation in crude oil. Paper SPE 26604, Tech. Conf. and Exhibit of the Soc. Of Pet. Engrs., Houston (Oct. 3-6, 1993).

Flöter, E.; Hollanders, B.; de Loos, T. W.; de Swaan Arons, J. The ternary system (n-heptane + docosane + tetracosane): The solubility of mixtures of docosane and

tetracosane in heptane and data on solid-liquid and solid-solid equilibria in the binary subsystem (docosane + tetracosane). *J. Chem. Eng. Data* **1997**, *42*, 562-565.

Fasman, G. D. Handbook of Biochemistry and Molecular Biology, 3rd edition, *Physical and Chemical Data*, vol. 1, CRC Press, Cleveland, OH, 1976.

Fredenslund, Aa.; Gmehling, J.; Rasmussen, P. Vapor-liquid equilibria using UNIFAC. A group-contribution method. Elsevier Scientific, Amsterdam, Netherlands. 1977.

Fullerton, G. D.; Ord, V. A.; Cameron, I. L. An evaluation of the hydration of lysozyme by an NMR titration method. *Biochim. Biophys. Acta* **1986**, *869(3)*, 230-246.

Geiger, A. Molecular-dynamics simulations study of the negative hydration effect in aqueous-electrolyte solutions. *Ber. Bunsenges. Phys. Chem.* **1981**, *85(1)*, 52-63.

Gekko, K; Idota, Y. Amino acid solubility and protein stability in aqueous maltitol solutions. *Agric. Biol. Chem.* **1989**, *53(1)*, 89-95.

Ghogomu, P. M.; Dellacherie, J.; Balesdent, D. Solubility of normal paraffin hydrocarbons (C20 to C24) and some of their binary mixtures (C22 +C24) and (C23 + C24) in ethylbenzene. *J. Chem. Thermodyn.* **1989,** *21*, 925-934.

Giron, D. Thermal analysis and calorimetric methods in the characterization of polymorphs and solvates. *Thermochimica Acta* **1995**, *248*, 1-59.

Givand, J. The effect of relative solubility on crystal purity. Ph. D. Dissertation, Georgia Institute of Technology, 1999a.

Givand, J.; Rousseau, R. W.;Teja, A. S. Manipulation of Thermodynamic Properties to Enhance Crystal Purity. *International Symposium on Industrial Crystallization* 14th **1999b**, 1688.

Givand, J. C.; Teja, A. S.; Rousseau, R. W. Effect of relative solubility on amino acid crystal purity. *AIChE Journal* **2001**, *47(12)*, 2705-2712.

Givand, J. C.; Teja A. S.; Rousseau, R. W. Correlation and prediction of crystal solubility and purity. *AIChE Journal* **2002a**, *48(11)*, 2629-2634.

Givand, J.; Chang, B-K.; Teja, A. S.; Rousseau, R. W. Distribution of isomorphic amino acids between a crystal phase and an aqueous solution. *Ind. Eng. Chem. Res.* **2002b,** *41,* 1873-1876.

Gmehling, J.; Onken, U. DECHEMA Chemistry Data Series; DECHEMA: Frankfurt/M., 1977; Vol. I.

Grant, D. J. W.; Higuchi, T. Solubility behavior of organic compounds. A Wiley-Interscience Publication, John Wiley & Sons, NY, 1990.

Grosch, L.; Noack, F. NMR relaxation investigation of water mobility in aqueous bovine serum-albumin solutions. *Biochim. Biophys. Acta* **1976**, *453(1)*, 218-232.

Guggenheim, E.A. *Thermodynamics, an advanced treatment for chemists and physicists.* North-Holland Publishing Co., Amsterdam, 1949.

Gupta, R. B.; Heidemann R. A. Solubility models for amino acids and antibiotics. *AIChE Journal* **1990**, *36(3)*, 333-341.

Hade, E. P. K. Solubilities of naturally occurring L-amino acids in water at various temperatures. PhD Dissertation, University of Chicago, 1963.

Hajmeer, M; Basheer, I. Comparison of logistic regression and neural network-based classifiers for bacterial growth. *Food Microbiology* **2003**, *20*, 43-55.

Hansen, H. K.; Rasmussen, P.; Fredenslund, Aa.; Schiller, M.; Gmehling, J. Vapor-liquid equilibria by UNIFAC group contribution 5. Revision and extension. *Ind. Eng. Chem. Res.* **1991**, *30*, 2352-2355.

Hansen, J. H.; Fredenslund, Aa.; Pedersen, K. S.; Ronningsen, H. P. A thermodynamic model for predicting wax formation in crude oils. *AIChE J.* **1988**, *34(12)*, 1937-1942.

He, B.; Martin, V.; Setterwall, F. Liquid-solid phase equilibrium study of tetradecane and hexadecane binary mixtures as phase change materials (PCMs) for comfort cooling storage. *Fluid Phase Equilibria* **2003**, *212*, 97-109.

He, X; Griesser, U. J.; Stowell, J. G.; Borchardt, T. B.; Byrn, S. R. Conformational color polymorphism and control of crystallization of 5-methyl-2-[(4-methyl-2-nitrophenyl)amino]-3-thiophenecarbonitrile. *Journal of Pharmaceutical Sciences*, **2001**, *90(3)*, 371-388.

Holder, G. A.; Winkler, J. Wax crystallization from distillate fuels. Part I. Cloud and pour point phenomena exhibited by solutions of binary n-paraffin mixtures *J. Inst. Pet.* **1965**, *51*, 228-234.

Hutchen, J. O.; Figlio K. M.; Granito, S. M. An isopiestic comparison method for activities. *J. Biol. Chem.* **1963**, *238*, 1419-1422.

Jin, X. Z.; Chao, K., Solubility of Four Amino Acids in Water and of four pairs of amino acids in their water solutions. *Journal of Chemical and Engineering Data* **1992**, *37*, 199-203.

Jones, B.N.; Pääbo, S.; Stein S. Amino acid analysis and enzymatic sequence determination of peptides by an improved o-phthaldialdehyde precolumn labeling procedure. *J. Liq. Chromatogr.* **1981**, *4(4)*, 565-586.

Kalra, A.; Nihal T.; Cramer, S.M.; Garde S. J. Salting-in and salting-out of hydrophobic solutes in aqueous salt solutions. *J. Phys. Chem. B* **2001**, *105*, 6380-6386.

Keener, C. R.; Fullerton, G. D.; Cameron, I. L.; Xiong, J. Solution nonideality related to solute molecular characteristics of amino acids. *Biophysical Journal* **1995**, *68*, 291-302.

Khan, A. R.; Riazi, M. R.; Al-Roomi, Y. A A thermodynamic model for liquid adsorption Isotherms. *Separation Purification Technology* **2000**, *18*, 237-250.

Kitamura, M.; Nakamura, T. Inclusion behavior of isomorphous impurities in crystallization of L-glutamic acid. *International Symposium of Industrial Crystallization* 14th **1999**, *12-16,*1604-1610.

Koolman, H. C.; Rousseau, R. W. Effect of isomorphic compounds on the purity and morphology of L-isoleucine crystals. *AIChE Journal* **1996**, *42*, 147-153.

Kuramochi, H.; Noritomi, H; Hoshino, D.; Nagahama, K. Measurements of Solubilities of two amino acids in water and prediction by the UNIFAC model. *Biotechnology Progress* **1996**, *12*, 371-379.

Kusumoto, I. Industrial production of L-glutamine. *J. Nutr.* **2001**, *131(9),* 2552S-2555S.

Lafferrere, L; Hoff, C.; Veesler, S. Polymorphism and liquid-liquid demixing in supersaturated drug solution. *Eng. Life Sci.* **2003**, *3*, 127-131.

Lakshml, T. S.; Nandi, P. P. K. Effects of sugar solutions on the activity coefficients of aromatic amino acids and their N-acetyl ethyl esters. *J. Phys Chem.* **1976**, *30(3)*, 249-252.

Larsen, B. L.; Rasmussen, P.; Fredenslund, A.; A modified UNIFAC group contribution model for prediction of phase equilibria and heats of mixing. *Ind. Eng. Chem. Res.* **1987**, *26*, 2274-2286.

Lewis, G.N.; Randall, M. *Thermodynamics and the free energy of chemical substances.* McGraw-Hill Book Company, Inc. NY and London, 1923.

Lira-Galeana, C.; Firoozabadi, A.; Prausnitz, J. M. Thermodynamics of wax precipitation in petroleum mixtures. *AIChE J.* **1996**, *42(1)*, 239-248.

Liu, G.; Nagahama, K. Solubility and ress experiments of solid solution in supercritical carbon dioxide. *Journal of Chemical Engineering of Japan* **1997**, *30,* 293 -301.

Liu, S. T.; Hurwitz, A. Effect of enantlomeric purity on solubility determination of dexclamol hydrochloride. *J. Pharm. Sci.,* **1978**, *67,* 636-638.

Lorenz, H.; Sapoundjiev, D.; Seidel-Morgenstern, A. Study of solubility equilibria in chiral systems. *15th ISIC proceedings*, **2002**, *1*, 167-172.

Makarov, E. S. Principles of the isomorphic interchangeability of atoms in solid solution crystals. *Materials Research Bulletin* **1972**, *7(11)*, 1293-1296.

Malanoski, A. P.; Monson, P. A. The phase behavior of a hard sphere chain model of a binary n-alkane mixture. *J. Chem. Phys.* **2000**, *112(6)*, 2870-2877.

Mansoori, G. A.; Carnahan, N. F.; Starling, K. E.; Leland, T. W. Equilibrium thermodynamic properties of mixture of hard spheres. *J. Chem. Phys.* **1971**, *54(4)*, 1523-1525.

Marlow, G. E.; Perkyns, J. S.; Pettitt, B. M. Salt effects in peptide solutions. Theory and Simulation. *Chem. Rev.* **1993**, *93(7)*, 2503-2521.

Matsuoka, M.; Garside, J. (ed); Davey, R.J (ed); Jones A. (ed).; *Advances in Industrial Crystallization*, Butterworth-Heinemann, pp.229-224, 1991.

McMeekin, T. L.; Cohn, E. J.; Weare, J. H. Studies in the physical chemistry of amino acids, peptides and related substances. VII. A comparison of the solubility of amino acids, peptides and their derivatives. *J. Amer. Chem. Soc.* **1936**, *58(11)*, 2173-2181.

Messer, C. E.; Malakoff, G.; Well, J.; Lablb, S. Phase equilibrium behavior of certain pairs of amino acids in aqueous solution. *The Journal of Physical Chemistry* **1981**, *85*, 3533-3540.

Mitchell, A. G. Racemic drugs: Racemic mixture, racemic compound, or pseudoracemates. *J. Pharm. Pharmaceut. Sci.*, **1998**, *1(1)*, 8-12.

Mitchell, J. P.; Butler, J. B.; Albright, J. G. Measurement of mutual diffusion coefficients, densities, viscosities, and osmotic coefficients for the system KSCN-H_2O at 25 ºC. *J. Sol. Chem.*

Morse, P. M. *Thermal Physics* W. A. Benjamin, NY, 1969.

Mullin, J. W. *Crystallization 4th ed.* Butterworth-Heinemann, MA 2001.

Nozaki, Y.; Tanford, C. The solubility of amino acids and two glycine peptides in aqueous ethanol and dioxane solutions. ESTABLISHMENT OF A HYDROPHOBICITY SCALE. *J. Biol. Chem.* **1971**, *246(7)*, 2211-2217.

Nývlt, J. *Solid-liquid Phase Equilibria.* Elsevier Scientific Publishing Company, NY, 1977.

Palecz, B.; Piekarski, H. Dissolution enthalpy of glycine in aqueous solutions of bivalent metal electrolytes. *Fluid Phase Equilibria* **1999**, *164(2)*, 257-265.

Palecz, B.; Piekarski, H.; Romanowski, S. Studies on homogeneous interactions between zwitterions of several L-a-amino acids in water at a temperature of 298.15 K. *J. Mol. Liq.* **2000**, *84(3)*, 279-288.

Park, B. H.; Yoo, K. –P.; Lee, C. S. Phase equilibria and properties of amino acids + water mixtures by hydrogen-bonding lattice fluid equation of state. *Fluid Phase Equilibria* **2003**, *212*, 175-182.

Park, H.; Englezos, P. Osmotic coefficient data for Na2SiO3 and Na2SiO3-NaOH by an isopiestic method and modeling using Pitzer's model. *Fluid Phase Equilibria* **1998**, *153*, 87-104.

Pedersen, W. B.; Hansen, A. B.; Larsen, E.; Nielsen, A. B.; Ronningsen, H. P. Wax precipitation from North-Sea crude oils: 2. Solid-phase content as function of temperature determined by pulsed NMR. *Energy and Fuels* **1991**, *5*, 908-913.

Pitzer, K.S. Electrolytes from dilute solutions to fused salts. *Journal of the American Chemical Society* **1980**, *102*, 2902-2906.

Pradhan, A. A.; Vera, J. H. Effect of acids and bases on the solubility of amino acids. *Fluid phase equilibria* **1998**, *152*, 121-132.

Pradhan, A. A; Vera, J. H. Effect of anions on the solubility of zwitterionic amino acids. *J. Chem. Eng. Data* **2000**, *45*, 140-143.

Prausnitz, J. M.; Lichtenthaler R. N.; de Azevedo D.G. *Molecular Termodynamics of Fluid-Phase Equilibria*, 2nd ed., PTR Prentice-Hall, Inc., Englewood Cliffs, NJ, 1986.

Prausnitz, J. M.; Lichtenthaler, R. N.; Azavedo, E. G. Molecular thermodynamics of fluid phase equilibria. 3rd Ed., Prentice-Hall, Upper Sadle River, NJ, 1999.

Ramasami, P. J. Solubilities of amino acids in water and aqueous sodium sulfate and related apparent transfer properties. *J. Chem. Eng. Data* **2002**, *47*, 1164-1166.

Renon, H.; Prausnitz, J. M. Local compositions in thermodynamic Excess Functions for Liquid Mixtures. *AIChE Journal* **1968**, *14,* 135.

Riazi, M. R.; Al-Roomi, Y. A. A thermodynamic model for liquid adsorption isotherms. *Separation and Purification Technology* **2000**, *18*, 237-250.

Robinson, R. A.; Sinclair, D. A. The activity coefficients of the alkali chlorides and of lithium iodine in aqueous solution from vapor pressure measurements. *J. Am. Chem. Soc.* **1934**, *56(9)*, 1830-1835.

Robinson, R.A.; Stokes, R.H. Activity coefficients in aqueous solutions of sucrose mannitol and their mixtures at 25º. *J. Phys. Chem.* **1961**, *65*, 1954-1958.

Rosenberger, F.; Riveros, H.G. Segregation in Alkali Halide Crystallization from Aqueous Solutions. *The Journal of Chemical Physics* **1974**, *60*, 668-673.

Rossky, P. J.; Karplus, M. Solvation-molecular-dynamics study of a dipeptide in water. *J. Amer. Chem. Soc.* **1979**, *101(8)*, 1913-1937.

Roth, M. Fluorescence reaction for amino acids. *Anal. Chem.* **1971**, *43(7)*, 880-882.

Rowe, R. C. Private prescription: A thought-provoking tonic on the lighter side. *Drug Delivery Today,* **2001**, *6(8)*, 395-397.

Smith, P. K.; Smith, E. R. B. Thermodynamic properties of solutions of amino acids and related substances. II. The activities of aliphatic amino acids in aqueous solution at twentyfive degrees. *J. Biol. Chem.* **1937**, *121*, 607-613.

Smith, P. K.; Smith, E. R. B. Thermodynamic properties of solutions of amino acids and related substances V. the activities of some hydroxy-and n-methylamino acids and proline in aqueous solution at twenty-five degrees. *J. Biol. Chem*. **1940a**, *132*, 57-64.

Smith, P. K.; Smith, E. R. B. Thermodynamic properties of solutions of amino acids and related substances. VI. The activities of some peptides in aqueous solution at twentyfive degrees. *J. Biol. Chem*. **1940b**, *135*, 273-279.

Snyder, R. G.; Srivatsavoy, V. J. P.; Cates, D. A.; Strauss, H. L.; White, J. W.; Dorset, D. L. Hydrogen/deuterium isotope effects on microphase separation in unstable crystalline mixtures of binary n-alkanes. *J. Phys. Chem.* **1994**, *98*, 674-684.

Sonnenschein, R.; Heinzinger, K. A molecular-dynamics study of water between lennard-jones walls. *Chem. Phys. Lett.* **1983**, *102(6)*, 550-554.

Sorensen, J. M.; Arlt, W. DECHEMA Chemistry Data Series, DECHEMA: Frankfurt/M., 1979; Vol. V, Parts 1-3.

Suda, A.; Ukyo, Y.; Sobukawa, H.; Sugiura, M. Formation mechanism of ceria-zirconia solid solution by solid phase reaction. *R&D Review of Toyota CRDL* **2002**, *37(4)*, 6-13.

Synder, L. R.; Stadalius, M.A.; Quarry, M.A. Gradient elution in reversed-phase HPLC. *Anal. Chem.* **1983,** *55(14)*, 1412A-1430A.

Toby, B. *The portable CMPR*, The NIST center for neutron research, Gaithersburg, MD 2000. http://www.ncnr.nist.gov/programs/crystallography/software/cmpr/cmpr.html

Torii, K.; Iitaka, Y. The crystal structure of L-valine. *Acta. Cryst.* **1970**, *B26*, 1317-1326.

Torii, K.; Iitaka, Y. The crystal structure of L-isoleucine. *Acta. Cryst.* **1971**, *B27*, 2237-2246.

Uedaira, H.; Uedaira, H. The effect of sugars on the thermal-denaturation of lysozyme. *Bull. Chem. Soc. Japan* **1980**, *53(9)*, 2451-2455.

Wang, F.; Wachter, J. A.; Antosz, F. J.; Berglund, K. A. An investigation of solvent-mediated polymorphic transformation of progesterone using in situ raman spectroscopy. *Organic Process Research & Development* **2000**, *4*, 391-395.

Yakubov, G. E.; Boiko, V. I. The thermodynamic equation for the dissolution of solids in liquids. *Journal of Molecular Liquids,* **2001**, *91*, 33-46.

Yoshimura, M; Ohmura, M.; Cho, W-S; Yashima, M.; Kakihana, M. Preparation of crystallized $Sr_{1-x}Ca_xMoO_4$ solid-solution films by an electrochemical method at room temperature and their luminescence. *J. Am Ceram. Soc.,* **1997**, *80(9)*, 2464-2466.

Yu, Lian Nucleation of one polymorph by another. *J. Am. Chem. Soc.* **2003**, *125*, 6380-6381.

Walter, J.H.; Wu, Yung-Chi Osmotic coefficients and mean activity coefficients of uni-univalent electrolytes in water at 25 ºC. *J. Phys. Chem. Ref. Data* **1972**, *1(4)*, 1047-1099.

Won, K.W. Thermodynamics for solid solution-liquid-vapor equilibria-Wax phase formation from heavy hydrocarbon mixtures. *Fluid Phase Equilibria* **1986**, 30, 265-279.

Zimmerman, S.; Zimmerman, A. M.; Fullerton, G. D.; Luduena, R. F. Water ordering during the cell-cycle-nuclear-magnetic-resonance studies of the sea-urchin egg. *J. Cell. Sci.* **1985**, *79*, 247-257.

Zumstein, R. C., Modeling, determination, and measurement of growth rate dispersion in crystallization. The crystallization of L-isoleucine in aqueous solutions. Ph. D. Dissertation, North Carolina State University, 1987.

Zumstein, R.C.; Rousseau, R.W. Solubility of L-isoleucine in and recovery of L-isoleucine from neutral and acidic aqueous solutions. *Ind. Eng. Chem. Res.* **1989**, *28*, 1226-1231.

Zuo, J. Y.; Zhang, D. D.; Ng, H. An improved thermodynamic model for wax precipitation from petroleum fluids. *Chemical Engineering Science* **2001**, *56*, 6941-6947.

VITA

Izumi Kurosawa was born in Chiba, Japan in 1973. She attended Tokyo Gakugeidaigaku Fuzoku High School until graduation in March of 1991. In April of 1993, she enrolled as a student at School of Engineering, Tohoku University in Miyagi, Japan. During her undergraduate tenure, she majored in Chemical Engineering. She worked at Department of Chemical Engineering, Prague Institute of Chemical Technology (Prague, Czech Republic) during the summer of 1996 for an internship program.

She started her academic career in her senior year under Dr. Kunio Arai at Department of Biochemistry and Engineering, School of Engineering, Tohoku University and received her Bachelors of Science degree in March, 1998.

After completing her Bachelor of Science, her admission to graduate school at Tohoku University was approved. She started graduate research under the direction of Dr. Hiroshi Inomata at Research Center of Supercritical Fluid Technology, Graduate School of Engineering, Tohoku University and received her Masters of Science in March, 2000.

She went to Atlanta, Georgia to attend School of Chemical Engineering at the Georgia Institute of Technology. She started her doctoral research under Dr. Ronald W. Rousseau and Dr. Amyn S. Teja in August, 2000. She successfully defended this thesis on April 28th, 2004 as part of the requirements for the Doctor of Philosophy degree in Chemical Engineering from the Georgia Institute of Technology.